TROPHIC STRUCTURE AND FOOD WEB DYNAMICS OF DEEP-PELAGIC MICRONEKTON IN THE GULF OF MEXICO

A Dissertation

by

TRAVIS MARK RICHARDS

Submitted to the Office of Graduate and Professional Studies of
Texas A&M University
in partial fulfillment of the requirements for the degree of

DOCTOR OF PHILOSOPHY

Chair of Committee,	Robert David Wells
Committee Members,	Jay Rooker
	Ron Eytan
	Gilbert Rowe
Head of Department,	Daniel Roelke

August 2020

Major Subject: Marine Biology

ABSTRACT

The deep-pelagic ocean is the largest but least studied ecosystem on Earth. As natural resource extraction and fisheries expand into the deep pelagic, there is increased need for comprehensive, ecosystem-based management plans for deep-pelagic ecosystems. Detailed knowledge of food webs is critical to effective ecosystem management, as trophic interactions regulate animal populations and influence the resilience of ecosystems to perturbation. Additionally, effective management strategies require data regarding feeding relationships amongst taxa, estimates of trophic position, and descriptions of energy transfer, which are lacking for the deep-pelagic Gulf of Mexico. This dissertation describes the trophic structure of deep-pelagic micronekton, which represent crucial components of deep-pelagic ecosystems worldwide, with the goal to provide data critical to the development of ecosystem-based management plans in deep-pelagic ecosystems. The first study describes fine-scale spatiotemporal variation in micronekton trophic structure in the Gulf of Mexico and presents evidence suggesting that micronekton inhabiting different regions of the water column feed within food chains supported by two different size classes of sinking particulate organic matter. The second study examines the trophic dynamics of deep-pelagic predatory fishes by providing estimates of their trophic position and quantifying their use of particulate organic matter from differing regions of the water column. Results indicate that all species occupy trophic positions between the third and fourth trophic level and receive the majority of their carbon from primary production derived near the surface of the ocean. These species, which often do not vertically migrate, access epipelagic primary production by consuming vertically migrating micronekton which forage in the epipelagic at night. The last study reveals that body size, depth of

occurrence, and proximity to major oceanographic features are important determinants of trophic structure within the deep-pelagic micronekton assemblage of the Gulf of Mexico. The emerging picture of deep-pelagic food webs is one of extreme interconnectedness, with animals inhabiting the deepest depths of the GoM connected to primary production and food resources in epipelagic waters. Taken together, the results of this research increase our understanding of deep-pelagic food webs and ecosystems and will be used to better inform the construction of deep-pelagic ecosystem-based management plans.

ACKNOWLEDGEMENTS

I would like to thank my committee chair, Dr. David Wells. His support and guidance over the years have been instrumental in completing my research. He has been an outstanding mentor, role model, counselor, and leader. I have been extremely fortunate to have been given the opportunity to work with him over these years and for this I will be forever grateful for the opportunities he has provided me.

Thanks to my committee members, Dr. Jay Rooker, Dr. Gil Rowe, Dr. Ron Eytan, and Dr. Tracey Sutton for their guidance and support throughout the course of this research. I would especially like to thank Dr. Tracey Sutton for providing me the opportunity to accompany him and other researchers on five expeditions into the Gulf of Mexico to sample deep-pelagic fauna. I would also like to thank Thomas TinHan and Jeff Plumlee for their support and the many conversations we had pertaining to experimental design and statistics. Thanks to April Cook, and Nina Pruzinski for their help organizing and collating all the data collected by the DEEPEND consortium which I frequently used throughout my dissertation. Thanks also to the faculty, staff and graduate students at Texas A&M University at Galveston for their friendship and guidance over the years as well as for assistance to acquire my degree.

Finally, thanks to my family for their love and support and to Mallory Mincberg for her patience, love, and constant encouragement.

CONTRIBUTORS AND FUNDING SOURCES

Contributors

This work was supervised by a dissertation committee consisting of Dr. David Wells of the Department of Marine Biology, Dr. Jay Rooker of the Department of Marine Biology, Dr. Gil Rowe of the Department of Marine Biology, Dr. Ron Eytan of the Department of Marine Biology, and Dr. Tracey Sutton of the Department of Marine and Environmental Sciences, Halmos College of Natural Sciences and Oceanography at Nova Southeastern University. The work for the dissertation was completed by Travis Richards, with field support from Tracey Sutton and April Cook.

Funding Sources

Graduate study was supported by Graduate student Teaching Assistantships from Texas A&M University. This work was also made possible in part by funding from the Gulf of Mexico Research Initiative. The analyses depicted in Chapter 3 were conducted by Travis Richards of the Marine Biology Department and were published in 2019.

NOMENCLATURE

GOM	Gulf of Mexico
POM	Particulate Organic Matter
SIA	Stable Isotope Analysis
AA-CSIA	Amino Acid Compound Specific Isotope Analysis
SCA	Stomach Content Analysis
DVM	Diel Vertical Migration

TABLE OF CONTENTS

Page

LIST OF FIGURES

Page

LIST OF TABLES

Page

CHAPTER I

INTRODUCTION

The deep-pelagic ocean is the largest cumulative ecosystem on the planet and provides a host of ecosystem services including carbon sequestration, nutrient regeneration, and waste absorption, which are vital to ocean health (Robison, 2004; Robison, 2009; Mengerink et al., 2014; Thurber et al., 2014). Despite its enormous volume and vital role in global carbon and climate cycles, deep-pelagic ecosystems are chronically understudied (Webb et al., 2010). Currently, deep-pelagic ecosystems face an increasing number of stressors including climate change, ocean acidification, overfishing, and natural resource extraction (Morato et al., 2006; Ramirez-Llodra et al., 2011; Mengerink et al., 2014). As threats to the diversity and stability of marine ecosystems increase and expand into deeper oceanic environments, there has been increasing concern regarding the status of deep-pelagic communities and a renewed interest in describing and understanding deep-sea ecosystem structure so that management plans can be developed and implemented (Ramirez-Lodra et al., 2011; Mengerink et al., 2014).

A detailed understanding of deep-pelagic ecosystem structure and function requires a thorough understanding of food web structure, including descriptions of feeding relationships among species and major functional groups and delineations of energy flow from carbon sources (primary producers) to apex predators (Polis and Strong, 1996). Trophic interactions regulate animal populations, determine energy pathways, and help determine the resilience of communities to perturbation (Winemiller and Polis, 1996). While our knowledge of deep-sea food webs has advanced considerably over the past few decades, in many regions fundamental information including species-specific feeding relationships, estimates of trophic position, and delineations of energy pathways, are lacking (Mengerink et al., 2014; Drazen and Sutton, 2017).

Micronekton, small (2-10 cm) swimming fishes, crustaceans, and cephalopods, are vital components of deep-pelagic food webs and represent a dominant proportion of the global fish and crustacean biomass (Irigoien et al., 2014; Vereshchaka et al., 2019). As highly abundant consumers, micronekton play important roles in ecological and biogeochemical processes that underpin ecosystem services including carbon sequestration and fisheries production (Longhurst et al., 1990). Many deep-pelagic micronekton undergo diel vertical migrations (DVM) through the water column to feed within the epipelagic zone (0 – 200 m) at night while avoiding visually cued predation, then return to daytime depths in the meso- (200-1000 m) or bathypelagic (1000-4000 m) zones. Through DVM micronekton represent an important source of connectivity between the epi-, meso-, and bathypelagic zones, and have been identified as important prey of consumers throughout the water column (Sutton and Hopkins, 1996b; Moteki et al., 2001; Cherel et al., 2008; Choy et al., 2013). By incorporating carbon derived from surface production and then respiring and excreting carbon at daytime depths in meso- and bathypelagic zones, micronekton also play an important role in the biological pump by vertically transporting carbon into the deep sea (Wilson et al., 2009; Thurber et al., 2014). As consumers, micronekton represent a significant top-down influence on lower trophic levels, with numerically dominant zooplanktivores such as the lanternfishes (Myctophidae) and lightfishes (Phosichthyidae) capable of regulating zooplankton populations (Hopkins and Gartner, 1992; Hopkins et al., 1996). Considering their high global abundance, importance as a trophic link between primary and higher-order consumers, and active role in the biological pump, understanding and describing the trophic structure of micronekton assemblages is critical to our understanding of deep-pelagic ecosystems.

The Gulf of Mexico (GOM) is a semi-enclosed ocean basin physically distinct from both the Caribbean Sea and greater Atlantic Ocean which exhibits physical and biological characteristics typical of oligotrophic low-latitude ecosystems worldwide (Sutton et al., 2017b). Circulation in the eastern GOM is dominated by the anticyclonic Loop Current, which brings warm, oligotrophic water from the Caribbean Sea in through the Yucatan Channel northward into the GOM before deflecting eastward and then exiting through the Florida Straits. Northward extension into the GOM by the Loop Current is highly variable and introduces significant spatial heterogeneity to the pelagic GOM through the shedding of anticyclonic and cyclonic eddies that propagate westward, eventually dissipating along the GOM's western boundary (Biggs, 1992; Davis et al., 2002). Previous studies have shown that currents associated with the Loop Current and mesoscale eddies can act to concentrate primary and secondary production and in turn can alter the spatial distribution of higher-order consumers such as tunas, billfishes, and marine mammals (Davis et al., 2002; Rooker et al., 2013; Cornic and Rooker, 2018). In addition to its unique oceanography, recent faunal inventories of the pelagic GOM identified 897 species of fishes, 120 species of crustaceans, and 94 species of cephalopods and was recently identified as one of the four most speciose pelagic ecoregions on the planet (Sutton et al., 2017b; Sutton et al., 2020). In addition to a diverse pelagic fauna, the GOM supports lucrative coastal and pelagic fisheries and is the focus of intense oil and gas exploration and extraction that has steadily expanded into the deep-pelagic realm (Murawski et al., 2020). Despite the deep-pelagic GOM's global importance to biological diversity and regional importance to local economies, comprehensive ecosystem management plans for the deep-pelagic GOM are lacking, a point amplified by the Deepwater Horizon oil spill.

Stable isotope analysis (SIA) is a popular tool in the field of food web ecology to trace energy pathways, delineate food web structure, and estimate trophic positions of consumers (Peterson and Fry, 1987; Vander Zanden and Rasmussen, 2001). Unlike stomach content analysis (SCA) which only provides a glimpse of an animal's feeding habits over short time scales (hours to days), SIA provides an integrated view of an organism's diet over time scales relevant to tissue turnover rates rather than digestion rates (Peterson and Fry, 1987; Post, 2002). Stable isotope analysis, which compares the ratio of heavy to light isotope in an organism with the ratio of heavy to light isotope in an international standard, provides an integrated view of an organism's diet over larger time scales than those offered by diet analysis (Peterson and Fry, 1987). Stable isotopes of carbon ($^{12}C/^{13}C$) are useful for determining the relative contributions of carbon sources to the production of consumers and for the delineation of energy pathways through food webs (Peterson and Fry, 1987). Carbon isotopes undergo relatively little fractionation (+ 0.5‰) during trophic transfer resulting in the isotopic carbon signature of consumers closely resembling the carbon signatures of their prey or basal carbon source (primary producer) (Peterson and Fry, 1987). Stable isotopes of nitrogen ($^{14}N/^{15}N$) undergo comparatively large levels of fractionation (~3.4‰) during trophic transfer resulting in large and predictable isotopic differences between consumers and their diet (Peterson and Fry, 1987; Post, 2002). The predictable level of enrichment of ^{15}N between consumers and prey allows nitrogen isotopes to be used to assign consumers to specific trophic positions, is useful for identifying trophic relationships among species or functional groups, and can be used to estimate food chain length (Peterson and Fry, 1987; Post, 2002).

This dissertation is successively organized into chapters to investigate the following research questions and themes.

Chapter II: How variable is the trophic structure of meso- and bathypelagic micronekton across horizontal (nearshore vs. offshore), vertical (migratory vs. non-migratory), and temporal (seasonal, annual) gradients?

Chapter III: What are the trophic dynamics of meso- and bathypelagic predatory fishes inhabiting the GOM? Specifically, I seek to focus on eight meso- and bathypelagic species and describe their trophic positions, isotopic niche sizes, degree of isotopic niche overlap, and quantify their relative use of food webs supported by particulate organic matter from regions throughout the water column.

Chapter IV: What biological, spatial, and temporal factors contribute to the trophic structure of deep-pelagic micronekton assemblages in the GOM? Specifically, how do factors such as body size, depth of occurrence, migration type, sampling location, and sampling season affect the trophic relationships of a diverse micronekton assemblage?

CHAPTER II

TROPHIC STRUCTURE AND SOURCES OF VARIATION INFLUENCING THE STABLE ISOTOPE SIGNATURES OF MESO- AND BATHYPELAGIC MICRONEKTON FISHES

Introduction

The deep-pelagic ocean represents the largest ecosystem on the planet and provides a suite of ecosystem services, including carbon sequestration, nutrient regeneration, and waste absorption, which are vital to ocean health (Mengerink et al., 2014; Thurber et al., 2014). Although its importance is well established, the deep pelagic is chronically understudied, with detailed knowledge of ecosystem function lagging behind coastal and shelf ecosystems (Webb et al., 2010). Despite a poor understanding of ecosystem structure and function, natural resource extraction and pelagic fisheries are currently expanding into the deep ocean before effective management strategies can be developed (Drazen, 2019; Murawski et al., 2020). As interest in these fisheries and untapped natural resources increases, there has been a concerted effort to study deep-pelagic ecosystems so that management plans can be implemented and the effects of anthropogenic activities can be assessed (Ramirez-Lodra et al., 2011; Mengerink et al., 2014). A major focus of recent deep-sea research has centered on understanding food webs, as trophic interactions regulate animal populations (especially in ecosystems with no physical refuge), determine energy pathways, and greatly influence the resilience of communities to perturbation (Winemiller and Polis, 1996). Additionally, ecosystem models, which are powerful tools used to inform ecosystem-based management, require data regarding feeding relationships amongst taxa, estimates of trophic position, and descriptions of energy transfer. These data are typically lacking from many deep-pelagic ecosystems (Choy et al., 2016; Pethybridge et al., 2018).

Micronekton, small (2-10 cm) swimming fishes, crustaceans, and cephalopods, are vital components of deep-pelagic food webs worldwide and represent a dominant proportion of the global fish and crustacean biomass (Irigoien et al., 2014; Vereshchaka et al., 2019). Ubiquitous throughout the world's oceans, micronekton play important roles in ecological and biogeochemical processes that underpin ecosystem services including carbon sequestration and fisheries production (Longhurst et al., 1990). Many deep-pelagic micronekton undergo diel vertical migrations (DVM) through the water column to feed within the epipelagic zone (0 - 200 m) at night while avoiding visually cued predation, then return to daytime depths in the meso- (200 - 1000 m) or bathypelagic (1000 - 4000 m). Through DVM, which for some species can exceed 1000 m, micronekton represent an important source of connectivity between the epi-, meso-, and bathypelagic zones, and have been identified as important components of the diets of consumers throughout the water column (Sutton and Hopkins, 1996b; Moteki et al., 2001; Cherel et al., 2008; Choy et al., 2013). As highly abundant consumers, micronekton represent a significant top-down influence on lower trophic levels, with numerically dominant zooplanktivores such as the lanternfishes (Myctophidae) and lightfishes (Phosichthyidae) capable of exerting control on zooplankton populations (Hopkins and Gartner, 1992; Hopkins et al., 1996). Considering their high global abundance and importance as a trophic link between primary and higher-order consumers, understanding and describing the trophic structure of micronekton assemblages is critical to the formation of accurate oceanic ecosystem models.

Stable isotope analysis (SIA) is a popular tool in the field of food web ecology to trace energy pathways, delineate food web structure, and estimate trophic positions (Peterson and Fry, 1987; Vander Zanden and Rasmussen, 2001). Stable isotopes of carbon, which undergo relatively small levels of fractionation during trophic transfer, are used to delineate the flow of

energy through food webs and can be used to identify contributions of different sources of primary production to consumers (DeNiro and Epstein, 1978; Wada et al., 1991). In contrast, stable isotope ratios of nitrogen undergo larger levels of fractionation during trophic transfer and are used to make estimations of trophic position and food chain length (Minagawa and Wada, 1984; Post, 2002).

While the utility of SIA in ecology is well established, correct interpretation of SIA data can be difficult as there are numerous sources of variation unrelated to an organism's diet that can contribute to isotopic variation within a consumer (Boecklen et al., 2011). For instance, because a consumer's isotopic signature is determined by both its trophic position and the isotope value of basal carbon sources, the high isotopic variability of primary producers over fine spatiotemporal scales has been shown to result in variation in higher order consumers that is not reflective of a change in trophic status (Popp et al., 2007).

Traditionally, variation at the base of the food web and its effect on consumer isotope values has been assessed through sampling of both primary producers and first order consumers. However, sampling primary producers over fine spatiotemporal scales is challenging, particularly in vast ecosystems such as the pelagic ocean. Amino acid compound-specific isotope analysis (AA-CSIA) is a promising technique that allows for changes in trophic position to be distinguished from isotopic variation at the base of the food web (Popp et al., 2007; Bradley et al., 2015). The method is based on two groups of individual amino acids which undergo differing levels of ^{15}N enrichment during trophic transfer. Amino acids that undergo minimal ^{15}N enrichment with each trophic step (<1‰) are termed "source" amino acids (e.g., phenylalanine, serine, glycine, lysine, tyrosine) and have been shown to accurately reflect the $\delta^{15}N$ values of primary producers at the base of food webs (McClelland and Montoya, 2002;

Popp et al., 2007; Chikaraishi et al., 2009). Comparatively, "trophic" amino acids (e.g., alanine, aspartic acid, glutamic acid, isoleucine, proline, valine) undergo larger levels of ^{15}N enrichment and can be used to provide estimations of trophic position (McClelland and Montoya, 2002; Chikaraishi et al., 2009). Additionally, because AA-CSIA incorporates both baseline and trophic information, highly accurate trophic position estimates can be made without having to characterize the isotopic values of the primary producers in a food web (Popp et al., 2007; Bradley et al., 2015).

Using a combination of SIA and AA-CSIA, this chapter describes the trophic structure of seven deep-pelagic fishes with similar diets but contrasting vertical distributions inhabiting the Gulf of Mexico (GOM). Specifically, the objectives of this study are threefold:

1) Determine the influence of depth of occurrence and vertical migration on the stable isotope values of species with similar diets

2) Determine to what extent interspecific variation in isotope values is driven by differences in feeding or by isotopic variation at the base of the food web

3) Characterize the extent of spatial (horizontal and vertical) and temporal variation in the isotopic values of primary producers and deep-pelagic micronekton in the GOM.

Methods

Study design and sample collection

This study was conducted as part of a larger collaborative project examining deep-pelagic nekton dynamics in the GOM (DEEPEND Consortium), and I refer readers to detailed descriptions of sampling design and methodologies outlined in Cook et al. (2020), with a brief description of methods as follows. Sample collections for this study took place during four

oceanographic cruises in the GOM in 2015-2016, with cruises conducted in spring (May) and summer (August) of each year. While sampling stations for each of the four cruises fell within the same geographic area, stations visited during each cruise varied due to the changing position of the Loop Current, the dominant oceanographic feature in the GOM (Figure 1). The anticyclonic Loop Current brings warm, oligotrophic water from the Caribbean in through the Yucatan Channel northward into the central GOM before deflecting eastward and then exiting through the Florida Straits. Northward extension of the Loop Current in the GOM is highly variable and introduces significant spatial heterogeneity to the pelagic GOM through the shedding of anticyclonic and cyclonic eddies that often propagate westward, eventually dissipating in the western GOM (Davis et al., 2002). Previous studies have shown that the Loop Current and associated mesoscale eddies can influence primary and secondary production and the spatial distribution of these flora and fauna, which in turn affects the distribution of higher-order consumers such as tunas, billfishes, and marine mammals (Davis et al., 2002; Rooker et al., 2013; Cornic and Rooker, 2018).

In order to examine the influence of the Loop Current on deep-pelagic trophic structure, sampling sites visited during each of the four cruises were classified as either falling within Loop Current water (LCW) or falling within the surrounding water mass, hereafter referred to as Gulf common water (GCW), following designations described by Johnston et al. (2019). In addition to LCW and GCW sites, Johnston et al. (2019) identified sampling sites along the fronts between the Loop Current and Gulf common water masses that exhibited characteristics intermediate to the two water masses. These sites, classified as "mixed" by Johnston et al. (2019), only

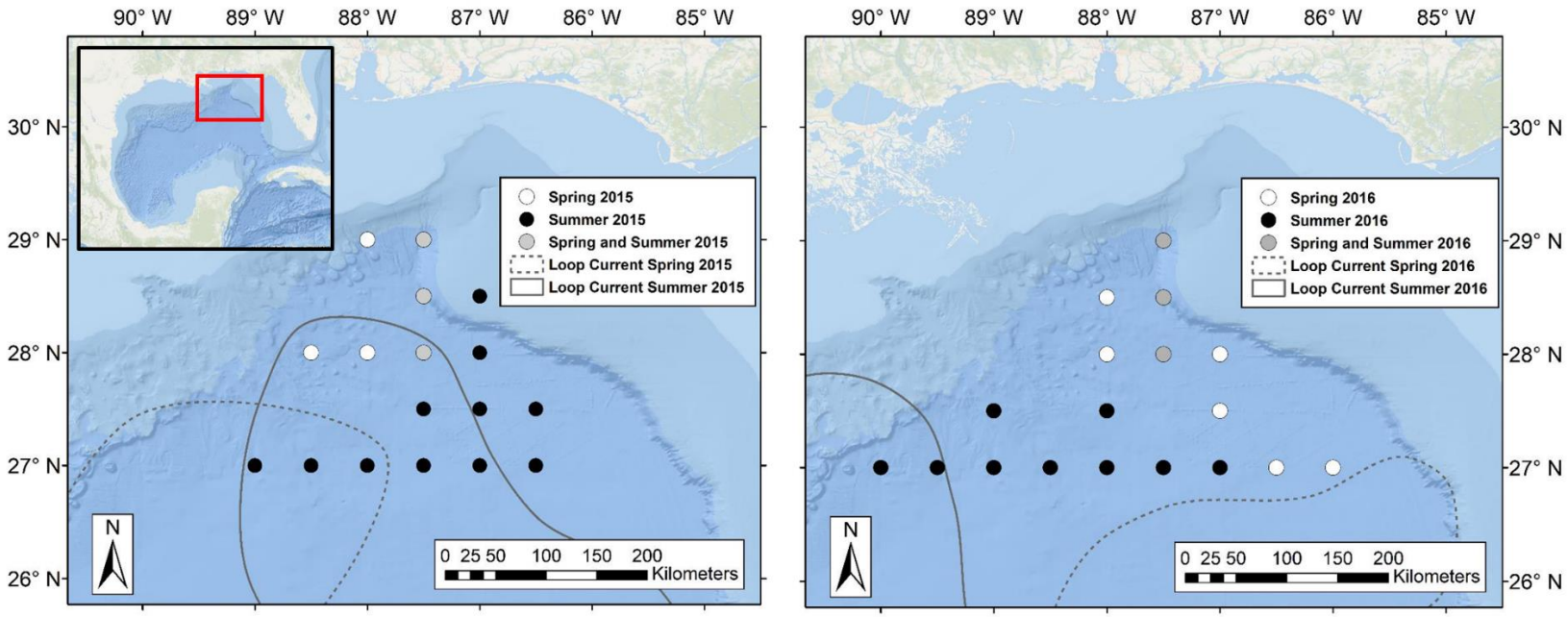

Figure 1. Maps of the northern Gulf of Mexico showing sampling locations. Samples collected in spring depicted as white circles, summer samples depicted as black circles and samples collected in spring and summer depicted as gray circles. Oceanographic cruises conducted in 2015 are shown in left panel and 2016 cruises in right panel. Dashed and solid lines represent approximate location of the Loop Current defined by 20-cm sea surface height anomaly (SSHA) during spring and summer sampling periods, respectively. Loop Current positions were created using remotely sensed sea surface height data available through the Copernicus Marine Environmental Monitoring Service.

represented three stations during sampling for this study and did not yield samples for SIA of fishes.

Micronekton were collected using a multiple opening and closing net with environmental sensing ecosystem (MOCNESS) which sampled discrete depth strata from the surface to 1500 m depth. The depth strata sampled included: 0 - 200 m (epipelagic), 200 - 600 m (upper mesopelagic), 600 - 1000 m (lower mesopelagic), 1000 - 1200 m (upper bathypelagic), and 1200 - 1500 m (lower bathypelagic) (Figure 2) (Milligan et al., 2018; Cook et al., 2020). Micronekton samples selected for SIA were measured to the nearest mm for standard length (SL) and frozen at -20ºC, while samples selected for AA-CSIA were stored in liquid nitrogen before long term storage at -80ºC. For this study, seven ubiquitous species of deep-pelagic fishes with similar diets and contrasting vertical depth distributions were selected for analysis (Figure 2) and included four migratory species (*Benthosema suborbitale*, *Lepidophanes guentheri*, *Melamphaes simus*, *Sigmops elongatus*) and three non-migratory species (*Argyropelecus hemigymnus*, *Cyclothone obscura*, *Sternoptyx pseudobscura*) (Hopkins et al., 1996). By selecting species with similar diets but contrasting vertical distributions and migratory patterns, my aim was to highlight isotopic variation caused by spatial and temporal factors while keeping variation related to diet at a minimum. The seven fish species selected are primarily zooplanktivorous and typically feed on copepods, ostracods, and polychaetes (Hopkins and Baird, 1985; Hopkins et al., 1996), with two species (*S. elongatus* and *S. pseudobscura*) known to undergo ontogenetic shifts in diet towards decapod crustaceans and fishes and occupy slightly higher trophic positions (Hopkins et al., 1996). In order to provide estimations of the isotopic baseline, samples of particulate organic matter (POM) were collected from the surface, epi-, meso-, and bathypelagic zones at each station sampled. Epipelagic and mesopelagic POM samples were collected from

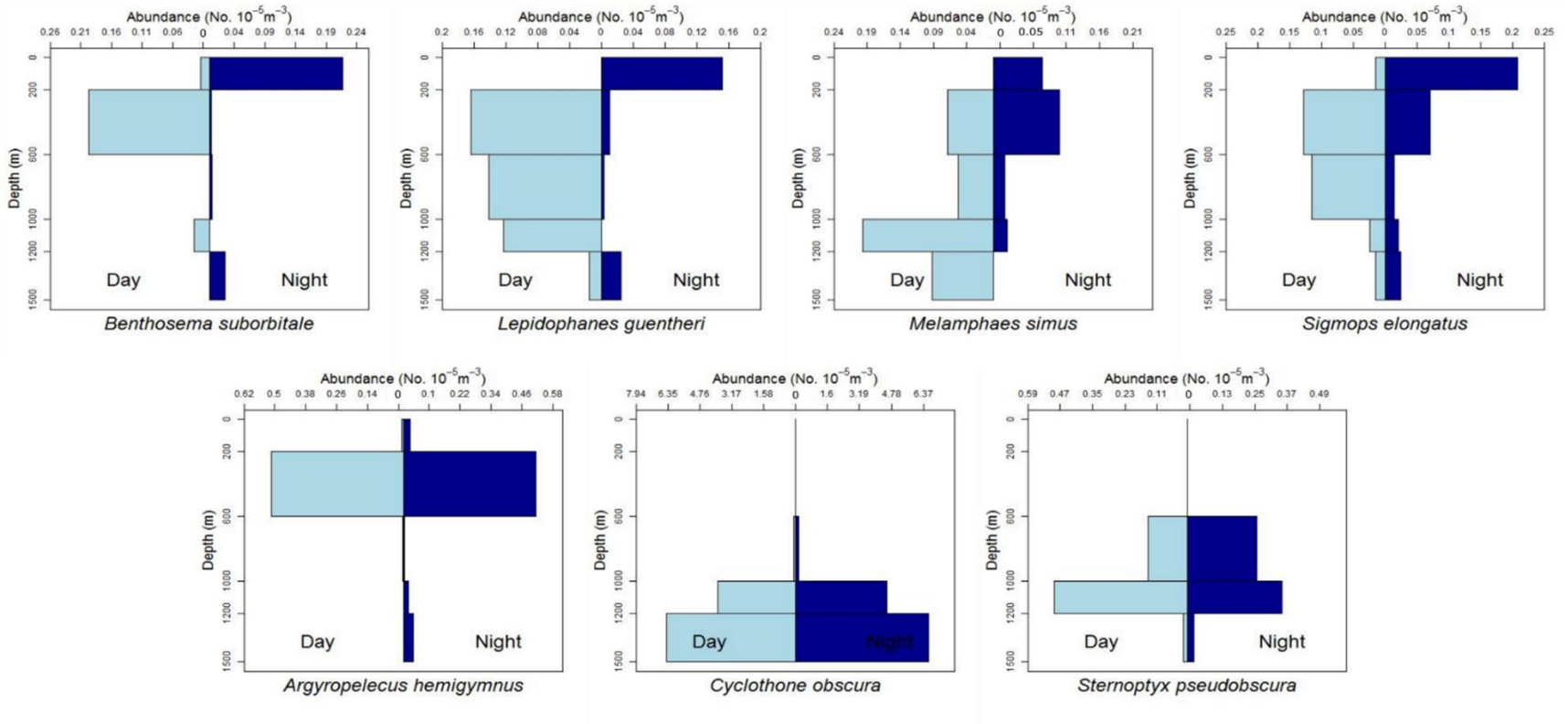

Figure 2. Vertical bar plots representing standardized abundances of migratory (top row) and non-migratory (bottom row) species. Bars represent specific depth bins sampled during day and night MOCNESS tows during four oceanographic cruises in 2015 and 2016. Plots represent catch data for each species combined across all four cruises and not data solely from individuals used for stable isotope analysis. Abundances were standardized by the volume of water filtered during MOCNESS tows as described in Cook et al. (2019).

the deep chlorophyll maximum (mean depth: 76.6 m) and oxygen minimum zone (mean depth: 426.6 m), respectively, while all bathypelagic POM samples were collected from maximum trawl depth (~1500 m). Exact depths for the deep chlorophyll maximum and oxygen minimum varied by station and were visually identified during the downcast of a CTD sensor conducted prior to each MOCNESS deployment. Water collections for POM samples were made using 12-L Niskin bottles attached to the CTD rosette and filtered across pre-combusted (2 h at 450ºC) 47-mm glass microfiber filters (GF/F) with a 0.7 μm pore size and frozen at -20ºC.

Stable isotope analysis

In total, 370 fish samples for SIA were collected with sample totals for each species ranging from 41 to 70 individuals (Table 1). Following collection, white muscle tissue was dissected from the lateral musculature, rinsed with deionized water and examined under a dissecting microscope for the presence of bones. Cleaned samples were then lyophilized, homogenized using a ceramic mortar and pestle, weighed (~1 mg sample) and wrapped in tin capsules. Prior to SIA, samples of POM were placed in a drying oven at 60ºC until a constant weight was achieved (~24 hours) and then folded and wrapped into tin capsules. As with previous studies of deep-pelagic micronekton in the GOM, the C:N of fishes in the present study were low (species mean C:N range 3.32–3.53), suggesting lipids would not significantly confound the interpretation of $\delta^{13}C$ values (McClain-Counts et al., 2017; Richards et al., 2018). Thus, samples were not treated for lipid removal and all statistical analyses were performed on uncorrected $\delta^{13}C$ values. Samples for SIA were analyzed at the University of California at Davis Stable Isotope Facility (UC Davis SIF) using an elemental analyzer (PDZ Europa ANCA-GSL) interfaced with an isotope ratio mass spectrometer (PDZ Europa 20-20). Long-term standard

Table 1. Summary table depicting sample totals of deep-pelagic fishes for each sampling year and each water type (LCW: Loop Current Water; GCW: Gulf Common Water) and mean (± *SD*) $\delta^{13}C$, $\delta^{15}N$, and C:N values for each species. Median nighttime depth distribution data were determined using depth data for adult life stages and excluded depth data for non-migratory juvenile stages. Depth data were derived from primary literature sources which incorporated finer scale depth stratified sampling (50 – 100 m depth bins) to allow for more accurate estimations of depth of occurrence. Depth references for species: *B. suborbitale* and *L. guentheri*: (Gartner, 1987), *M. simus*: (Sutton et al., 2017a), *S. elongatus*: (Lancraft et al., 1998), *A. hemigymnus* and *S. pseudobscura*: (Hopkins and Baird, 1985), *C. obscura*: (McEachran and Fechhelm, 1985)

Species	Median nighttime depth (m)	n	2015 LCW	2015 GCW	2016 LCW	2016 GCW	SL range (mm)	$\delta^{13}C$ (‰)	$\delta^{15}N$ (‰)	C:N
Migrators										
B. suborbitale	80	63	4	17	4	38	16 - 31	-19.41 ± 0.40	8.05 ± 0.74	3.40 ± 0.70
L. guentheri	80	48	6	17	4	21	21 - 66	-19.10 ± 0.46	7.18 ± 0.94	3.38 ± 0.23
M. simus	300	45	8	9	4	24	14 - 27	-19.58 ± 0.48	8.94 ± 0.95	3.44 ± 0.06
S. elongatus	175	70	11	17	10	32	49 - 196	-19.05 ± 0.45	8.70 ± 0.70	3.34 ± 0.05
Non-migrators										
A. hemigymnus	400	41	8	11	7	15	16 - 37	-18.75 ± 0.45	8.87 ± 0.63	3.40 ± 0.10
C. obscura	1950	61	2	16	9	34	28 - 51	-18.29 ± 0.40	10.61 ± 0.74	3.32 ± 0.05
S. pseudobscura	850	41	1	13	4	23	14 - 46	-19.85 ± 0.29	8.27 ± 0.56	3.53 ± 0.07

deviation for instrumentation precision at the UC Davis SIF for SIA is 0.2‰ and 0.3‰ for $\delta^{13}C$ and $\delta^{15}N$, respectively. Isotopic ratios are presented in delta notation relative to the international standards VPDB (Vienna PeeDee Belemnite) and air for carbon and nitrogen, respectively.

A total of 37 samples (species totals: 4-6) were analyzed for AA-CSIA at the UC Davis SIF. Sample dissection and preparation for AA-CSIA followed a similar protocol to SIA except a larger amount of tissue (~3 mg) was dissected, lyophilized, homogenized and stored in 2-ml glass dram vials prior to sample submission. Sample preparation for AA-CSIA at UC Davis SIF followed protocols outlined in (Yarnes and Herszage, 2017). Briefly, dried and homogenized samples were hydrolyzed with 6M HCl in order to isolate amino acids from other compounds before derivatization using esterification-acetylation to yield N-acetyl isopropyl esters prior to gas chromatograph (GC) analysis. The nitrogen isotope compositions of the resulting N-acetyl amino acid isopropyl esters were determined using a gas chromatograph (Thermo Trace GC 1310) coupled to an isotope-ratio mass spectrometer (Thermo Scientific Delta V Advantage IRMS) via a GC IsoLink II combustion interface. Samples were injected into a DB-1301 (Agilent Technologies) column (60 m x 0.25 mm x 1.0 µm film) at a temperature of 255°C (splitless, 1 min.) under a constant flow rate of 1.2 mL/min (Yarnes and Herszage, 2017). During analysis, all samples were analyzed in duplicate with triplicate measurements made if the average standard deviation of duplicate samples exceeded ± 1‰ (Yarnes and Herszage, 2017). Norleucine was used as an internal standard during analysis, while two amino acid compounds developed by the UC Davis SIF were co-measured during analysis of fish samples and were used for calibration and normalization of amino acid data. Standard deviation for all amino acids averaged ± 0.38‰. The $\delta^{15}N_{source\ AA}$ for each species is presented as the weighted mean of the four source amino acids phenylalanine, lysine, glycine and serine while $\delta^{15}N_{Trophic\ AA}$ represents

the weighted mean of the three trophic amino acids alanine, leucine, and glutamic acid (Bradley et al., 2015; Gloeckler et al., 2018). Both source and trophic amino acids were weighted by the standard deviation of each amino acid (Bradley et al., 2015; Gloeckler et al., 2018).

Data analysis

Interspecific differences in the $\delta^{13}C$ and $\delta^{15}N$ values of POM and fishes were examined using a three-factor multivariate analysis of variance (MANOVA) with $\delta^{13}C$ and $\delta^{15}N$ included as dependent variables and species, sampling year (2015, 2016), and water type (LCW, GCW) as independent variables. Any interactions between independent variables found to be non-significant were removed from the final model. Following MANOVA, univariate tests for $\delta^{13}C$ and $\delta^{15}N$ were performed using analysis of variance (ANOVA) to test for interspecific differences with POM, species, sampling year, and water type included as independent variables. Intraspecific variation of each species was explored using ordinary least squares regression to characterize the relationship between standard length (SL) and $\delta^{13}C$ and $\delta^{15}N$. For species with statistically significant relationships between standard length and $\delta^{13}C$ and $\delta^{15}N$, length was used as a covariate in univariate analysis of covariance (ANCOVA) models used to assess the effects of sampling year and water type on each isotope. Variation in POM $\delta^{13}C$ and $\delta^{15}N$ within each depth zone was assessed using ANCOVA with sampling year and water type included as independent variables. Following ANOVA/ANCOVA, *a posteriori* differences among means were analyzed using Shaffer's multiple comparison procedure (Shaffer's MCP), as it is less affected by unbalanced sample sizes relative to other post-hoc tests while controlling the familywise error rate (Shaffer, 1986). All statistical analyses were performed in R using the multcomp package (R version 3.6.0).

Trophic position estimates

Trophic position (TP) estimates were made using both SIA and AA-CSIA data. TP estimations using SIA followed Equation 1 where $\delta^{15}N_i$ represents the nitrogen signature of an individual, $\delta^{15}N_{base}$ represents the nitrogen signature of the pyrosome, *Pyrosoma atlanticum*, and TEF (trophic enrichment factor) represents the enrichment of ^{15}N with each trophic step (3.15‰ following Valls et al., 2014). Primary consumers are useful when setting isotopic baselines because their slower tissue turnover rates and longer generation times allow for the integration of isotopic baselines over broader spatiotemporal scales (Post, 2002). Pyrosomes are filter feeding pelagic tunicates known to feed on POM and have been used as model primary consumers in several studies examining pelagic food web structure (Cherel et al., 2008; Menard et al., 2014). The utility of pyrosomes to characterize isotopic baselines is enhanced in regions such as the GOM which are characterized by relatively low chlorophyll *α* concentrations and phytoplankton communities dominated by small flagellates rather than diatoms which have been shown to be unassimilated during pyrosome feeding (Harbou et al., 2011; Pakhomov et al., 2019). The mean $\delta^{13}C$ (-22.40 ± 0.63) and $\delta^{15}N$ (3.15 ± 0.92) values of 22 *P. atlanticum* collected during this study were higher than the $\delta^{13}C$ and $\delta^{15}N$ values of epipelagic POM suggesting pyrosomes are suitable for setting an isotopic baseline in the pelagic GOM.

$$\text{Equation 1:} \quad TP_{SIA} = \frac{\delta^{15}N_i - \delta^{15}N_{base}}{TEF} + 1$$

TP estimations made using AA-CSIA followed equation 2. In the equation, $\delta^{15}N_{Tr\text{-}AA}$ represents the weighted mean of the three trophic amino acids alanine, leucine, and glutamic acid and $\delta^{15}N_{Src\text{-}AA}$ the weighted mean of three source amino acids glycine, lysine, and phenylalanine

(Bradley et al., 2015; Gloeckler et al. 2018). The terms β, which represents the difference in $\delta^{15}N$ values of trophic and source amino acids of primary producers, and $TEF_{Tr\text{-}Src}$, which represents the average isotopic enrichment between trophic and source amino acids in consumers, were set to 3.6‰ and 5.7‰, respectively, following Bradley et al. (2015).

Equation 2: $$TP_{Tr\text{-}Src} = \frac{\delta^{15}N_{Tr-AA} - \delta^{15}N_{Src-AA} - \beta}{TEF_{Tr-Src}} + 1$$

Results

Particulate organic matter stable isotope analysis

Isotopic values of POM differed significantly among depth zones with epipelagic POM displaying lower $\delta^{13}C$ and $\delta^{15}N$ values relative to meso- and bathypelagic POM. Within each depth zone, isotope values of POM were variable, with individual POM $\delta^{13}C$ values ranged from 4.0‰ in the bathypelagic to 6.69‰ in surface samples. Similarly, individual POM $\delta^{15}N$ values spanned a minimum of 4.25‰ in the mesopelagic and varied by as much as 6.7‰ in the epipelagic zone. Mean $\delta^{13}C$ values of POM were lowest in the epipelagic zone (-24.82 ± 1.49) and highest in the mesopelagic zone (-22.01 ± 1.57), while surface (-23.11 ± 1.46) and bathypelagic (-23.62 ± 1.22) samples were intermediate (Table 2, Figure 3A).

POM $\delta^{13}C$ differed among depth zones (ANOVA: $F_{3,63} = 17.10$, $p < 0.001$), with differences among zones changing between years (ANOVA: $F_{3,63} = 0.08$, $p < 0.001$), but remaining similar between LCW and GCW water types (ANOVA: $F_{3,63} = 1.82$, $p = 0.15$). In 2015, bathypelagic $\delta^{13}C$ values were lower than all other depth zones, but only significantly different from surface samples ($p < 0.01$, Shaffer's MCP). In 2016, $\delta^{13}C$ values of POM significantly differed among all depth zones ($p < 0.01$, Shaffer's MCP for each) except for

Table 2. Summary table depicting sample totals of particulate organic matter for each sampling period and mean (± *SD*) $\delta^{13}C$, $\delta^{15}N$, and C:N values for each depth zone.

Depth Zone	n	2015 LCW	2015 GCW	2016 LCW	2016 GCW	$\delta^{13}C$ (‰)	$\delta^{15}N$ (‰)
Surface (0-3 m)	20	4	1	2	13	-23.11 ± 1.46	2.54 ± 1.74
Epipelagic (~76.6 m)	24	4	6	2	12	-24.82 ± 1.49	2.87 ± 1.67
Mesopelagic (~426.6 m)	17	2	2	1	12	-22.01 ± 1.57	6.05 ± 1.15
Bathypelagic (~1500 m)	14	0	2	1	11	-23.62 ± 1.22	4.76 ± 1.75

samples collected from the surface and bathypelagic ($p = 0.91$, Shaffer's MCP). Differences in POM $\delta^{15}N$ values among depth zones were significant (ANOVA: $F_{3,63} = 20.11$, $p < 0.001$) but differences among zones did not change between water types (ANOVA: $F_{3,63} = 2.582$, $p = 0.07$) or sampling years (ANOVA: $F_{3,63} = 0.06$, $p = 0.98$). Among depth zones, POM $\delta^{15}N$ values from the surface (2.54 ± 1.74) and epipelagic (2.87 ± 1.67) were similar to one another ($p > 0.05$, Shaffer's MCP), but significantly lower than samples from the meso- (6.05 ± 1.15) and bathypelagic (4.76 ± 1.75) ($p < 0.05$, Shaffer's MCP for each) (Table 2, Figure 3A).

Within each depth zone, the influence of sampling year and water type on POM isotope values differed between $\delta^{13}C$ and $\delta^{15}N$. Differences between sampling years were only observed in $\delta^{13}C$ data, while differences between water types only occurred in $\delta^{15}N$ data (Table 3). Significant interannual differences in $\delta^{13}C$ values occurred in all depth zones, with surface and epipelagic POM $\delta^{13}C$ values higher in 2015 relative to 2016, while meso- and bathypelagic samples were higher in 2016 relative to 2015 ($p < 0.05$, Shaffer's MCP for each). Mean $\delta^{15}N$ values from surface and epipelagic samples were lower in LCW relative to samples collected from GCW ($p < 0.05$, Shaffer's MCP for each). No differences in $\delta^{13}C$ and $\delta^{15}N$ values were observed between water types in meso- or bathypelagic samples (Table 3).

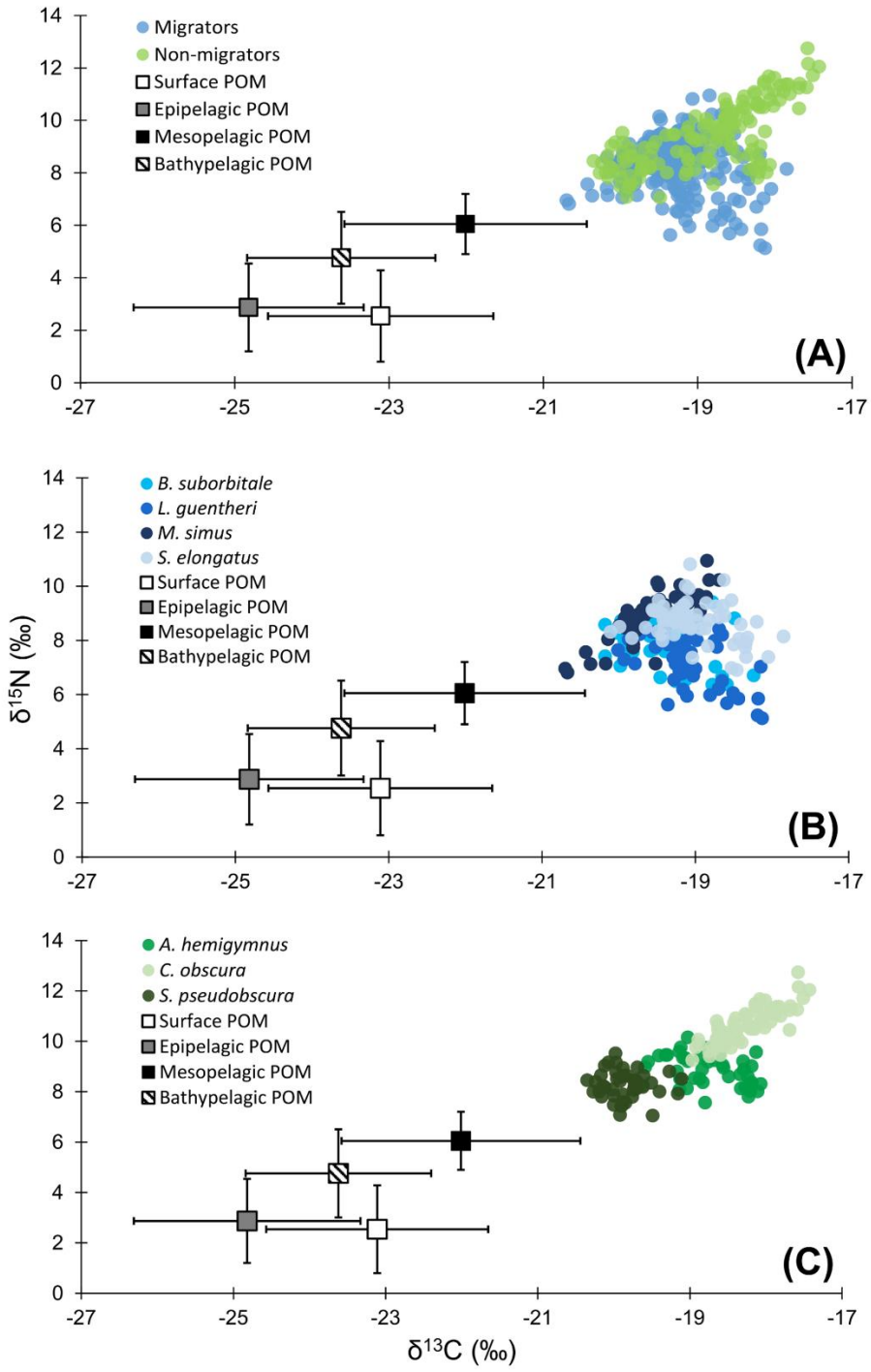

Figure 3. Isotope bi-plot of mean (± *SD*) $\delta^{13}C$ and $\delta^{15}N$ values for particulate organic matter (squares) and individual $\delta^{13}C$ and $\delta^{15}N$ values for all vertically migrating (blue circles) and non-migrating (green circles) fish species. (B) Individual $\delta^{13}C$ and $\delta^{15}N$ values of vertically migrating species. (C) Individual $\delta^{13}C$ and $\delta^{15}N$ values of non-migrating species.

Table 3. Mean (± SD) $\delta^{13}C$ and $\delta^{15}N$ stable isotope ratios of particulate organic matter from both sampling years (2015/2016), and water types (Loop Current/Common Water). Values in bold represent significant differences identified during post hoc pairwise comparisons of means using Shaffer's multiple comparison procedure.

	$\delta^{13}C$ (‰)	$\delta^{15}N$ (‰)
Surface		
Year (2015/2016)	**-22.18 ± 0.43/**	1.20 ± 1.48/
	-23.42 ± 1.56	2.99 ± 1.63
Water Type (Loop/Common)	-23.22 ± 2.42/	**0.83 ± 1.09/**
	-23.06 ± 0.92	**3.27 ± 1.43**
Epipelagic		
Year (2015/2016)	**-23.94 ± 0.85/**	2.21 ± 1.34/
	-25.45 ± 1.55	3.34 ± 1.76
Water Type (Loop/Common)	-24. 95 ± 1.99/	**1.37 ± 0.77/**
	-24.78 ± 1.35	**3.37 ± 1.59**
Mesopelagic		
Year (2015/2016)	**-23.20 ± 1.43/**	5.96 ± 1.79/
	-21.64 ± 1.47	6.08 ± 0.98
Water Type (Loop/Common)	-21.91 ± 1.17/	6.39 ± 2.21/
	-22.03 ± 1.68	5.98 ± 0.92
Bathypelagic		
Year (2015/2016)	**-25.20 ± 0.28/**	4.18 ± 1.22/
	-23.36 ± 1.10	4.86 ± 1.85
Water Type (Loop/Common)	-24.79 ± NA/	6.07 ± NA/
	-23.53 ± 1.22	4.66 ± 1.78

Deep-pelagic fish stable isotope analysis

$\delta^{13}C$ and $\delta^{15}N$ values of the seven species of deep-pelagic fishes examined displayed considerable variation between migratory and non-migratory taxa. Mean $\delta^{13}C$ values of non-migratory fishes were more variable (range: 1.56‰) than migratory species (range: 0.53‰) (Figure 3A). The non-migratory *S. pseudobscura* (-19.85 ± 0.29) and non-migratory *C. obscura* (-18.29 ± 0.40) displayed the lowest and highest mean $\delta^{13}C$ values, respectively, with all migratory species and *A. hemigymnus* displayed intermediate values (Table 1, Figure 3B). The $\delta^{13}C$ values of migratory species overlapped considerably suggesting these species rely on production from a similar region within the water column, most likely the epi- and upper mesopelagic (Figure 3B). Considered separately, $\delta^{13}C$ values of non-migratory species were

almost completely separated in isotope space from one another and displayed a pattern of enrichment that echoed the pattern observed in POM $\delta^{13}C$ (Figure 3C). Fish $\delta^{13}C$ values differed significantly among species (ANOVA: $F_{6,353} = 92.58$, $p < 0.001$), with interspecific relationships varying between GCW and LCW (ANOVA: $F_{6,353} = 5.37$, $p < 0.001$). In GCW, interspecific differences were driven by high $\delta^{13}C$ values in C. *obscura* and low values in *S. pseudobscura*, with the four migratory species and the non-migratory *A. hemigymnus* displaying intermediate $\delta^{13}C$ values (Figure 4A).

Interspecific differences for $\delta^{13}C$ in LCW differed slightly due to higher $\delta^{13}C$ values in *A. hemigymnus, B. suborbitale, L. guentheri*, and *S. elongatus* relative to samples from GCW which resulted in $\delta^{13}C$ values similar to those of the non-migratory *C. obscura* (Figure 4A). Fish $\delta^{15}N$ values spanned 7.62‰, with mean $\delta^{15}N$ values of non-migratory fishes encompassing a wider range (2.34‰) than migratory species (1.76‰). The $\delta^{15}N$ values of fishes differed significantly among species (ANOVA: $F_{6,354} = 129.53$, $p < 0.001$), with interspecific differences varying between GCW and LCW (ANOVA: $F_{6,354} = 7.97$, $p < 0.001$). In both water types, differences among species were primarily driven by high $\delta^{15}N$ values in *C. obscura* and low values in *L. guentheri* and *B. suborbitale* (Figure 4B), while the migratory *M. simus*, *S. elongatus* and the non-migratory *A. hemigymnus* and *S. pseudobscura* were characterized by intermediate $\delta^{15}N$ values (Figure 4B).

Standard length was significantly correlated with $\delta^{13}C$ and $\delta^{15}N$ values in both migratory and non-migratory fishes. Specifically, statistically significant positive relationships between $\delta^{13}C$ and standard length were observed in the migratory *L. guentheri* ($p < 0.05$; $R^2 = 0.11$), *S.*

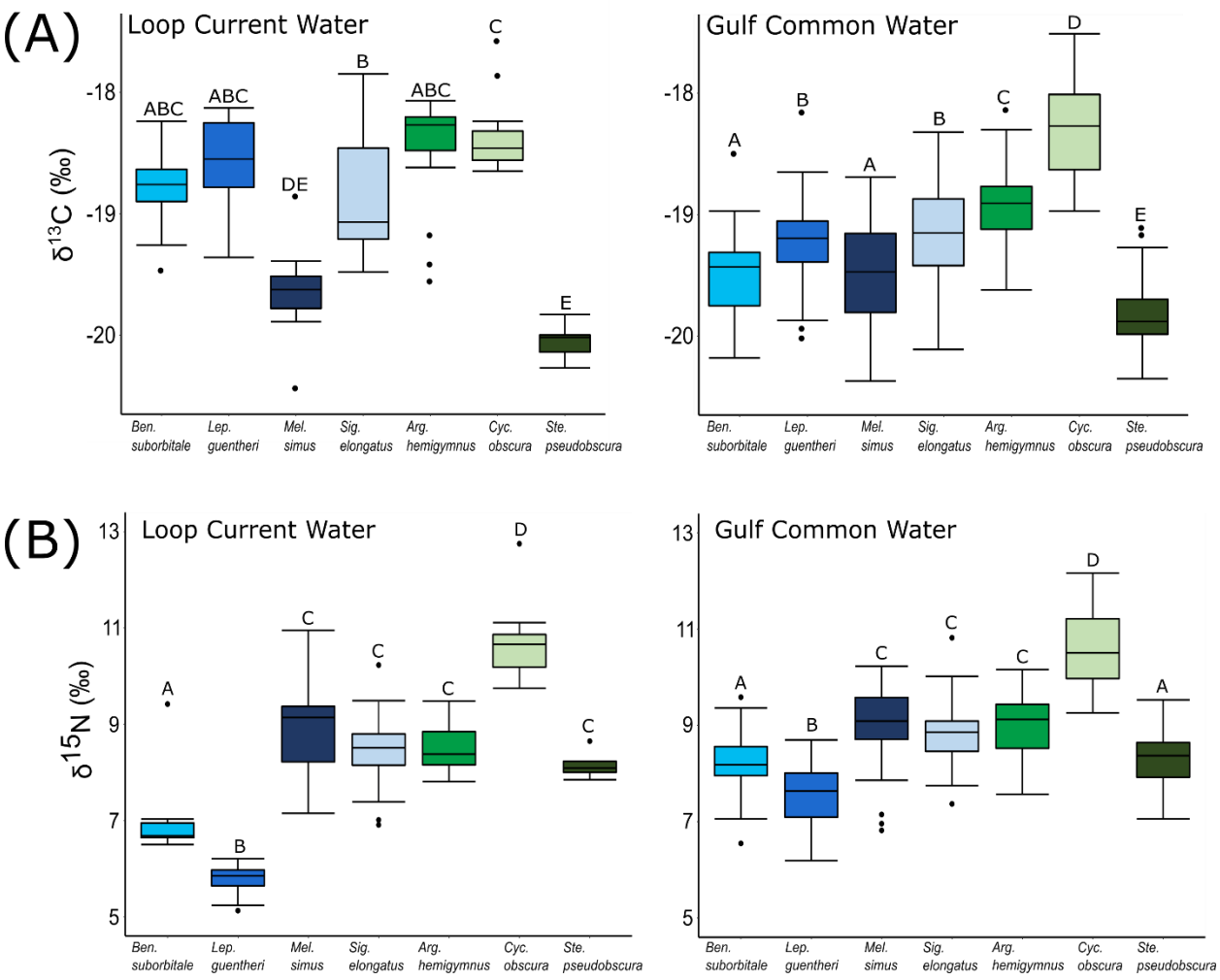

Figure 4. Boxplots depicting interspecific differences in (A) $\delta^{13}C$ values and (B) $\delta^{15}N$ values for migratory (blue shades) and non-migratory (green shades) deep-pelagic fishes collected in Loop Current water and Gulf common water. Boxes represent 25th%, 50th% and 75th% percentile, while whisker lengths represent 1.5*interquartile range. Outliers (filled circles) are observations falling beyond the range defined by the whiskers. Differing letters among species denote significant differences identified during *post hoc* pairwise comparisons of means.

elongatus ($p < 0.001$; $R^2 = 0.15$), and *M. simus* ($p < 0.001$; $R^2 = 0.40$) and in the non-migratory *C. obscura* ($p < 0.001$; $R^2 = 0.25$). Similarly, significant positive relationships between standard length and $\delta^{15}N$ were observed for all migratory species: *L. guentheri* ($p < 0.001$; $R^2 = 0.43$), *S.*

elongatus ($p < 0.001$; $R^2 = 0.23$), *M. simus* ($p < 0.001$; $R^2 = 0.73$), *B. suborbitale* ($p < 0.01$; $R^2 = 0.12$) and for the non-migratory *C. obscura* ($p < 0.01$; $R^2 = 0.15$). Results of subsequent ANCOVA indicated the effect of sampling year and water type on $\delta^{13}C$ and $\delta^{15}N$ varied by species with no consistencies between migrators and non-migrators (Table 4). Intraspecific interannual variability was minimal, with no statistical differences in $\delta^{13}C$ observed between sampling years and interannual differences in $\delta^{15}N$ only occurring in the migratory *L. guentheri* and non-migratory *A. hemigymnus* and *S. pseudobscura* ($p < 0.05$, Shaffer's MCP for each). The effect of water type was more pronounced, with the migratory *B. suborbitale*, *L. guentheri*, and *S. elongatus*, and the non-migratory *A. hemigymnus* possessing significantly higher $\delta^{13}C$ and lower $\delta^{15}N$ values in LCW relative to GCW ($p < 0.05$, Shaffer's MCP for each) (Table 4, Figure 4).

Compound specific isotope analysis and trophic position estimates

Mean $\delta^{15}N_{sourceAA}$ values of fishes echoed patterns in $\delta^{15}N$ values, with the migratory *L. guentheri* (-0.15 ± 0.80) and *B. suborbitale* (0.91 ± 1.34) displaying the lowest mean $\delta^{15}N_{sourceAA}$ values and the non-migratory and deepest dwelling *C. obscura* (5.00 ± 1.58) displaying the highest values of $\delta^{15}N_{sourceAA}$. The migratory *M. simus* (1.29 ± 2.10), *S. elongatus* (1.93 ± 1.12), non-migratory *A. hemigymnus* (2.49 ± 2.01) and *S. pseudobscura* (1.94 ± 1.76) had similar $\delta^{15}N_{sourceAA}$ values that all fell between the end members of *L. guentheri* and *C. obscura*. Significant positive linear relationships were observed between bulk $\delta^{15}N$ values and $\delta^{15}N_{sourceAA}$ values ($p < 0.01$; $R^2 = 0.90$) (Figure 5A) and between mean $\delta^{15}N_{sourceAA}$ values and median nighttime depth ($p < 0.05$; $R^2 = 0.81$), providing further evidence supporting the idea that interspecific isotopic variation is caused by differing use of isotopically distinct baselines (Figure

Table 4. Mean (± *SD*) $\delta^{13}C$ and $\delta^{15}N$ stable isotope ratios of deep-pelagic fishes from both sampling years (2015/2016), and water types (Loop Current/Common Water). Values in bold represent significant differences identified during *post hoc* pairwise comparisons of means using Shaffer's multiple comparison procedure.

	$\delta^{13}C$ (‰)	$\delta^{15}N$ (‰)
B. suborbital		
Year (2015/2016)	-19.42 ± 0.58/	7.94 ± 0.92/
	-19.41 ± 0.27	8.11 ± 0.64
Water Type (Loop/Common)	**-18.13 ± 0.38/**	**6.96 ± 1.12/**
	-19.50 ± 0.32	**8.21 ± 0.55**
L. guentheri		
Year (2015/2016	-18.99 ± 0.62/	**6.95 ± 0.91/**
	19.18 ± 0.25	**7.39 ± 0.92**
Water Type (Loop/Common)	**-18.60 ± 0.41/**	**5.76 ± 0.35/**
	-19.22 ± 0.39	**7.56 ± 0.62**
M. simus		
Year (2015/2016)	-19.56 ± 0.28/	8.92 ± 0.66/
	-19.58 ± 0.57	8.96 ± 1.10
Water Type (Loop/Common)	-19.64 ± 0.37/	8.92 ± 1.08/
	-19.56 ± 0.51	8.95 ± 0.92
S. elongatus		
Year (2015/2016)	-19.00 ± 0.54/	8.48 ± 0.88/
	-19.08 ± 0.38	8.85 ± 0.50
Water Type (Loop/Common)	**-18.86 ± 0.49/**	**8.43 ± 0.80/**
	-19.13 ± 0.41	**8.82 ± 0.62**
A. hemigymnus		
Year (2015/2016)	-18.67 ± 0.40/	**8.64 ± 0.61/**
	-18.83 ± 0.49	**9.11 ± 0.56**
Water Type (Loop/Common)	**-18.48 ± 0.48/**	**8.55 ± 0.52/**
	-18.92 ± 0.35	**9.01 ± 0.63**
C. obscura		
Year (2015/2016)	-18.36 ± 0.42/	10.42 ± 0.69/
	-18.26 ± 0.39	10.68 ± 0.75
Water Type (Loop/Common)	-18.35 ± 0.33/	10.67 ± 0.81/
	-18.27 ± 0.41	10.59 ± 0.73
S. pseudobscura		
Year (2015/2016)	-19.73 ± 0.30/	**8.57 ± 0.60/**
	-19.91 ± 0.27	**8.12 ± 0.48**
Water Type (Loop/Common)	-20.05 ± 0.16/	8.16 ± 0.30/
	-19.82 ± 0.29	8.29 ± 0.59

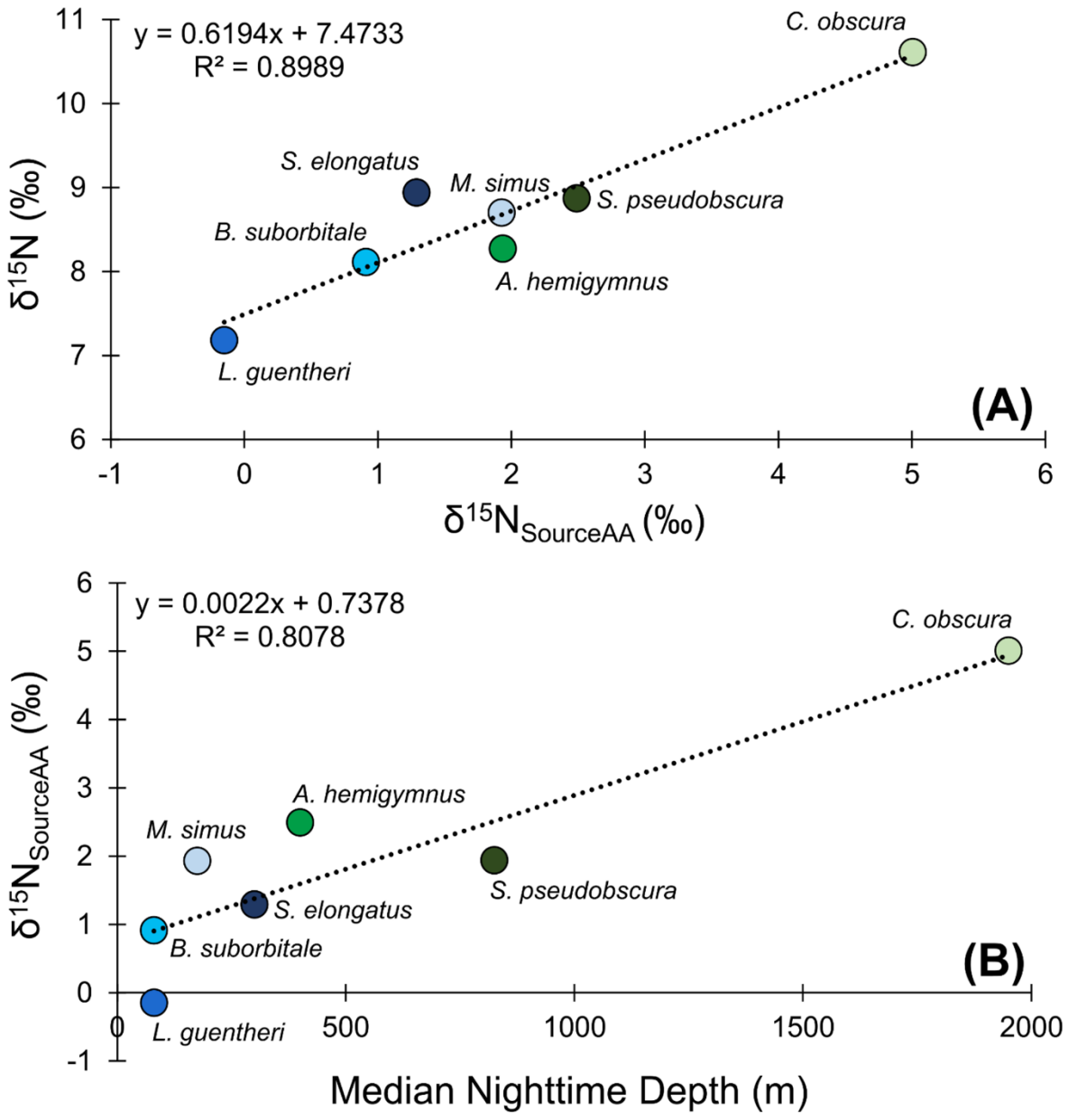

Figure 5. Mean (± *SE*) bulk tissue $\delta^{15}N$ values of deep-pelagic fishes as a function of mean (± SE) $\delta^{15}N_{SourceAA}$ values (A). Mean (± *SE*) $\delta^{15}N_{SourceAA}$ values as a function of median nighttime depth of occurrence (B). Blue circles represent vertical migrators and green circles represent non-migrators.

5B). Mean TP_{SIA} estimates spanned 1.09 trophic levels with all species except *C. obscura* placed between the third and fourth trophic level (Table 5). Comparatively, $TP_{AA\text{-}CSIA}$ estimates exhibited a narrower range of 0.62 trophic levels and placed all species between the third and fourth trophic level. Differences in mean TP estimates between the two methods varied by species with close agreement between estimates for *S. pseudobscura*, *L. guentheri*, and *M. simus* but a relatively large disparity in *C. obscura*, with $TP_{AA\text{-}CSIA}$ estimates (3.47 ± 0.26) 0.9 TLs lower than TP_{SIA} estimates (4.37 ± 0.24) (Table 5).

Table 5. Comparison of mean (± *SD*) trophic position estimates for each fish species created using bulk SIA and AA-CSIA.

Species	TP: Bulk	TP: AA-CSIA
Migrators		
B. suborbitale	3.56 ± 0.24	3.11 ± 0.22
L. guentheri	3.28 ± 0.30	3.38 ± 0.22
M. simus	3.84 ± 0.30	3.73 ± 0.35
S. elongatus	3.76 ± 0.22	3.44 ± 0.29
Non-migrators		
A. hemigymnus	3.82 ± 0.20	3.38 ± 0.36
C. obscura	4.37 ± 0.24	3.47 ± 0.26
S. pseudobscura	3.63 ± 0.18	3.61 ± 0.41

Discussion

Variation in particulate organic matter stable isotope signatures

The isotopic values of POM varied considerably among and within the vertical depth zones of the northern GOM. The high level of variation in POM is consistent with previous studies in the northern GOM that documented POM values spanning 6-10‰ and 5-13‰ for $\delta^{13}C$ and $\delta^{15}N$, respectively, for similar depths (Fernandez-Carrera et al., 2016). Despite the high degree of variation, differences in POM $\delta^{13}C$ and $\delta^{15}N$ values among depth zones, and a general

pattern of enrichment among the epipelagic, meso-, and bathypelagic zones was observed. It should be noted, however, that the trend of enrichment was not perfectly correlated with depth, as mesopelagic POM $\delta^{13}C$ and $\delta^{15}N$ values were higher relative to bathypelagic samples. The observed enrichment in ^{15}N between the epipelagic zone and deep pelagic (> 200 m) POM samples is consistent with previous studies which have shown meso- and bathypelagic $\delta^{15}N$ values to be 3-10‰ higher than in the epipelagic (Altabet, 1988; Hannides et al., 2013; Ferrnandez-Correra et al., 2016). However, at deeper depths, the steady pattern of ^{15}N enrichment with increasing depth does not continue, with $\delta^{15}N$ values of POM remaining constant from the mesopelagic to bathypelagic (Altabet et al., 1991; Emeis et al., 2010; Ferrnandez-Carrera et al., 2016). Thus, it is interesting to note that I observed relatively low POM $\delta^{15}N$ values in bathypelagic samples relative to samples from the mesopelagic. Due to the high level of isotopic variation in POM documented in previous studies, lower POM $\delta^{15}N$ values in bathypelagic may be an artifact of sampling, as the mean values reported for both zones are well within the wide range of values previously reported (Ferrnandez-Correra et al., 2016). The high level of isotopic variation of POM documented by this and previous studies underscores both the need to delineate isotopic baselines when conducting isotope studies in the pelagic realm and the potential utility of AA-CSIA in accounting for highly variable isotopic baselines.

Isotopic enrichment of POM with depth, particularly regarding ^{15}N, has been demonstrated in pelagic ecosystems throughout the world's oceans and is attributed to microbial degradation as POM sinks through the water column (Altabet, 1988; Mintenbeck et al., 2007; Hannides et al. 2013). During microbial reworking, bonds containing ^{14}N are preferentially broken leaving the residual material isotopically heavier and isotopically distinct from newly formed particles in the epipelagic (Mintenbeck et al., 2007; Hannides et al., 2013). Additionally,

as POM sinks, microbial activity and disturbance from zooplankton swimming and feeding enhances physical degradation resulting in different size fractions that vary from large (> 53 µm), fast sinking particles to small (0.7-53 µm), suspended particles (Altabet, 1988; Gloeckler et al., 2018). SIA and AA-CSIA of different size classes of POM have shown small suspended particles at depths >200 m to have $\delta^{15}N$ and $\delta^{15}N_{sourceAA}$ values that are enriched relative to large particles. Large particles, which are subjected to less microbial activity and isotopic change due to increased sinking rates, do display a pattern of enrichment from epi- to mesopelagic depths, but remain ^{15}N depleted relative to small, suspended particles throughout the water column (Hannides et al., 2013, Gloeckler et al., 2018). The recent descriptions of size fractions of POM with distinct $\delta^{15}N$ and $\delta^{15}N_{sourceAA}$ values provide important context to the observed vertical variation in POM samples, as it suggests variation among higher-order consumers could reflect variation at the base of the food web and may not be reflective of changes in trophic status.

Variation in deep-pelagic fish stable isotope signatures

The isotopic values of deep-pelagic fishes differed significantly among species, with interspecific variation appearing to be depth-related and similar to patterns documented in the isotopic values of POM. The $\delta^{13}C$ values of migratory species, which overlapped broadly with one another, are suggestive of shared reliance on recently formed primary production within the epipelagic characterized by depleted $\delta^{13}C$ and $\delta^{15}N$ values. Despite interspecific differences in day and nighttime depth distributions, no discernable patterns between depth of occurrence and $\delta^{13}C$ values were evident in the migratory species examined. Variation in $\delta^{13}C$ was more evident in non-migratory species, with minimal isotopic overlap among species and significantly different mean $\delta^{13}C$ values between each species in GCW. The pattern of ^{13}C enrichment within

non-migratory species is interesting as it did not perfectly align with vertical distributions due to lower $\delta^{13}C$ values in *S. pseudobscura* relative to the upper mesopelagic dwelling *A. hemigymnus*. The low $\delta^{13}C$ values in *S. pseudobscura*, which overlapped broadly with $\delta^{13}C$ values of the migratory *B. suborbitale* and *L. guentheri*, suggests *S. pseudobscura* uses food webs supported by production derived in the epipelagic despite a depth of distribution that centers below 700 m (see discussion below). By contrast, higher $\delta^{13}C$ values in *A. hemigymnus* and *C. obscura* relative to all migratory species and *S. pseudobscura*, suggest that both species may feed within food webs supported by POM with higher $\delta^{13}C$ values within the meso- and bathypelagic.

Depth-driven variation in micronekton $\delta^{15}N$ values has been observed in deep-pelagic assemblages in the Atlantic Ocean (Parzanini et al., 2017), Pacific Ocean (Gloeckler et al., 2018; Romero et al., 2019), and Mediterranean Sea (Valls et al., 2014). Similarly, our data suggest that depth is an important factor influencing $\delta^{15}N$ values for deep-pelagic fishes in the GOM. Non-migratory species exhibited a wider range of mean $\delta^{15}N$ values (2.34‰) relative to migratory species (1.76‰), although interspecific differences in $\delta^{15}N$ suggest depth-driven variation was present in both groups. For example, *B. suborbitale* and *L. guentheri,* which have epipelagic nighttime distributions, displayed lower $\delta^{15}N$ values relative to *S. elongatus* and *M. simus* and the non-migratory *A. hemigymnus,* which have nighttime distributions in the mesopelagic zone. Additionally, the highest $\delta^{15}N$ values belonged to the non-migratory *C. obscura*, which has the deepest depth of occurrence of the species examined. Interestingly, the trend of higher $\delta^{15}N$ values in deeper-dwelling species was not reflected in the values of *S. pseudobscura*, which was isotopically similar to *L. guentheri* and characterized by lower $\delta^{15}N$ values relative to the shallower dwelling *A. hemigymnus*, *M. simus*, and *S. elongatus*. Despite a center of distribution below 700 m, $\delta^{15}N$ values for *S. pseudobscura* suggests use of food webs with similar isotopic

baselines to those of migratory species foraging in the upper meso- and epipelagic (Hopkins and Baird, 1985; Hopkins et al., 1996). Diet analysis of *S. pseudobscura* in the GOM has shown selection for epipelagic prey, with > 90% of the identified copepod species consumed by *S. pseudobscura* possessing population centers above 75 m (Hopkins et al., 1996). To date there has been no explanation for the occurrence of epipelagic prey in *S. pseudobscura*, but downwelling of epipelagic prey items, net feeding, and the hypothesis that epipelagic copepods are the prey of *S. pseudobscura's* prey have been ruled out during previous studies (Hopkins and Baird, 1985; Hopkins et al., 1996). While our results cannot offer a mechanism to link *S. pseudobscura* to epipelagic prey, the isotopic similarities between *S. pseudobscura* and migratory species provides additional support for the assertion that *S. pseudobscura* feeds at depth in the lower meso- and upper bathypelagic on prey with $\delta^{15}N$ values indicative of an epipelagic origin, and offers an interesting example of vertical connectivity in GOM pelagic food webs.

Interspecific differences observed in $\delta^{15}N$ values could potentially be explained by dietary variation of the species examined. With the exception of larger *S. elongatus* and *S. pseudobscura*, which feed on higher-order prey such as decapod crustaceans and fishes, other species examined have diets predominantly comprised of small crustaceans (copepods, ostracods), including frequent consumption of copepods from the genus *Pleuromamma* (Hopkins and Baird, 1985; Hopkins et al., 1996; Burghart et al., 2010). Based on available diet data, *S. elongatus* and *S. pseudobscura* appear to occupy trophic positions slightly higher than the other five zooplanktivorous species. Assuming dietary relationships among taxa remained similar to those outlined by Hopkins et al. (1996), the observed interspecific variation in $\delta^{15}N$ was greater than, and different from, variation predicted from interspecific feeding relationships alone.

Specifically, elevated $\delta^{15}N$ values in the smaller-bodied and zooplanktivorous *M. simus*, *A. hemigymnus*, and *C. obscura* relative to the larger bodied *S. elongatus* and *S. pseudobscura* is counter to known trophic relationships and suggests that interspecific differences in $\delta^{15}N$ are instead likely driven by differences in the relative use of food webs supported by isotopically enriched POM baselines in the meso- and bathypelagic zones.

The $\delta^{15}N_{sourceAA}$ values in fishes were variable but broadly reflected trends in $\delta^{15}N$ with lower $\delta^{15}N_{sourceAA}$ values in the shallowest migratory species (*L. guentheri*, *B. suborbitale*), intermediate $\delta^{15}N_{sourceAA}$ values in *M. simus*, *S. elongatus*, and *A. hemigymnus*, and highest values in the deepest dwelling *C. obscura*. Contrasting $\delta^{15}N_{sourceAA}$ values within this group of fishes supports the assertion that isotopic variation among species is underpinned by differential use of POM pools with isotopically distinct signatures. Evidence supporting the hypothesis that deep-dwelling micronekton are increasingly supported by POM with enriched isotopic signatures was recently described in a deep-pelagic assemblage in the Pacific Ocean and our results suggest similar mechanisms exist in the GOM (Hannides et al., 2013; Gloeckler et al., 2018). Using CS-SIA, Gloeckler et al. (2018) examined the $\delta^{15}N_{sourceAA}$ values of small (0.7-53 μm) and large (> 53 μm) size fractions of POM and observed increasing $\delta^{15}N_{sourceAA}$ values in both POM size classes with increasing depth, with small POM $\delta^{15}N_{sourceAA}$ values consistently elevated relative to large particles. By comparing the $\delta^{15}N_{sourceAA}$ values of micronekton to the $\delta^{15}N_{sourceAA}$ values of two size fractions of POM, Gloeckler et al. (2018) demonstrated that micronekton in the lower meso- and bathypelagic zones have $\delta^{15}N_{sourceAA}$ values similar to those of suspended particles, suggesting a shift from food webs supported by large, fresh particles in the epi- and upper mesopelagic to food webs supported by small, suspended particles in the lower meso- and bathypelagic. Taken together, the contrast between lower $\delta^{15}N_{sourceAA}$ values in the four

mesopelagic migratory species relative to higher $\delta^{15}N_{sourceAA}$ values in the mesopelagic *A. hemigymnus* and bathypelagic *C. obscura*, suggests a transition from the use of food webs supported by newly formed particles in the epipelagic and large fast sinking particles in the upper mesopelagic towards food webs supported by smaller, suspended particles at depth (Gloeckler et al., 2018).

It is noteworthy that *C. obscura* in my sample appeared to receive carbon from deep-suspended particles as it was the second most abundant micronekton species collected during intensive midwater sampling of the GOM behind its congener, *Cyclothone pallida* (Sutton et al., 2017). The $\delta^{15}N_{sourceAA}$ values of *C. pallida*, which has a median depth distribution slightly shallower than *C. obscura*, displayed elevated $\delta^{15}N_{sourceAA}$ values (4.3 ± 2.7) and appeared to be supported by small particle food webs in the Pacific Ocean (Gloeckler et al., 2018). Members of the genus *Cyclothone* are one of the most numerous vertebrates on the planet, and it is interesting that two of the most abundant species within the pelagic GOM appear to feed within food webs supported by small, suspended particles at depth which, until recently, were not known to significantly contribute to the production of deep-pelagic micronekton (Gloeckler et al., 2018). While *C. pallida* and *C. obscura* both appear to utilize small particle-based organic matter in the lower meso- and bathypelagic, Gloeckler et al. (2018) found $\delta^{15}N_{sourceAA}$ values for the upper mesopelagic dwelling *Cyclothone braueri* and *C. alba* more closely resembled source values form large, sinking particles. Contrasting $\delta^{15}N_{sourceAA}$ values among members of *Cyclothone* with differing depth distributions suggests that utilization of small particle food webs may be more closely related to species-specific to depth of occurrences than phylogeny (Gloeckler et al., 2018).

Effects of water type on isotopic values

The $\delta^{15}N$ values of surface and epipelagic POM and $\delta^{13}C$ and $\delta^{15}N$ values of four fish species (three migratory, one non-migratory) were significantly lower in LCW relative to samples collected in GCW. Isotopic variation between the two water types appeared to be depth related as differences in POM $\delta^{15}N$ values were greatest at the surface and decreased with increasing depth. Similarly, differences in fish $\delta^{13}C$ and $\delta^{15}N$ values between water types were greatest for *B. suborbitale* and *L. guentheri* which have epipelagic nighttime distributions, less pronounced in *S. elongatus* and *A. hemigymnus* which have nighttime distributions extending into the upper mesopelagic, and absent for the deepest dwelling *S. pseudobscura* and *C. obscura*. The pattern of lower $\delta^{13}C$ and $\delta^{15}N$ values for fishes collected from anticyclonic features like the Loop Current is consistent with previous investigations which documented lower isotopic values in epipelagic fishes, crustaceans and zooplankton in anticyclonic features relative to cyclonic features and common water in the northern GOM (Dorado et al., 2012; Wells et al., 2017). However, the differences in mean $\delta^{15}N$ values of fishes between LCW and GCW, which ranged from 1.80‰ (*L. guentheri*) to 0.39‰ (*S. elongatus*), were generally less than the isotopic differences observed in juvenile flyingfishes (1.75‰) and *Sargassum*-associated crustaceans (5.4‰) collected from anticyclonic and cyclonic features by Wells et al. (2017).

Isotopic differences in POM and mirconekton between cyclonic and anticyclonic features are driven by differences in nitrogen cycling which result in isotopically distinct nitrogen sources fueling production at the base of the food web (Montoya et al., 2002; Dorado et al., 2012; Wells et al., 2017). The Loop Current and other anticyclonic features in the GOM are areas of convergence, characterized by increased stratification and downwelling, which depresses nitracline depths and limits the amount of isotopically enriched deep-water nitrate entering the

photic zone (Biggs, 1992). In the absence of new, upwelled nitrate, phytoplankton and higher-order consumers in the Loop Current and anticyclonic eddies have been shown to be supported by regenerated nitrogen and by isotopically light nitrogen derived from diazotrophy (cyanobacteria *Trichodesmium* spp.), which results in phytoplankton with lower $\delta^{15}N$ values that can then be reflected in the $\delta^{15}N$ values of higher-order consumers (McClleland and Montoya, 2002; Dorado et al., 2012). By contrast, phytoplankton in cyclonic eddies or neritic waters (i.e., common water) are largely supported by isotopically enriched deep-water nitrate resulting in higher $\delta^{15}N$ values in phytoplankton and, subsequently, higher-order consumers. To our knowledge, a study by Menard et al. (2014) is the only other study to examine the isotopic values of deep-pelagic micronekton across mesoscale features, which documented relatively few differences in the $\delta^{15}N$ and $\delta^{13}C$ values of micronekton among cyclones, anticyclones, and frontal regions. The authors suggest that the lack of isotopic variation between mesoscale features was likely due to micronekton moving and feeding between features on timescales shorter than tissue turnover rates, resulting in an integration of multiple isotopic baselines (Menard et al., 2014). Although turnover rates for deep-pelagic fishes are unknown, *B. suborbitale*, *L. guentheri*, and *S. elongatus* have life spans of one to three years, so assumed tissue turnover rates of several weeks is reasonable (Lancraft et al., 1988; Gartner, 1991). While the currents associated with mesoscale features in the GOM are likely not strong enough to trap micronekton, and movement in and out of mesoscale features is likely, the Loop Current and associated eddies can be 100s of kilometers in diameter, persist for months to years, and dominate circulation in the upper layer (surface to 1000 – 1200 m) of the GOM (Biggs, 1992; Vukovitch, 2007). Thus, due to the persistence of the Loop Current or anticyclonic eddies over timescales greater than hypothesized tissue turnover rates, the conservation of isotopic baselines

unique to a water type in micronekton is feasible, particularly for short-lived species with relatively shallow distributions. While these results should be interpreted carefully due to low sample sizes in LCW and narrow differences between water types for *S. elongatus* and *A. hemigymnus*, our results, combined with those of previous studies in the GOM, suggest that the distinct isotopic baselines that characterize anticyclonic features can be conserved and reflected in the isotopic values of deep-pelagic micronekton in the GOM. This finding supports the notion that heterogeneity in the isotopic baseline of pelagic ecosystems is an important consideration when studying the trophic structure of pelagic assemblages.

CHAPTER III

TROPHIC ECOLOGY OF MESO- AND BATHYPELAGIC PREDATORY FISHES IN THE GULF OF MEXICO*

Introduction

The deep-pelagic zone (waters deeper than 200 m to just above the seafloor) represents the largest cumulative habitat on earth and is home to a diverse array of specialized fauna (Robison, 2004; Robison, 2009). The deep pelagic and its inhabitants provide an array of ecosystem services that are important to humans, including carbon sequestration, nutrient regeneration, fisheries production, and waste absorption (Danavaro et al., 2008; Mengerink et al., 2014; Thurber et al., 2014). Despite its enormous volume and the economic and ecological importance of its fauna, deep-pelagic ecosystems remain chronically understudied (Webb et al., 2010) and face an increasing number of stressors including climate change, ocean acidification, overfishing, and natural resource extraction (Morato et al., 2006; Ramirez-Llodra et al., 2011; Mengerink et al., 2014). As threats to the diversity and stability of marine ecosystems increase and expand into deeper oceanic environments, there has been increasing concern regarding the status of deep-sea communities and a renewed interest in describing and understanding deep-sea ecosystem structure.

Central to our understanding of ecosystem and community structure is a thorough knowledge of food webs (Polis and Strong, 1996; McCann, 2000). In addition to providing important information regarding ecosystem functioning, the study of food webs provides

*Reprinted with permission from "Trophic ecology of meso-and bathypelagic predatory fishes in the Gulf of Mexico" by Richards et al., (2019) ICES Journal of Marine Science, https://doi.org/10.1093/icesjms/fsy074.

understanding of how animal communities are structured and sheds light on the mechanisms underlying species coexistence and persistence in the face of perturbations. While our knowledge of deep-sea food webs has advanced considerably over the past few decades (Robison, 2009; Sutton, 2013), in many regions fundamental information including species-specific feeding relationships, trophic position estimates, and delineation of energy pathways connecting disparate trophic levels and communities are lacking (Mengerink et al., 2000; Drazen and Sutton, 2017).

Fishes are a dominant component of deep-pelagic ecosystems worldwide and are among the main taxa that undertake diel vertical migrations (DVM). While standardized abundances (no. per unit volume) of meso- and bathypelagic fishes are relatively low (Angel and Baker, 1982), their global distributions have resulted in high cumulative biomass, estimated at 7-10 billion metric tons (Iriogen et al., 2014). Due to their sheer numbers and vertical migration behavior, which can exceed 1000 m in vertical extent, it is increasingly being recognized that fishes play key ecological and biogeochemical roles in open ocean ecosystems (Wilson et al., 2009; Drazen and Sutton, 2017). As highly abundant mid-level consumers, deep-pelagic fishes help regulate zooplankton populations (Hopkins and Gartner, 1992; Pakhomov et al., 1996). Deep-pelagic fishes also serve as trophic links between zooplankton and higher-order consumers such as epipelagic fishes (Moteki et al., 2001; Choy et al., 2013), marine mammals (Pauly et al., 1998), and seabirds (Raclot et al., 1998; Cherel et al., 2008). Diel vertical migrations of fishes have been shown to connect epi-, meso-, and bathypelagic habitats with each other and with deep-benthic habitats (Portiero and Sutton, 2007; Trueman et al., 2014).

Stable isotope analysis (SIA) has been widely used to delineate food web structure and provides an integrated view of an organism's diet over time scales relevant to tissue turnover

rates rather than digestion rates (Peterson and Fry, 1987; Post, 2002). Carbon isotopes undergo relatively small amounts of fractionation (~0.5‰) during trophic transfers and are useful for determining the relative contributions of carbon sources to the production of consumers (Peterson and Fry, 1987). Stable isotopes of nitrogen undergo comparatively large levels of fractionation (~3.4‰) during trophic transfer resulting in predictable differences in the isotopic signatures of consumers and their prey (Post, 2002). The relatively predictable level of enrichment of ^{15}N during trophic transfer allows for the determination of trophic levels and can be used to identify trophic relationships within assemblages of organisms (Peterson and Fry, 1987; Post, 2002).

To date, much of the research describing the trophic ecology of deep-pelagic fishes has focused on zooplanktivorous groups (myctophids, sternoptychids, gonostomatids), while less attention has been paid to micronektonivores (stomiids, alepisauroids) occupying higher trophic levels. The numerical importance of micronektonivores (Hopkins et al., 1996; Sutton and Hopkins, 1996a), their propensity to prey heavily on zooplanktivorous fishes (Hopkins et al., 1996; Sutton and Hopkins, 1996b), and documented importance as prey to higher trophic level consumers (Moteki et al., 2001; Choy et al., 2013) underscores the importance of describing their trophic structure. Here, I describe the trophic ecology of eight putative high-trophic-level fishes: common fangtooth (*Anoplogaster cornuta)*, Sloane's viperfish (*Chauliodus sloani),* atlantic sabretooth (*Coccorella atlantica*), Chun's telescope fish (*Gigantra chuni*), Indian telescopefish (*Gigantura indica*), hammerjaw (*Omosudis lowii*), *Photostomias guernei*, and Gunther's boafish (*Stomias affinis*). These species are meso- and bathypelagic fishes with circumglobal distributions, some of which have been documented as numerically important components of deep-pelagic assemblages (Sutton and Hopkins, 1996a; Moore et al., 2003; Sutton et al., 2008).

Specific goals of this study are to provide estimates of trophic position, describe the isotopic niche areas and the extent of niche overlap among species and detail ontogenetic shifts in trophic position. Additionally, following the trophic analysis of seven zooplanktivorous micronekton species which suggested non-migratory species feed within food webs supported by small particles in the meso- and bathypelagic zones (Chapter II), I attempt to quantify the relative contributions of particulate organic matter (POM) from the epi-, meso-, and bathypelagic zones to determine if a similar pattern occurs in higher-order predators.

Methods

Sample collection and study site

Fishes were collected from the northern GOM during three oceanographic cruises conducted during 2011 in the spring (22-Mar to 11-Apr), summer (23-Jun to 13-Jul), and fall (08-Sep to 27-Sep) (Table 6). All cruises were part of the Offshore Nekton Sampling and Analysis Program (ONSAP) that was implemented following the *Deepwater Horizon* oil spill in support of NOAA's Natural Resource Damage Assessment (NRDA). ONSAP stations were situated every half degree of latitude and longitude in the northern GOM. Specimens were collected using large midwater trawls fitted with large mesh panels (~80 cm) near the mouth that gradually tapered to smaller mesh (~6 cm) sizes before the cod end. Trawls were fished obliquely from the surface to depths of either 700 m or 1400 m. Once the trawls were retrieved, animals were sorted, enumerated and visually identified to species. Samples for SIA were selected haphazardly to maximize spatial and temporal coverage. All specimens for SIA were frozen whole at -20˚C until processed at Texas A&M University at Galveston.

Table 6. Species-specific sample descriptions and bulk $\delta^{13}C$ and $\delta^{15}N$ isotope data (mean ± SD). [1] Denotes no diel vertical migration, [2] denotes asynchronous diel vertical migration (not all individuals of population migrate vertically each day). References for vertical migration patterns: *A. cornuta* (Clarke and Wagner, 1976), *C. sloani* (Sutton and Hopkins, 1996a), *C. atlantica* (McEachran and Fechhelm, 1998), *G. chuni* (McEachran and Fechhelm, 1998), *G. indica* (Sutton et al., 2010), *O. lowii* (McEachran and Fechhelm, 1998; Sutton et al., 2010), *P. guernei* (Sutton and Hopkins, 1996a), *S. affinis* (Sutton and Hopkins, 1996a)

Species	*N*	Spring	Summer	Fall	Standard Length Range (mm)	Mean Standard length (mm) ± SD	$\delta^{13}C$ (‰) ± SD	$\delta^{15}N$ (‰) ± SD	C:N ± SD
A. cornuta [1]	23	2	12	9	84 – 148	114.35 ± 19.09	-18.93 ± 0.67	11.14 ± 0.96	3.66 ±0.44
C. sloani [2]	30	10	20	0	143 – 237	191.43 ± 23.32	-18.68 ± 0.43	9.51 ± 0.42	3.42 ± 0.23
C. atlantica [2]	19	0	19	0	44 – 125	89.53 ± 26.53	-18.50 ± 0.47	9.96 ± 0.83	3.67 ± 0.34
G. chuni [1]	24	6	9	9	34 – 186	134.57 ± 40.11	-18.25 ± 0.44	11.13 ± 1.08	3.31 ±0.15
G. indica [1]	21	8	6	7	75 – 192	141.95 ± 28.83	-18.25 ± 0.94	10.70 ± 0.64	3.43 ± 0.29
O. lowii [1]	32	12	10	10	36 – 261	120.66 ± 61.60	-19.04 ± 0.32	9.79 ± 0.60	3.40 ± 0.08
P. guernei [2]	37	14	13	10	56 – 127	98.08 ± 14.03	-18.61 ± 0.40	9.18 ± 0.63	3.44 ± 0.13
S. affinis [2]	26	5	16	5	55 – 205	127.31 ± 38.66	-19.38 ± 0.84	9.98 ± 0.89	3.86 ± 0.63

Stable isotope analysis

White muscle tissue for SIA was dissected from the dorsal musculature of fishes and visually examined under a dissecting microscope for the presence of bones, which were subsequently removed. Cleaned samples were rinsed with deionized water, frozen and lyophilized for 48 h. Freeze-dried samples were homogenized using a mortar and pestle, weighed, wrapped in tin capsules and shipped to the University of California at Davis' Stable Isotope Facility for analysis. Analysis of muscle tissue $\delta^{13}C$ and $\delta^{15}N$ was carried out using an elemental analyzer (PDZ Europa ANCA-GSL) coupled with an isotope ratio mass spectrometer (PDZ Europa 20-20). The long-term standard deviation of UC Davis' stable isotope facility is 0.2‰ for $\delta^{13}C$ and 0.3‰ for $\delta^{15}N$. Stable isotope data are expressed relative to international standards of Vienna PeeDee belemnite and atmospheric N_2 for carbon and nitrogen, respectively. The C:N of fishes in this study were low (species mean C:N range 3.31 – 3.86; 92% of individuals C:N <4.0) compared to C:N from similar species collected in the Atlantic Ocean and Southern Ocean (C:N 3.3 – 12.5; Hoffman and Sutton, 2010), suggesting lipids did not significantly confound the interpretation of $\delta^{13}C$ data. Therefore, all statistical analyses were performed on uncorrected $\delta^{13}C$ values.

Stable isotope data of particulate organic matter (POM) used in this study were derived from the published data set of Fernandez-Carrera et al. (2016) (**https://data.gulfresearchinitiative.org** R1.x132.134:0073, R1.x132.134:0074, R1.x132.139:0016 and R1.x132.139:0017). For detailed descriptions of methodologies and sample locations of POM I refer the reader to Fernandez-Carrera et al. (2016), but a brief description of their sampling methodologies follows. POM samples were collected during summer of 2011 (02-July to 21-July) in the northern GOM. In addition to samples collected in

pelagic waters, the complete published data set included samples taken from waters over the continental shelf and from waters near the Mississippi River. In order to maximize the spatial overlap between POM samples and the collection locations of fishes, only POM data collected within proximity to ONSAP sampling stations in waters ≥1000 m deep (Figure 6) were utilized. POM samples were collected throughout the water column using remotely fired 10-L Niskin bottles. Samples were then filtered across 47-mm glass fiber filters at low pressure and dried at 60˚C for 24 hours prior to isotope analysis (Fernandez-Carrera et al., 2016). In order to determine if the isotopic signatures of POM samples changed with depth, I used collection depth to designate POM samples as epipelagic (0-200 m), mesopelagic (200-1000 m) or bathypelagic (> 1000 m) so that statistical comparisons could be made.

Statistical analysis

Multivariate analysis of variance (MANOVA) was used to test for differences in $\delta^{13}C$ and $\delta^{15}N$ among species and POM depth zones. Species and season were included as factors in the linear model and tested for the presence of an interaction. Univariate tests for both $\delta^{13}C$ and $\delta^{15}N$ were performed using analysis of variance (ANOVA) among fish species and POM depth zones. *A posteriori* differences among means were detected using Tukey's honestly significant difference (HSD) test. Using equation 3 (Post et al., 2007), trophic position was calculated for each species:

$$\text{Equation 3:} \quad TrP_i = ((\delta^{15}N_i - \delta^{15}N_{base})/ \Delta^{15}N) + \lambda$$

where $\delta^{15}N_i$ is the mean species $\delta^{15}N$, $\delta^{15}N_{base}$ is the mean $\delta^{15}N$ of the primary producer or primary consumer being used to set the isotopic baseline, $\Delta^{15}N$ is the trophic discrimination factor, and λ represents the trophic level of the organism being used to set the baseline. Because primary consumer data were not available for the time period of this study, trophic position

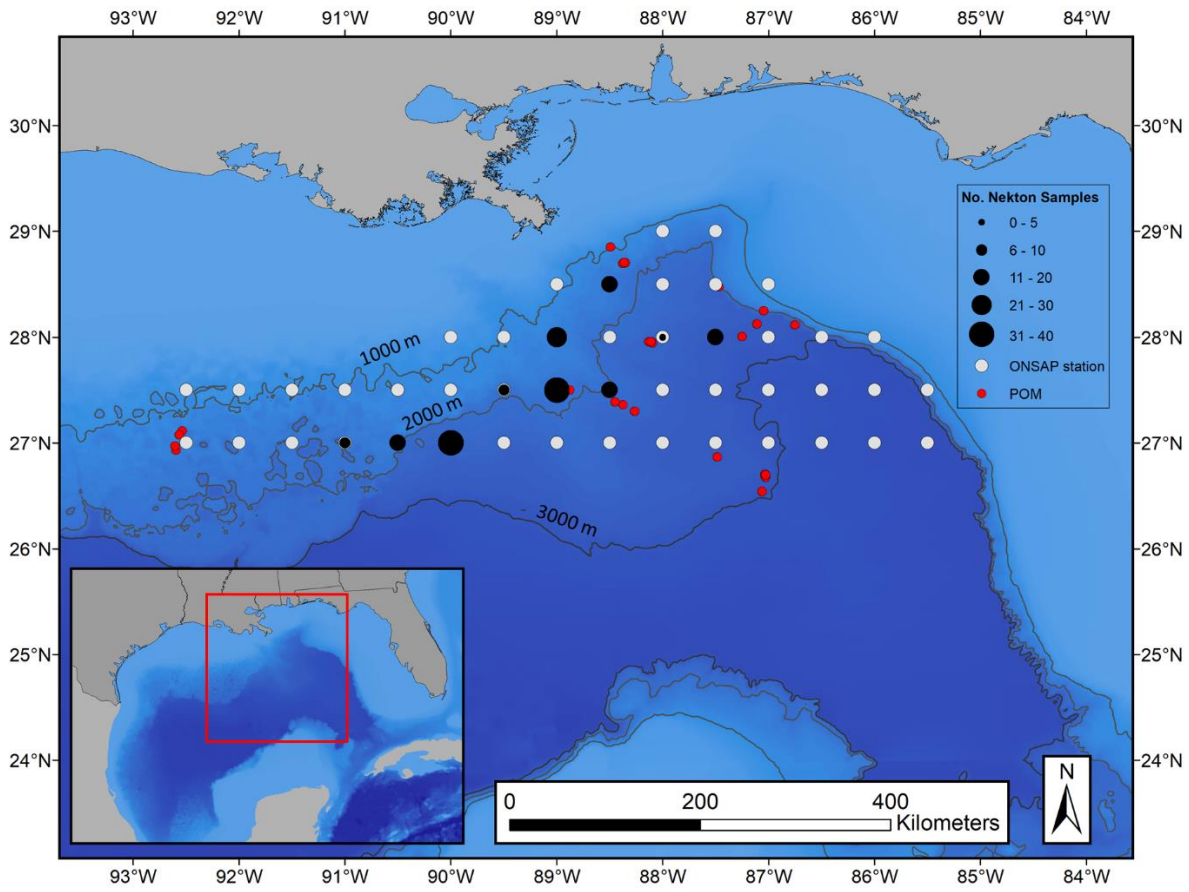

Figure 6. Map of sampling stations (white circles) in northern Gulf of Mexico. Locations of POM samples depicted as red circles, and locations of fish samples for stable isotope analysis depicted by black circles (specimen number denoted by circle diameter).

estimates made using mean $\delta^{15}N$ values of POM collected from the epipelagic zone were compared with estimates calculated from published $\delta^{15}N$ values of vertically migrating euphausiids collected from the epi- and mesopelagic zones in the northern GOM during 2007 (McClain-Counts et al., 2017). In order to explore the relationship between fish size and $\delta^{13}C$ and $\delta^{15}N$, least-squares linear regression analysis was conducted for each species.

Spatial variation in $\delta^{13}C$ and $\delta^{15}N$ of both fishes and POM was investigated using least-squares linear regression between isotopic values and longitude and latitude (0.5-degree intervals). Due to the limited spatial coverage within each fish species, spatial trends in fishes had to be tested by pooling individuals from all species together. Latitudinal and longitudinal variation in POM $\delta^{13}C$ and $\delta^{15}N$ was minimal, with the only significant correlation occurring between epipelagic POM $\delta^{13}C$ and longitude, although correlation coefficients were low (p = 0.04, R^2 = 0.04). All other pairwise combinations between $\delta^{13}C$ and $\delta^{15}N$ and latitude or longitude within the epi-, meso-, and bathypelagic depth zones were non-significant (Appendix Table A-1). The $\delta^{13}C$ values of fishes were significantly correlated with latitude ($p < 0.01$, R^2 = 0.08) and longitude ($p < 0.01$, R^2 = 0.04), with $\delta^{13}C$ values becoming more enriched at southern latitudes and western longitudes. In contrast, the $\delta^{15}N$ values of fishes did not correlate with latitude (p = 0.46) or longitude (p = 0.19). Due to the low correlation coefficients observed between fish $\delta^{13}C$ values and latitude and longitude, isotope data for each species were pooled across lines of latitude and longitude during subsequent analysis. All statistical analyses were performed in R (R Development Core Team 2014) v. 3.3.2.

The trophic breadth of each species and trophic similarity among species were assessed by calculating standard ellipse areas (SEA) using the R package SIBER (Jackson et al., 2011) and following methods outlined by Jackson et al. (2011). Bayesian standard ellipses encompass ~40% of the isotope data for each species, are less affected by increases in sample size or statistical outliers than convex hull analysis and represent the core isotopic niche area of a species (Jackson et al., 2011). Size corrected SEAs (SEA_c) were calculated for each species, which adjusts for underestimation of ellipse area at small sample sizes and allows for comparison of ellipse sizes to other studies with larger sample sizes (Jackson et al., 2011). Overlap of size-

corrected ellipses was used as a proxy for trophic similarity and was examined by calculating the extent of overlap between each pairwise combination of species. The percentage of overlap between species pairs was calculated by dividing the area of overlap ($‰^2$) by the total combined ellipse area ($‰^2$) of the two species being compared. Isotopic niche overlap was considered significant when overlap between two species was >60% following Schoener (1968). Differences in size-corrected ellipse area, a proxy for trophic breadth that assumes species with larger SEAc feed more broadly within the food web than those with smaller SEAc, were compared among species and considered to be significantly different when 95% of posterior draws were smaller in one species compared to the other.

The Bayesian mixing model, MixSIAR (Stock and Semmens, 2015), was used to estimate the relative contribution of epi- (0-200 m), meso- (200-1000 m), and bathypelagic (>1000 m) POM to each species. Bayesian mixing models provide the most accurate estimations of source or prey contributions when tissue and species-specific discrimination factors are used (Caut et al., 2008), but discrimination factors for meso- and bathypelagic fishes are currently unknown. I chose to run mixing models using discrimination factors of 3.15‰ ± 1.28‰ and 0.97‰ ± 1.08‰ for $\delta^{15}N$ and $\delta^{13}C$, respectively (Sweeting et al., 2007a,b), which have been previously used to study the trophic structure of meso- and bathypelagic fishes (Valls et al., 2014). Mixing models in MixSIAR estimate probability density functions using Markov Chain Monte Carlo methods and each model was run with identical parameters (number of chains = 3; chain length = 100,000; burn in = 50,000; thin = 50). Model convergence was determined using Gelman-Rubin and Geweke diagnostic tests (Stock and Semmens, 2015).

Results

Stable isotope values of fishes and particulate organic matter

Individual consumer $\delta^{13}C$ values ranged from -21.49 to -16.63‰, with mean differences among species spanning 1.13‰ between *S. affinis* (-19.38‰ ± 0.83) and *G. chuni* (-18.25‰ ± 0.44) and *G. indica* (-18.25‰ ± 0.94) (Table 6; Figure 7). Individual $\delta^{15}N$ values varied between 7.10‰ and 13.0‰ with 1.96‰ separating the mean $\delta^{15}N$ values of *A. cornuta* (11.1‰ ± 0.96) and *P. guernei* (9.18‰ ± 0.63) (Table 6; Figure 7). Interspecific differences in $\delta^{13}C$ and $\delta^{15}N$ were detected (MANOVA: $F_{14,382} = 17.24$, $p < 0.001$); however, no significant seasonal effects were found (MANOVA: $F_{14,382} = 1.29$, $p = 0.27$) and no significant interaction effect among species and season was detected (MANOVA: $F_{22,382} = 1.05$, $p = 0.40$). Significant differences in $\delta^{13}C$ values among species (ANOVA: $F_{7,204} = 11.62$, $p < 0.001$) were driven by *G. chuni* and *G. indica* which were enriched in ^{13}C compared to species such as *O. lowii* and *S. affinis* (Figure 7). Significant differences in $\delta^{15}N$ among species (ANOVA: $F_{7,204} = 25.55$, $p < 0.001$) were primarily driven by *A. cornuta*, *G. chuni*, and *G. indica* which were enriched in ^{15}N compared to *C. sloani* and *P. guernei* (Figure 7). Results of all pairwise comparisons for $\delta^{13}C$ and $\delta^{15}N$ values among species are listed in the Appendix Table A-2.

A total of 154 samples of POM collected from depths ranging from 1 to 2500 m were analyzed from the publicly available dataset described in Fernandez-Correra et al. (2016). POM exhibited a wide range of $\delta^{13}C$ (-27.17 to -16.41) and $\delta^{15}N$ values (-3.58 to 11.69), with POM samples generally becoming more ^{15}N enriched with increasing depth (Figure 7). Significant differences in POM $\delta^{13}C$ and $\delta^{15}N$ among vertical depth zones (MANOVA: $F_{4,302} = 14.54$, $p < 0.001$) were observed. Significant differences in $\delta^{15}N$ were found among depth zones (ANOVA: $F_{2,151} = 34.41$, $p < 0.001$), with epipelagic POM more ^{15}N depleted than POM collected from

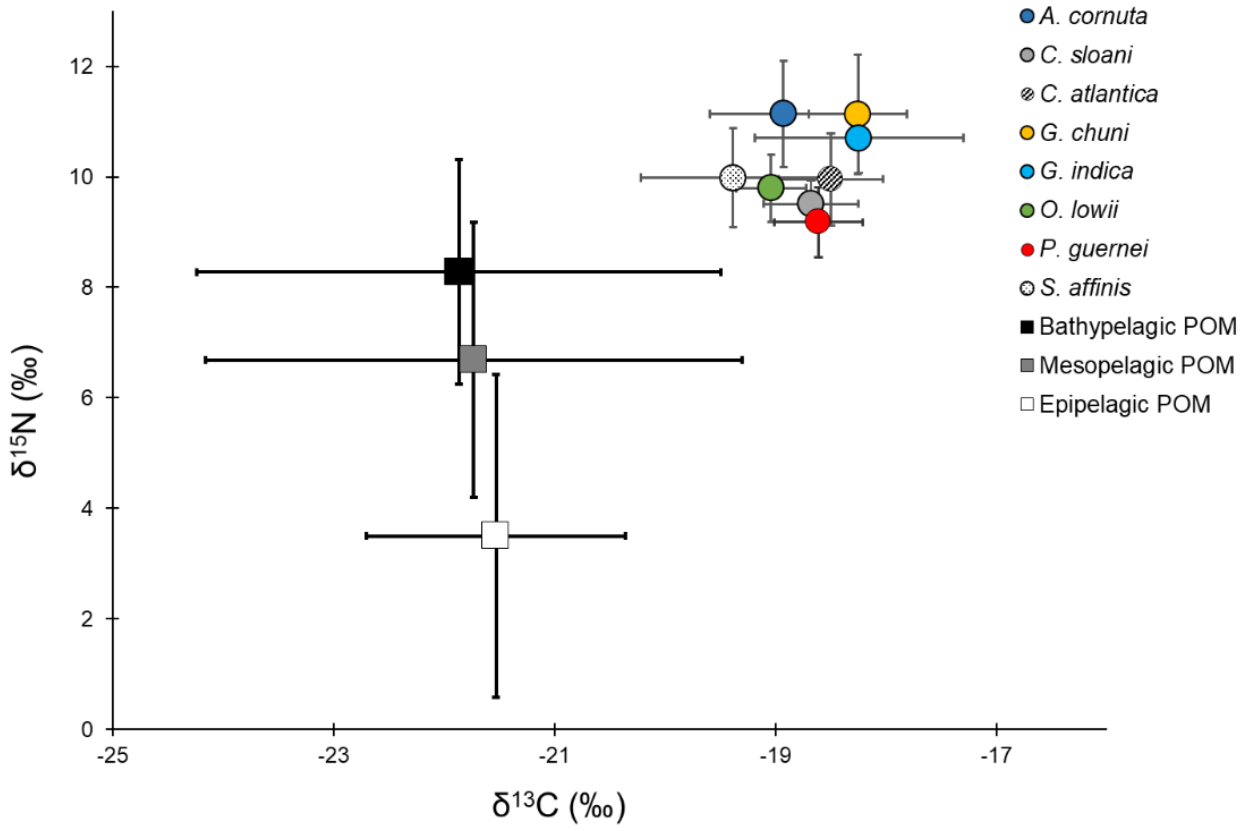

Figure 7. Isotope bi-plot of $\delta^{13}C$ and $\delta^{15}N$ values from POM (squares) and fishes (circles). Data points represent means and error bars represent ± 1 SD.

mesopelagic and bathypelagic depths. The $\delta^{13}C$ values of POM did not significantly differ across depth zones (ANOVA: $F_{2,151} = 0.42$, $p = 0.66$).

Trophic position estimates

The use of primary producers or primary consumers to set the isotopic baseline had no effect on the relative trophic positions among consumers but resulted in slight differences (0.32) in calculated trophic position (TP) within each species. When primary producer (POM) data were used to set the baseline, consumer TP ranged from 2.8 (*P. guernei*) to 3.4 (*A. cornuta*, *G. chuni*), while all species fell within the third and fourth trophic position when primary consumers

were used to set the baseline (*P. guernei* = 3.1, *A. cornuta* and *G. chuni* = 3.7) (Figure 8; Appendix Table A-3).

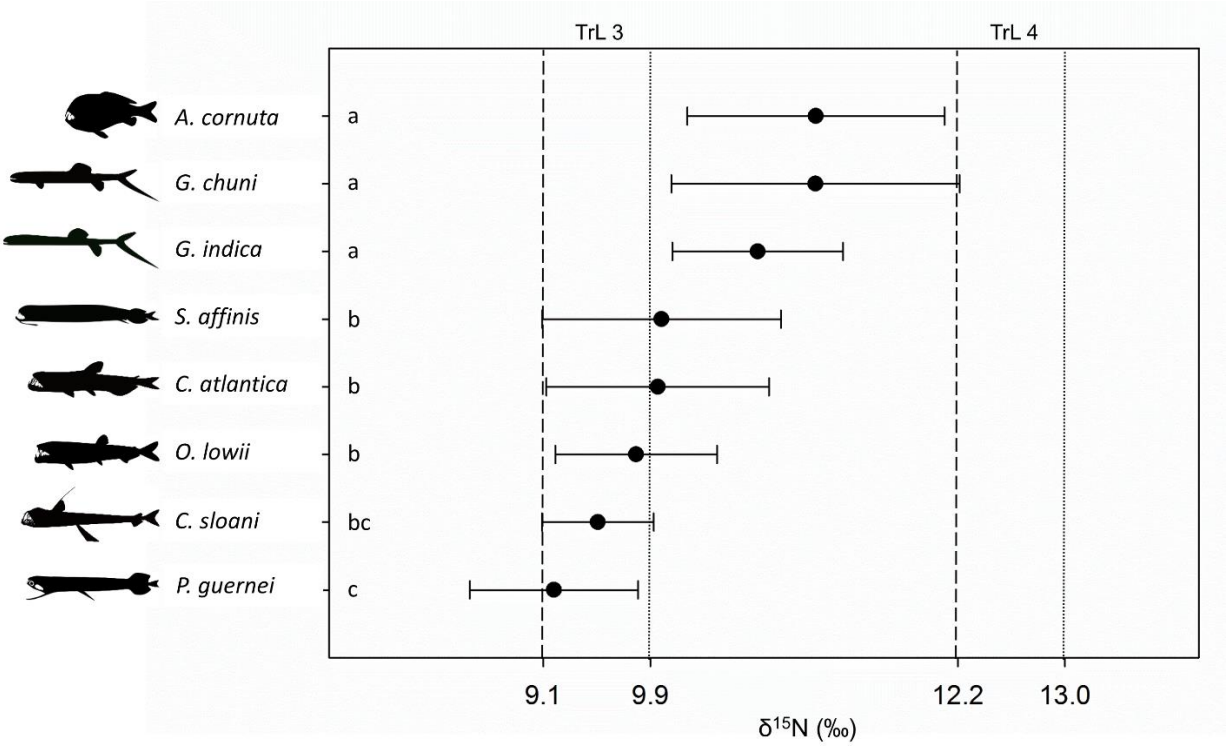

Figure 8. Trophic position (TP) estimates for each fish species. Letters represent significant differences in TP among species with like letters being similar and non-like letters significantly different. Dashed lines represent the δ ^{15}N threshold values of TP 3 and TP 4 when using primary consumers (euphausiids) to set the isotopic baseline; dotted lines represent the δ ^{15}N threshold values of TL 3 and TL 4 when using primary producers (POM) to establish isotopic baseline. For species-specific TP estimates (± SD) see Appendix Table A-3.

Of the species examined, *A. cornuta* ($p < 0.001$, $R^2 = 0.63$), *C. atlantica* ($p < 0.001$, $R^2 = 0.74$), *G. chuni* ($p < 0.001$, $R^2 = 0.41$), *C. sloani* ($p < 0.001$, $R^2 = 0.22$), *P. guernei* ($p < 0.001$, R^2

= 0.25), and *S. affinis* ($p < 0.001$, $R^2 = 0.53$) exhibited significant positive relationships between $\delta^{15}N$ and SL (Figure 9). Relationships between $\delta^{13}C$ and SL were more variable than those observed with $\delta^{15}N$, with two species, *G. chuni* ($p < 0.01$, $R^2 = 0.33$), and *O. lowii* ($p < 0.01$, $R^2 = 0.44$) displaying significant positive relationships between $\delta^{13}C$ and SL (Figure 9).

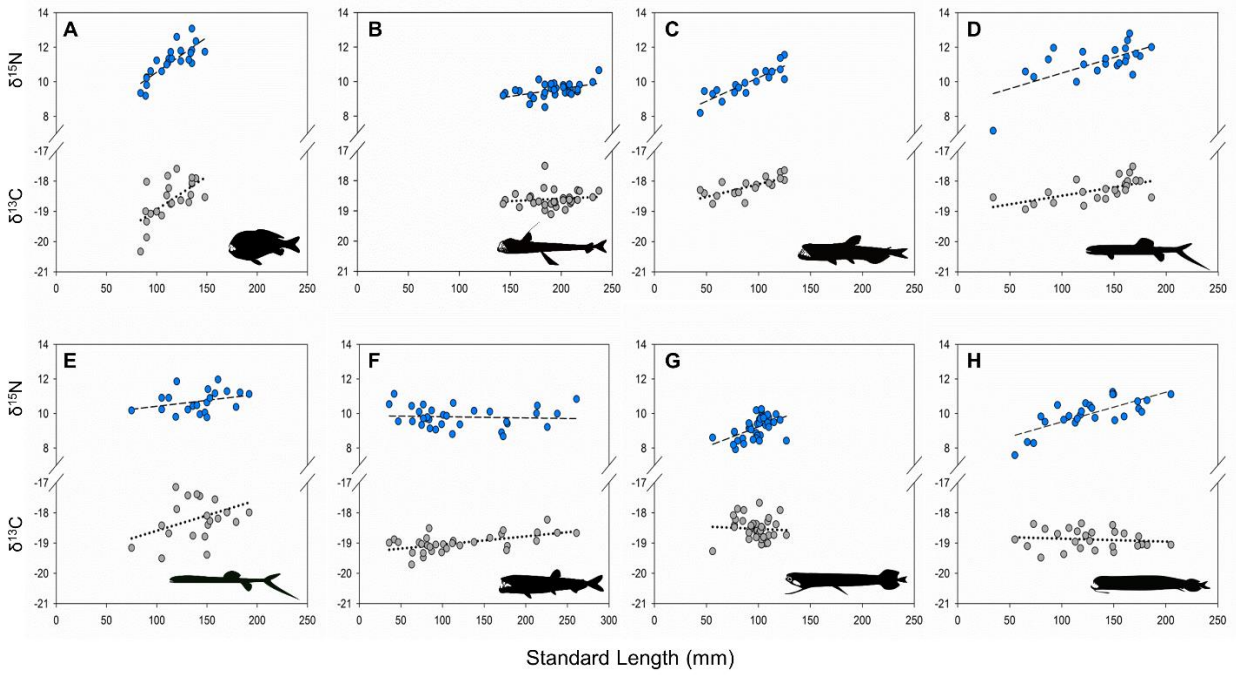

Figure 9. Results of least squares regression analysis between standard length (mm) and $\delta^{15}N$ (blue circles) and $\delta^{13}C$ (gray circles) values. (A) *A. cornuta* (B) *C. sloani* (C) *C. atlantica* (D) *G. chuni* (E) *G. indica* (F) *O. lowii* (G) *P. guernei* (H) *S. affinis*.

Isotopic niche breadth, calculated using SEA_c, was largest for the piscivorous *S. affinis* ($SEA_c = 2.27$), *G. indica* ($SEA_c = 1.98$), *A. cornuta* ($SEA_c = 1.96$) and *G. chuni* ($SEA_c = 1.53$), which collectively occupied the highest trophic positions within the guild of predators examined.

C. atlantica (SEA_c = 0.1.19) occupied an intermediate relative trophic position and intermediate-sized trophic niche. *P. guernei* (SEA_c = 0.71), and *O. lowii* (SEA_c = 0.62) which feed primarily on crustaceans and cephalopods, respectively, occupied lower relative trophic positions and were characterized by relatively small isotopic niches (Table 7, Figure 10).

Table 7. Metrics for estimating isotopic niche size in eight meso- and bathypelagic predators. TA: Total area (expressed in ‰) encompassed by all data points of each species; SEA: Standardized ellipse area for each species; SEAc: Size-corrected standardized ellipse area; CD: Centroid distance calculated by taking average distance of each data point from the centroid for each species.

Species	TA	SEA	SEAc	CD
A. cornuta	6.81	1.87	1.96	0.97
C. sloani	2.68	0.53	0.56	0.46
C. atlantica	3.02	1.13	1.19	0.82
G. chuni	5.82	1.46	1.53	0.83
G. indica	5.17	1.88	1.98	0.98
O. lowii	2.33	0.60	0.62	0.58
P. guernei	2.58	0.69	0.71	0.66
S. affinis	7.01	2.18	2.27	1.04

Interestingly, the smallest isotopic niche also belonged to a known piscivore, *C. sloani* (SEA_c = 0.56), although the small calculated isotopic niche area could have been due to a limited size range of specimens for this species resulting in a loss of any length-based variation in isotope values (Figure 9). In the twenty instances where overlap in SEAc occurred, the percentage of shared isotopic niche space ranged from 1% (*A. cornuta* and *C. atlantica; G. indica and O. lowii*) to 27% (between *G. chuni* and *G. indica*) (Table 8), while directional overlap, or the percentage

of one species' ellipse covering the ellipse of another species, varied widely from 2% to 100% (Table 8, Figure 10).

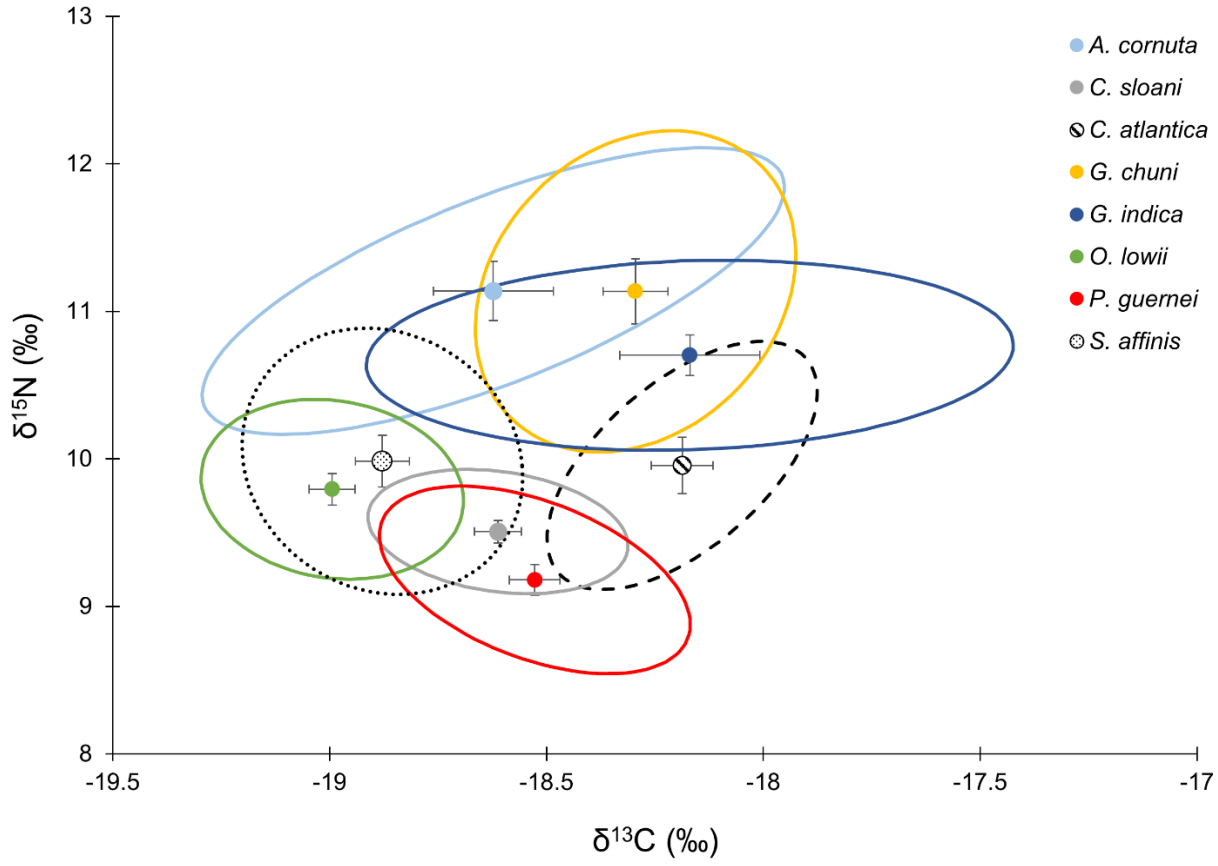

Figure 10. Size corrected Bayesian standard ellipse areas plotted around mean $\delta^{13}C$ and $\delta^{15}N$ values for each species.

Table 8. Isotopic niche overlap measured in percentage of shared space (‰) between each pairwise combination of species. Numbers in parentheses represent the percent overlap of species A (column) with species B (row) and vice versa. Numbers in bold represent shared overlap >50%. Second column of numbers represents the likelihood of differences in SEAc size. Numbers in bold represent statistically significant differences in SEAc size between the pair of species examined.

	A. cornuta		*C. sloani*		*C. atlantica*		*G. chuni*		*G. indica*		*O. lowii*		*P. guernei*	
C. sloani	0 (0,0)	**0**												
C. atlantica	1 (2,3)	**0.05**	26 (**81**, 38)	**0.99**										
G. chuni	9 (23, 30)	0.19	0 (0,0)	**0.99**	14 (32, 25)	0.80								
G. indica	16 (33, 32)	0.49	0 (0,0)	**0.99**	20 (41, 25)	0.94	27 (**61**, 47)	0.80						
O. lowii	3 (4, 12)	**0**	18 (39, 34)	0.66	11 (16,32)	**0.01**	0 (0,0)	**0.01**	1 (2,5)	**0**				
P. guernei	0 (0,0)	**0**	30 (**68**, **54**)	0.85	7.5 (28, 47)	**0.04**	0 (0,0)	**0.01**	0 (0,0)	**0**	11 (23, 20)	0.73		
S. affinis	9 (19, 17)	0.70	12 (**63**, 15)	**0.99**	11 (33,17)	**0.98**	0 (0,0)	0.15	4 (7, 7)	0.70	21 (**100**, 27)	**1**	9 (37, 11)	**1**

Mean POM $\delta^{13}C$ and $\delta^{15}N$ values collected from the meso- and bathypelagic were not significantly different from each other, thus mixing models were run using epipelagic POM data and data combined from the meso- and bathypelagic zones. Mixing model results suggest that all consumers included in this study derive the bulk of their carbon from epipelagic POM (Figure 11). Relative contributions of epipelagic POM ranged from 97.87% ± 1.43% in *P. guernei* to 73.30% ± 3.19% in *G. chuni*, while contributions from meso- and bathypelagic POM were much lower, ranging from 26.70% ± 3.19% in *G. chuni* to 2.13% ± 1.43% in *P. guernei.* Diagnostic plots of posterior distributions revealed a high negative correlation between the two sources (epipelagic POM and meso-/bathypelagic POM). Considering the producer data fully constrain consumer data when an appropriate trophic enrichment factor is applied and that model diagnostics (Gelman-Rubin Diagnostic: all variables <1.01; Gweke Diagnostic: <5% of variables outside ±1.96 for each chain) indicate the model fully converged, the negative correlation is likely caused by the similar $\delta^{13}C$ signatures of sources and not from a missing carbon source.

Discussion

Trends in particulate organic matter and fish isotope values

Results from the analysis of POM samples taken by Fernandez-Carrera et al. (2016) in 2011 revealed POM $\delta^{13}C$ and $\delta^{15}N$ values in the northern GOM are highly variable throughout the water column, with a clear trend of enrichment in ^{15}N with increasing depth. Similar increases in POM $\delta^{15}N$ values from the epi- to bathypelagic zones were observed in POM samples collected from the same region of the GOM in 2015-2016 (Chapter II) and are driven by the preferential removal of isotopically light nitrogen (^{14}N) during bacterial degradation of POM as it sinks through the water column (Mintenbeck et al., 2007; Hannides et al., 2013). Despite

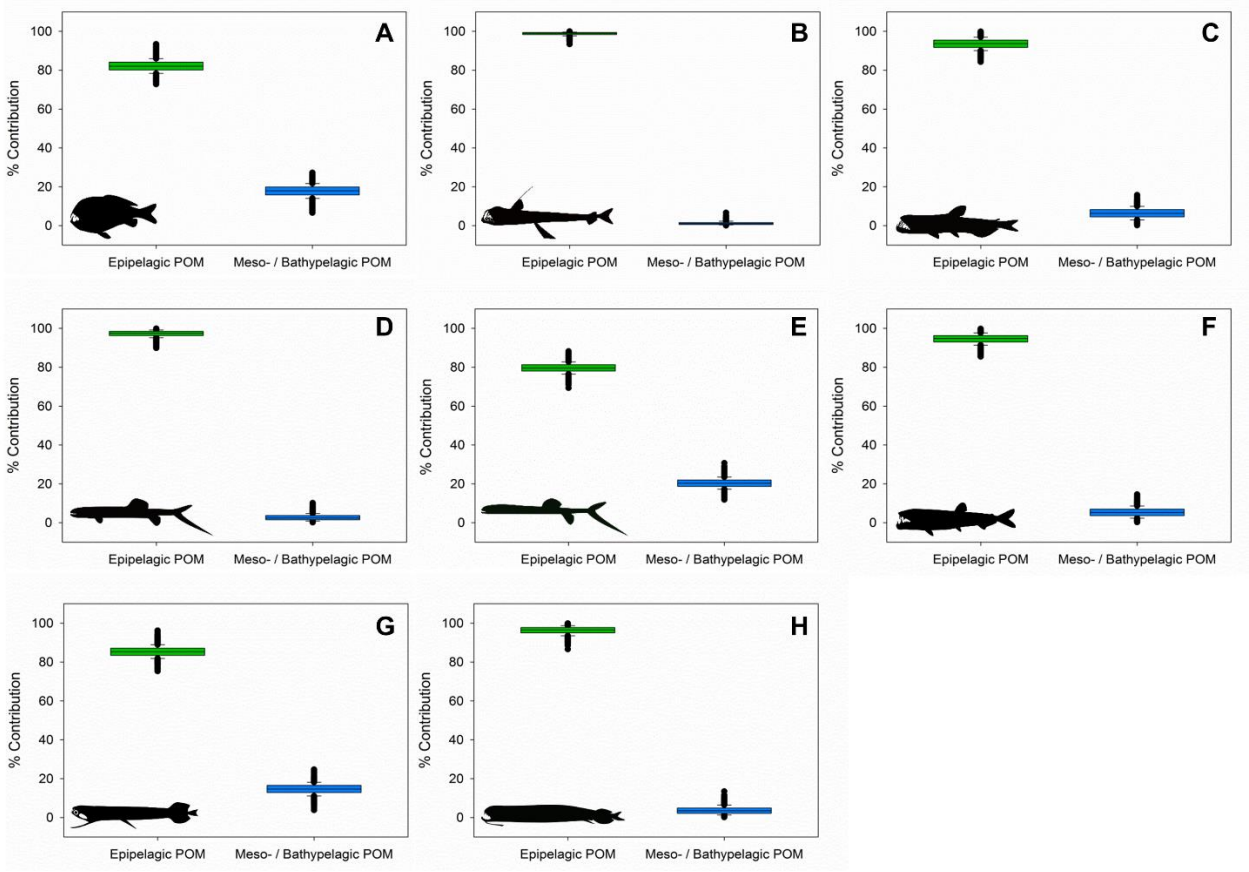

Figure 11. Estimated relative contributions of POM collected from epipelagic (green) and meso- and bathypelagic (blue) depths to meso- and bathypelagic fishes. (A) *A. cornuta* (B) *C. sloani* (C) *C. atlantica* (D) *G. chuni* (E) *G. indica* (F) *O. lowii* (G) *P. guernei* (H) *S. affinis.*

high variability in POM $\delta^{13}C$ and $\delta^{15}N$ values, the isotopic values of the fish species examined were much less variable, with mean $\delta^{13}C$ and $\delta^{15}N$ values spanning <2.0‰ among species and the narrow range of $\delta^{13}C$ values supports the notion that all consumers examined in this study are supported by a single carbon source, phytoplankton. Despite differences in vertical migration patterns, which was shown to affect the $\delta^{15}N$ values of non-migratory zooplanktivorous species (Chapter II), mean $\delta^{15}N$ values of the piscivorous species spanned a relatively narrow 1.96‰ when compared to the span of 3.43‰ observed in zooplanktivorous species in chapter II. Thus,

the relatively narrow range of $\delta^{13}C$ and $\delta^{15}N$ values examined in this predatory guild of fishes suggests that all species are likely feeding within food webs supported by POM from the same region of the water column in the epipelagic zone. Interestingly, even though these samples were collected in 2011, the range of $\delta^{13}C$ values observed in this study were extremely similar to those observed in Chapter II. Specifically, mean $\delta^{13}C$ values in zooplanktivorous species ranged between -19.85 to -18.29, while $\delta^{13}C$ values of the higher-order predators in this study varied between -19.38 to -18.25. The consistent range of $\delta^{13}C$ values in consumers collected >4 years apart, combined with no interannual differences observed in the $\delta^{13}C$ values of zooplanktivorous species in Chapter II, suggests that interannual variability in $\delta^{13}C$ values of deep-pelagic micronekton is relatively low.

Horizontal variation in POM and fish isotope values in the northern GOM was minimal, with only $\delta^{13}C$ values of POM showing a pattern of depletion in eastern longitudes, and $\delta^{13}C$ values of fishes becoming more enriched at southern latitudes and western longitudes. Shifts in the isotopic signatures of POM in the GOM have been observed between nearshore and offshore regions and between mesoscale cyclonic and anticyclonic oceanographic features (Wissel and Fry, 2005; Dorado et al., 2012, Wells et al., 2017). These shifts are thought to be caused by phytoplankton in offshore regions relying more heavily on isotopically light nitrogen produced by diazatrophic cyanobacteria (*Trichodesmium* spp.) relative to phytoplankton that are less influenced by *Trichodesmium spp*. and typically characterized by signatures that are ^{15}N enriched and ^{13}C depleted (Holl et al., 2007; Dorado et al., 2012). The pattern of POM samples becoming ^{13}C depleted at eastern longitudes and fishes becoming ^{13}C enriched at lower latitudes and western longitudes is consistent with the idea that organisms collected closer to the continental

shelf are more likely to be partially supported by terrestrially derived organic matter from the Mississippi River (Dorado et al., 2012).

Trophic position estimates inferred through stable isotope data suggest that within this group of fishes the highest trophic positions are held by the largely piscivorous *A. cornuta*, *G. chuni*, *G. indica*, and *S. affinis;* intermediate trophic positions are occupied by species preying on mixtures of cephalopods and fishes (*C. atlantica* and *O. lowii*), and fishes and crustaceans (*C. sloani*); and the lowest trophic position is occupied by *P. guernei*, which eats primarily macrocrustaceans (Hopkins et al., 1996; Sutton and Hopkins, 1996b). For the species examined, individual $\delta^{15}N$ values spanned 5.91‰ or 1.9 TPs, while species mean $\delta^{15}N$ values spanned 1.96‰ and 0.62 TPs (assuming TEF of 3.15). Using mean $\delta^{15}N$ values and applying a TEF of 3.15, our observed range of estimated trophic positions (0.62) appears to be in line with other studies examining Mediterranean Sea (1.1 TPs), Pacific Ocean (1.6 TPs), and GOM (1.1 TPs) fish assemblages that included both micronektonivores (stomiids, anoplogastrids) and lower-order zooplanktivores (myctophids, gonostomatids), which have been shown to be up to 0.6 lower TPs than micronektonivores (Valls et al., 2014; Choy et al., 2015; McClain-Counts et al., 2017).

Trophic position estimates determined using a primary consumer to set the isotopic baseline placed each species between the third and fourth trophic position. Where species-specific comparisons of trophic positions could be made, and applying a $\delta^{15}N$ TEF of 3.15 to reported mean $\delta^{15}N$ values, our estimated TP for *A. cornuta* (3.7) and *C. sloani* (3.2) were similar to estimates from the Pacific Ocean (TP = 3.5 for both species) and to the GOM (*C. sloani* TP = 2.8) (Choy et al., 2015; McClain-Counts et al., 2017). The observed difference in TP estimates for *C. sloani* in the GOM was likely caused by the inclusion of smaller *C. sloani* (< 50 mm SL)

by McClain-Counts et al. (2017). Estimates of TP for *S. affinis* (3.4) were similar to *Stomias boa* collected in the Mediterranean Sea (TP = 3.5) (Valls et al., 2014) while estimates of the three stomiid species, *C. sloani* (3.2), *S. affinis* (3.4) and *P. guernei* (3.1), were within the estimated worldwide TP range of stomiid fishes (TP = 3.0 – 3.5) (Choy et al., 2012). This study represents the first descriptions of trophic positions using stable isotope analysis for *C. atlantica*, *G. chuni*, *G. indica*, *O. lowii*, and *P. guernei* so comparisons to TP estimates in other studies were not possible.

Isotopic niche size, estimated using SEAc, was largest for fishes occupying the highest TP within the guild (*A. cornuta*, *C. chuni*, *G. indica*, *S. affinis*) and smallest in fishes with intermediate and lower TP (Figure 10). The larger SEAc of the highest TP fishes within this guild could suggest more generalized feeding compared to other species. Differences in SEAc can also be influenced by an organism's size distribution, which was not equally comprehensive in all species. The small SEAc of *C. sloani*, for example, was likely affected by samples that only included the largest individuals (>140 mm SL). Isotopic niche overlap was common although the extent of the overlap was typically non-significant (< 50%) (Table 8). In species displaying significant isotopic niche overlap (*S. affinis* and *O. lowii*), available SCA data suggest prey resource overlap is not as strong as isotopic niche overlap would make them appear (Hopkins et al., 1996; Sutton and Hopkins, 1996b).

Ontogenetic shifts in $\delta^{13}C$ and $\delta^{15}N$

Ontogenetic enrichment in ^{15}N was documented in six of the eight species examined. While significant relationships between $\delta^{15}N$ and length suggest ontogenetic patterns in feeding ecology, in some cases observed trends were driven by a few points and the nature of size-based relationships with $\delta^{15}N$ could change with the inclusion of different size classes and more

samples. Observed enrichment in ^{15}N with length could be caused by ontogenetic shifts in prey selection as has been suggested for *A. cornuta*, *C. sloani* and *P. guernei* or by ingestion of larger sized prey (Hopkins et al., 1996; Sutton and Hopkins, 1996b). For species such as *S. affinis* and *C. sloani* which have been shown to feed on myctophid fishes across their ontogeny, observed positive relationships between $\delta^{15}N$ and length could be a result of ingestion of larger myctophid fishes which have been shown to become enriched in ^{15}N with increasing size (Sutton and Hopkins, 1996b; Cherel et al., 2010; McClain-Counts et al., 2017). The negative relationship between length and $\delta^{15}N$ of *O. lowii* contrasts with published diet data suggesting *O. lowii* undergoes an ontogenetic diet shift from eating fishes as juveniles to feeding primarily on squid and fish as adults (Hopkins et al., 1996). *Omosudis lowii* are known to have highly distensible stomachs and have been reported to feed on prey much larger than themselves (Hopkins et al., 1996). However, the tendency to feed on large prey appears to occur primarily during juvenile stages as adults have been found to feed on both large and small prey (Hopkins et al., 1996). Thus, the lack of a relationship between SL and $\delta^{15}N$ of *O. lowii* could be a function of adults and juveniles feeding on similarly sized prey or by switching to prey that occupy lower TPs. The observed relationships between $\delta^{15}N$ and body length are not necessarily the result of ontogenetic shifts in diet and can instead reflect spatial and temporal changes in the isotopic signature of nitrogen sources at the base of the food web (Wells et al., 2017). Horizontal spatial variation in the isotopic signatures of primary producers has been documented in the GOM but the increased movements and longer tissue turnover rates of fishes likely diminishes spatial variation by increasing the likelihood of an organism integrating the isotopic signatures of multiple isotopic baselines. Additionally, the observed enrichment in ^{15}N with increasing length could reflect an ontogenetic shift in the relative use of food webs supported by isotopically enriched POM at

deeper depths. While some species of deep-pelagic fishes do show ontogenetic shifts in depth (Gartner, 1987), the major shifts in depth distribution typically occur in the larval and post-larval stage. For all species examined in this study, samples were taken from juvenile and adult stage individuals that do not undergo the rapid ontogenetic shift in depth distribution seen in early life stages. Thus, it is likely that the observed ontogenetic shifts in ^{15}N are likely driven by changes in feeding and not habitat use.

Relative contributions of epi-, meso-, and bathypelagic POM to deep-pelagic fishes

A paradigm of deep-sea ecology is that meso- and bathypelagic organisms feed within food webs largely supported by epipelagic POM and that POM suspended at deeper depths contributes little carbon to higher order consumers. Recently, through the use of compound specific stable isotope analysis (CS-SIA) of amino acids (AAs), that paradigm was challenged by evidence which suggests zooplankton and micronekton can partly rely on small particle (0.7 – 53 µm) suspended POM as a carbon source (Hannides et al., 2013; Choy et al., 2015; Gloeckler et al., 2018). Choy et al. (2015) estimated the relative contributions of epipelagic and deep-water POM to the production of four fishes (including *A. cornuta*) in the North Pacific Ocean and found that two meso- and bathypelagic zooplanktivores received contributions from small particle, deep-pelagic suspended POM ranging between 39-81%, while contributions to the micronektonivore, *A. cornuta*, were far less (0-23%). Gloeckler et al. (2018) examined the $\delta^{15}N$ values of source AAs from a micronekton assemblage and found that relative contributions of small, suspended particles to micronekton were greatest in non-migratory species with nighttime distributions in the lower mesopelagic and upper bathypelagic. Species with nighttime distributions within the epi- and mesopelagic, however, were found to be supported by either

surface particles or large, fast sinking particles (>53 μm) at depth (Hannides et al., 2013; Gloeckler et al. 2018).

The results from our mixing model analyses suggest that the majority of carbon (≥ 73%) supporting the species examined in this study appears to be derived from epipelagic sources or from fast sinking particles at depth which carry similar isotopic signatures to particles within the epipelagic (Hannides et al., 2013). These contribution estimates, combined with vertical distribution data which suggest the collective nighttime distributions of these predatory fishes span the epi-, meso- and upper bathypelagic (Sutton and Hopkins, 1996a; Sutton et al., 2010), are in alignment with estimations for micronekton with similar depth distributions made by Choy et al. (2015) and Gloeckler et al. (2018). It should be noted that the relative contribution of small suspended particles to these species cannot be fully assessed without conducting CSIA-AA and that further investigation into the relative importance of small particles to these higher trophic level consumers is warranted (Gloeckler et al., 2018). Additional support for the assertion that these species are largely supported by surface derived carbon is provided by diet studies which suggest these species consume migratory prey that feed within food chains supported by surface production (Hopkins et al., 1996; Sutton and Hopkins, 1996b) highlighting the extent to which spatially distinct consumers are connected in the northern GOM.

CHAPTER IV

TROPHIC STRUCTURE AND FOOD WEB DYNAMICS OF A DIVERSE MESO- AND BATHYPELAGIC MICRONEKTON ASSEMBLAGE IN THE GULF OF MEXICO

Introduction

Worldwide, marine ecosystems are threatened by a variety of stressors including climate change, ocean acidification, eutrophication, habitat loss, overfishing, and natural resource extraction which have resulted in profound changes to ecosystem structure and function (Meyers & Worm, 2003; Syvitski et al., 2005; Lotze et al., 2006; Halpern et al., 2008; Menegerink et al., 2014). A thorough understanding of the scale and nature of changes to marine ecosystem functioning, and their subsequent effects on the provision of ecosystem services is critical to the formation of informed ecosystem management and policy (Thurber et al., 2014).

Ecosystem models, conceptual and theoretical frameworks representing a synthesized understanding of all major parts of an ecosystem, are powerful ecosystem management tools as they can be used to forecast ecosystem responses to hypothetical environmental, resource use, and management scenarios (Choy et al., 2013; Pethybridge et al., 2018). The construction of effective ecosystem models, which demands large quantities of data relevant to physical, chemical, biological and ecological processes, can be difficult to obtain, particularly in oceanic ecosystems due to their complexity, vast size, and the logistical constraints associated with their study. Of all marine ecosystems, the deep-pelagic ocean (waters beyond shelf break >200 m depth to above the seafloor) is the largest, most difficult to study, and most poorly understood ecosystem on the planet (Webb et al., 2010). Encompassing >90% of the world's living space by volume, the deep-pelagic realm affects all life on the planet through its vital roles in the global

carbon and climate cycles. Additionally, the deep pelagic and deep seafloor provide essential ecosystem services including carbon sequestration, nutrient recycling, fisheries production and contain massive stores of energy resources, precious metals and minerals (Thurber et al., 2014). Despite their vast size and remoteness, deep-pelagic ecosystems are changing rapidly due to climate change, ocean acidification, overfishing, and increasing natural resource extraction, with the rate and scale of change far outpacing our ability to describe and manage these changes (Sutton et al., 2020; Murawski et al., 2020). In light of these persistent threats and subsequent changes to ecosystem structure and function, there has been a concerted effort to develop comprehensive deep-pelagic ecosystem models so that management plans can be implemented and the effects of anthropogenic activities can be assessed (Ramirez-Lodra et al., 2011; Mengerink et al., 2000).

Of critical importance to the construction of ecosystem models is a thorough understanding of food web structure including descriptions of feeding relationships among species and major functional groups. Descriptions of food webs are particularly important for ecosystem models as they delineate the flow of energy and can be used to quantify the strength of relationships among species (Polis and Strong, 1996; Winemiller and Polis, 1996). Traditionally, the study of food webs has been conducted using stomach content analysis (SCA) as it provides direct evidence of feeding relationships among species and allows for the effect of one species on another through predation to be quantified (Hyslop, 1980; Winemiller and Polis, 1996). Despite its utility, SCA only provides a glimpse of an animal's feeding habits over short time scales (hours to days) necessitating large sample sizes (hundreds) to identify meaningful patterns across comprehensive spatial and temporal scales (Hyslop, 1980). Additionally, the taxonomic resolution of identified prey items is highly dependent on the taxonomic expertise of

the researchers and prey identification is easier in taxa that swallow their prey whole, resulting in a bias in the types of consumers studied (Hyslop, 1980). The shortcomings of SCA are particularly problematic in the deep-pelagic realm where samples are expensive and difficult to obtain and many species are present are uncommon or rare, making the procurement of large sample sizes difficult. Stable isotope analysis (SIA) is a complimentary tool in food web analysis that addresses many of the shortcomings of SCA. Unlike SCA, SIA provides feeding information that is integrated over longer timescales (weeks to months), which reduces variation among samples and allows for the identification of meaningful patterns and trends using smaller sample sizes (Layman et al., 2007). In ecological studies, isotopes of carbon, which undergo relatively low levels of fractionation during trophic transfer are used to trace the flow of energy from primary producers to higher-order consumers (Peterson and Fry, 1987), while stable isotopes of nitrogen undergo relatively larger levels of fractionation during trophic transfer and can be used to estimate trophic position within the food web and identify trophic relationships among consumers (Post, 2002; Layman et al., 2005). When combined, SIA and SCA provide complimentary views of food webs that can be used to directly parameterize ecosystem models by integrating feeding information of consumers differing timescales.

When considering the structure of deep-pelagic food webs and deep-pelagic ecosystems, perhaps the most critical functional group is comprised of small (2-10 cm) fishes, crustaceans, and cephalopods collectively known as micronekton. As dominant proportions of the global fish, crustacean and cephalopod biomass, deep-pelagic micronekton are critical to the structure and function of deep-pelagic ecosystems (Choy et al., 2013; Irigoien et al., 2014; Vereshchaka et al., 2019). Highly abundant throughout the world's oceans, micronekton play critical roles in deep-pelagic food webs as both predators and prey (Hopkins et al., 1996; Choy et al., 2013;

Drazen and Sutton, 2017). As predators, micronekton have been shown to be important consumers capable of exerting top-down control on zooplankton populations and, in turn, are known to be important contributors to the diets of marine mammals, seabirds, and economically valuable fishes including tunas and billfishes (Hopkins and Gartner, 1992; Moteki et al., 1991; Choy et al., 2013). Many species of micronekton undertake diel vertical migrations (DVM) at night from the deep-pelagic to access the nutrient and food-rich waters of the epipelagic while remaining hidden from visually cued predators. By incorporating carbon derived from surface production and then respiring and excreting carbon at daytime depths in the meso- and bathypelagic, micronekton play an important role in the biological pump by vertically transporting carbon into the deep sea (Wilson et al., 2009; Thurber et al., 2014). Additionally, through their vertical migrations, micronekton serve as vectors for the transport of surface derived production to deep-pelagic communities by falling prey to non-migratory deep-pelagic and demersal species (Sutton and Hopkins, 1996b; Portiero and Sutton, 2007; Trueman et al., 2014). Due to their high global biomass, pivotal roles in the global carbon cycle, and their importance to deep-pelagic food webs and vertical connectivity in the pelagic ocean, detailed data regarding the trophic ecology of micronekton are critical to the formation of effective ecosystem models.

The GOM is a semi-enclosed ocean basin physically distinct from both the Caribbean Sea and greater Atlantic Ocean, which exhibits physical and biological characteristics typical of oligotrophic, low-latitude pelagic ecosystems worldwide. With recent faunal inventories identifying 897 species of fishes, 120 species of crustaceans, and 94 species of cephalopod, the micronekton assemblage in the GOM is diverse and was recently identified as one of the four most speciose marine ecoregions on the planet (Sutton et al., 2017b; Sutton et al., 2020). In

addition to a diverse pelagic fauna, the GOM supports lucrative coastal and pelagic fisheries and is the focus of intense oil and gas exploration and extraction that has steadily expanded into the deep-pelagic realm (Murawski et al., 2020). Despite the deep-pelagic GOM's global importance to biological diversity and regional importance to local economies, detailed knowledge of GOM pelagic food webs are lacking, a point amplified by the *Deepwater Horizon* oil spill. In this chapter I build upon the findings presented in Chapters II and III by examining the trophic structure of 55 species of micronekton collected from the northern GOM. Specifically, I employ the use of SIA and SCA data from the literature to 1.) Delineate major functional groups within the GOM micronekton assemblage 2.) Model isotopic variation in the micronekton assemblage using multiple linear regression to examine how differences in diet, vertical migration, and spatial distribution affect trophic structure of the assemblage 3.) Provide detailed trophic position estimates for each species micronekton with a comparison between estimations made using SCA and SIA data.

Methods

Sample collection and study design

This study was conducted within the framework of a larger, collaborative research consortium tasked with describing deep-pelagic nekton dynamics in the GOM (DEEPENDConsortium.org). Sampling methodologies and detailed oceanographic cruise descriptions are outlined by Cook et al. (2020) and Milligan et al. (2019) but a succinct methodological description follows. Micronekton samples were collected in 2016 in the northern GOM (Figure 12) using a 10-m2 multiple opening and closing net with environmental

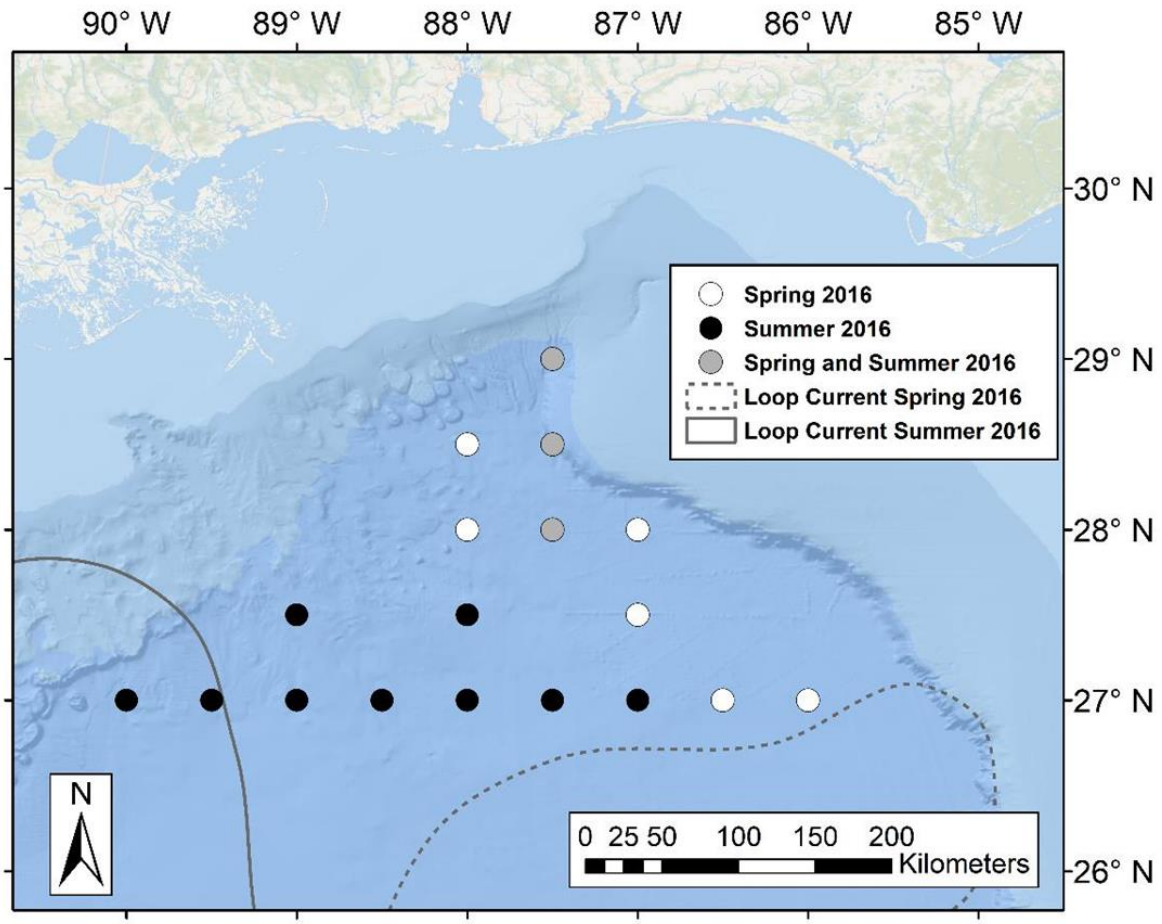

Figure 12. Map of the northern Gulf of Mexico showing sampling locations during spring (white circles), summer (black circles) and spring and summer (gray circles) for oceanographic cruises conducted in 2016. Dashed and solid lines represent approximate location of the Loop Current defined by 20-cm sea surface height anomaly (SSHA) during spring and summer sampling periods, respectively. Loop Current positions were created using remotely sensed sea surface height data available through the Copernicus Marine Environmental Monitoring Service.

sensing ecosystem (MOCNESS). The MOCNESS consisted of six individual nets fitted with 3-mm stretch nylon mesh able to be deployed at specific depths throughout the water column. During each deployment, depth strata sampled by the MOCNESS included samples within the epipelagic (0-200 m), upper-mesopelagic (200-600 m), lower-mesopelagic (600-1000 m), and

two samples within the upper bathypelagic (1000-1200 m & 1200-1500 m). Upon retrieval of the MOCNESS, micronekton were sorted, identified to species, and enumerated. Samples for SIA were frozen whole at -20ºC until processing at Texas A&M University at Galveston.

For this study, 55 species of deep-pelagic micronekton with contrasting migratory patterns and vertical distributions representing a range of trophic strategies (detritivores, zooplanktivores, micronektonivores, piscivores) were selected to provide as broad a view of deep-pelagic trophic structure as possible (Table 9). Additionally, I purposefully selected species that were included in previous diet studies of deep-pelagic micronekton in the GoM (Passarella and Hopkins, 1991; Hopkins et al., 1996; Sutton and Hopkins, 1996b; Burghart et al., 2010) to allow for comparisons between trophic structure estimates derived from SCA and SIA.

Stable isotope analysis

Samples for SIA were dissected from the lateral musculature of fishes, the anterior mantle of cephalopods, and from the abdomen of crustaceans. Following dissection, tissue samples were examined under a dissection microscope to ensure skin, scales, bones, or exoskeleton were completely removed. Isotope samples were then rinsed thoroughly with deionized water to remove any trace carbonates. All isotope samples were freeze dried, homogenized using an agate mortar and pestle, and wrapped in tin capsules before shipment to the UC Davis Stable Isotope Facility. Samples were analyzed for ^{13}C and ^{15}N isotopes using a PDZ Europa ANCA-GSL elemental analyzer coupled with a PDZ Europa 20-20 isotope ratio mass spectrometer. Stable isotope data are expressed in δ-notation as the deviation from the international standards Vienna PeeDee belemnite and atmospheric N_2 for carbon and nitrogen, respectively. The UC Davis Stable Isotope Facility reports a long-term standard deviation of

Table 9. Summary table depicting sample sizes, length, $\delta^{13}C$, $\delta^{15}N$ values (mean ± SD), median day and nighttime depth of occurrence, and trophic position estimates for micronekton.
***n*: number of samples; M/NM: M, migrator; NM, non-migrator; TP:SCA: trophic position derived from stomach content analysis; TP:SIA: trophic position derived from stable isotope analysis.**

Species	*n*	Family	M/ NM	Length (cm)	$\delta^{13}C$ (‰)	$\delta^{15}N$ (‰)	Med. Night Depth (m)	Med. Day Depth (m)	Diet Guild	TP: SCA	TP: SIA
Argyropelecus aculeatus	5	Sternoptychidae	M	3.7 ± 1.0	-19.4 ± 0.3	8.4 ± 0.4	150	325	Zoo 3	3.7	3.7 ± 0.1
Benthosema suborbitale	15	Myctophidae	M	2.6 ± 0.4	-19.3 ± 0.2	8.2 ± 0.9	80	500	Zoo 1	3.4	3.6 ± 0.3
Bolinichthys photothorax	7	Myctophidae	M	3.1 ± 1.0	-19.5 ± 0.3	7.5 ± 0.7	150	675	Zoo 1	--	3.4 ± 0.2
Ceratoscopelus warmingii	8	Myctophidae	M	4.0 ± 1.6	-19.7 ± 0.5	7.4 ± 1.0	100	750	Zoo 2	3.4	3.4 ± 0.3
Chauliodus sloani	17	Stomiidae	M	18.6 ± 3.4	-18.6 ± 0.3	9.1 ± 0.6	600	600	Pisc.	4.3	3.9 ± 0.2
Diaphus dumerilii	8	Myctophidae	M	3.7 ± 0.8	-19.5 ± 0.4	8.4 ± 0.6	105	450	Zoo 1	--	3.7 ± 0.2
Diaphus lucidus	10	Myctophidae	M	5.2 ± 1.7	-19.8 ± 0.6	8.9 ± 0.8	180	725	Zoo 3	--	3.8 ± 0.3
Diaphus mollis	10	Myctophidae	M	3.7 ± 0.8	-19.6 ± 0.3	9.1 ± 0.7	155	650	Zoo 1	--	3.9 ± 0.1
Diaphus splendidus	5	Myctophidae	M	3.5 ± 1.8	-19.5 ± 0.3	8.1 ± 1.1	140	450	Zoo 1	--	3.6 ± 0.2
Diogenichthys atlanticus	4	Myctophidae	M	1.8 ± 0.2	-20.6 ± 0.2	6.8 ± 0.4	135	525	Zoo 1	3.1	3.2 ± 0.3
Echiostoma barbatum	5	Stomiidae	M	19.8 ± 7.8	-18.3 ± 0.6	9.8 ± 0.6	500	800	Pisc.	4.1	4.1 ± 0.2
Hygophum benoiti	6	Myctophidae	M	1.8 ± 0.1	-19.0 ± 0.4	8.0 ± 0.9	125	500	Zoo 1	--	3.6 ± 0.3
Hygophum taaningi	10	Myctophidae	M	3.0 ± 0.6	-19.0 ± 0.3	7.8 ± 1.1	155	675	Zoo 1	3.1	3.5 ± 0.3
Lampadena luminosa	8	Myctophidae	M	2.3 ± 0.5	-19.3 ± 0.5	6.1 ± 0.7	210	750	Zoo 5	--	3.0 ± 0.2
Lampanyctus alatus	15	Myctophidae	M	3.5 ± 0.8	-19.7 ± 0.3	8.0 ± 0.7	115	625	Zoo 2	3.2	3.6 ± 0.2
Lepidophanes guentheri	15	Myctophidae	M	3.6 ± 1.3	-19.2 ± 0.3	7.3 ± 1.1	115	650	Zoo 2	--	3.3 ± 0.3
Melamphaes simus	15	Melamphaeidae	M	2.3 ± 0.4	-19.3 ± 0.6	9.3 ± 1.1	600	850	Zoo 1	--	4.0 ± 0.4
Myctophum affine	10	Myctophidae	M	3.1 ± 1.1	-19.4 ± 0.6	8.4 ± 1.2	80	500	Zoo 1	--	3.7 ± 0.4
Nannobrachium lineatum	9	Myctophidae	M	8.7 ± 0.7	-19.3 ± 0.2	8.7 ± 0.5	500	700	Zoo 2	--	3.8 ± 0.2
Notolychnus valdiviae	10	Myctophidae	M	1.8 ± 0.2	-19.9 ± 0.3	7.3 ± 0.7	105	450	Zoo 1	3.1	3.3 ± 0.2
Notoscopelus resplendens	4	Myctophidae	M	3.4 ± 1.2	-19.8 ± 0.4	7.5 ± 1.6	105	1050	Zoo 2	--	3.4 ± 0.5
Photostomias guernei	5	Stomiidae	M	8.4 ± 2.5	-18.7 ± 0.5	8.7 ± 0.3	485	700	Micro.	3.5	3.8 ± 0.1
Pollichthys mauli	5	Phosichthyidae	M	3.5 ± 0.7	-19.1 ± 0.2	7.5 ± 0.9	100	400	Zoo 2	3.7	3.4 ± 0.3
Sigmops elongatus	15	Gonostomatidae	M	9.5 ± 2.6	-19.0 ± 0.4	8.7 ± 0.5	175	575	Zoo 2	3.3	3.8 ± 0.2
Stomias affinis	5	Stomiidae	M	13.7 ± 1.7	-18.6 ± 0.6	9.7 ± 0.7	435	650	Pisc.	4.3	4.1 ± 0.2
Vinciguerria nimbaria	5	Phosichthyidae	M	2.8 ± 0.7	-19.1 ± 0.3	7.8 ± 0.6	100	400	Zoo 1	3.1	3.5 ± 0.2

Table 9 Continued

Species	*n*	Family	M/ NM	Length (cm)	$\delta^{13}C$ (‰)	$\delta^{15}N$ (‰)	Med. Night Depth (m)	Med. Day Depth (m)	Diet Guild	TP: SCA	TP: SIA
Pterygioteuthis gemmata	6	Pyroteuthidae	M	1.1 ± 0.4	-19.5 ± 0.3	8.0 ± 0.3	100	750	Zoo 1	--	3.6 ± 0.1
Stigmatoteuthis arcturi	4	Histioteuthidae	M	1.0 ± 0.2	-19.7 ± 0.2	9.5 ± 0.7	600	750	Zoo 1	--	4.0 ± 0.2
Acanthephyra purpurea	14	Oplophoridae	M	3.6 ± 2.7	-18.3 ± 0.5	7.8 ± 0.6	175	900	Zoo 2	--	3.8 ± 0.2
Sergia splendens	11	Sergestidae	M	3.5 ± 0.3	-19.6 ± 0.5	6.7 ± 0.7	250	975	Zoo 2	3.6	3.4 ± 0.3
Systellaspis debilis	6	Oplophoridae	M	--	-18.8 ± 0.6	7.2 ± 0.7	175	675	Zoo 2	3.5	3.6 ± 0.3
Thysanopoda acutifrons	5	Euphausiidae	M	3.4 ± 0.2	-19.3 ± 0.1	9.1 ± 0.5	600	700	Zoo 1	3.7	4.3 ± 0.2
Anoplogaster cornuta	4	Anoplogastridae	NM	12.4 ± 0.8	-19.1 ± 0.2	9.9 ± 1.1	628	950	Pisc.	4.0	4.2 ± 0.3
Argyropelecus hemigymnus	14	Sternoptychidae	NM	2.5 ± 0.4	-18.7 ± 0.4	9.1 ± 0.6	325	375	Zoo 4	3.1	3.9 ± 0.2
Cyclothone acclinidens	10	Gonostomatidae	NM	3.2 ± 0.3	-18.3 ± 0.3	10.5 ± 0.5	900	900	Zoo 1	3.6	4.4 ± 0.2
Cyclothone alba	10	Gonostomatidae	NM	2.6 ± 0.2	-19.6 ± 0.3	7.5 ± 0.5	425	425	Zoo 1	--	3.4 ± 0.1
Cyclothone braueri	10	Gonostomatidae	NM	2.3 ± 0.1	-19.1 ± 0.3	6.9 ± 0.5	400	400	Zoo 1	3.1	3.2 ± 0.2
Cyclothone obscura	15	Gonostomatidae	NM	4.4 ± 0.6	-18.4 ± 0.4	10.5 ± 0.9	1950	1950	Zoo 1	--	4.4 ± 0.3
Cyclothone pallida	10	Gonostomatidae	NM	4.3 ± 0.7	-18.7 ± 0.7	9.6 ± 0.9	850	850	Zoo 1	3.2	4.1 ± 0.3
Cyclothone pseudopallida	10	Gonostomatidae	NM	3.3 ± 0.4	-19.4 ± 0.3	8.2 ± 0.3	600	600	Zoo 1	3.1	3.6 ± 0.1
Poromitra gibbsi	3	Melamphaeidae	NM	10.4 ± 1.0	-19.2 ± 0.1	10.9 ±	800	900	Gelat.	--	4.5 ± 0.1
*Rhynchoconger flavus**	5	Congridae	NM	--	-21.6 ±0.1	5.5 ±	100	100	Detr.	--	2.8 ± 0.1
Scopeloberyx opercularis	7	Melamphaeidae	NM	2.6 ± 0.1	-18.9 ± 0.2	11.1 ± 0.4	1050	1050	Zoo 1	3.1	4.6 ± 0.1
Scopeloberyx opisthopterus	7	Melamphaeidae	NM	2.3 ± 0.2	-20.0 ± 0.3	9.4 ± 0.8	900	1050	Zoo 1	--	4.0 ± 0.3
Scopeloberyx robustus	6	Melamphaeidae	NM	2.1 ± 0.4	-19.7 ± 0.6	9.2 ± 0.9	1050	1050	Zoo 1	--	3.9 ± 0.3
Sternoptyx diaphana	14	Sternoptychidae	NM	2.2 ± 0.7	-19.5 ± 0.2	8.6 ± 0.7	600	600	Zoo 5	3.2	3.7 ± 0.2
Sternoptyx pseudobscura	15	Sternoptychidae	NM	2.9 ± 1.0	-19.7 ± 0.3	8.2 ± 0.5	1000	1000	Zoo 2	3.4	3.6 ± 0.3
Valenciennellus tripunctulatus	5	Sternoptychidae	NM	2.4 ± 0.1	-19.8 ± 0.2	9.0 ± 0.4	340	400	Zoo 1	3.1	3.9 ± 0.1
Bolitaena pygmaea	6	Amphitretidae	NM	1.1 ± 0.3	-19.4 ± 0.7	6.5 ± 1.2	750	750	Zoo 1	3.7	3.1 ± 0.4
Japatella diaphana	10	Amphitretidae	NM	2.6 ± 2.0	-19.2 ± 0.5	6.1 ± 1.3	750	750	Zoo 1	3.6	2.9 ± 0.4
Mastigoteuthis agassizii	2	Mastigoteuthidae	NM	6.9 ± 0.4	-18.3 ± 0.1	11.5 ± 0.8	1050	1050	Pisc.	--	4.7 ± 0.2
Vampyroteuthis infernalis	3	Vampyroteuthidae	NM	1.4 ± 0.7	-19.0 ± 0.2	10.4 ± 2.3	1050	1050	Zoo 1	3.5	4.3 ± 0.7
Acanthephyra curtirostris	13	Oplophoridae	NM	4.3 ± 3.5	-18.5 ± 0.2	9.1 ± 0.5	1050	1050	Micro.	3.8	4.3 ± 0.2
Acanthephyra stylorostrata	11	Oplophoridae	NM	2.7 ± 2.0	-18.7 ± 0.2	8.9 ± 0.3	1300	1300	Micro.	4.0	4.2 ± 0.1
Eucopia sculpticauda	4	Eucopiidae	NM	--	-18.8 ± 0.3	10.4 ± 0.4	1650	1650	Zoo 1	--	4.8 ± 0.2

0.2‰ for $\delta^{13}C$ and 0.3‰ for $\delta^{15}N$. Mean C:N values of micronekton species ranged between 3.17-4.33, suggesting lipid content in samples could confound the interpretation of $\delta^{13}C$ values (Post, 2007). Thus, all $\delta^{13}C$ values were mathematically corrected according to Post et al. (2007) before any statistical analyses were performed.

Trophic position designations

Trophic position estimates using SIA (TP-SIA) were made using equation 3:

$$\text{Equation 3:} \quad TrP_i = (\delta^{15}N_i - \delta^{15}N_{Base})/\Delta^{15}N + \lambda$$

where $\delta^{15}N_i$ is the nitrogen isotopic signature of an individual belonging to species i, $\delta^{15}N_{Base}$ is the nitrogen isotopic signature of the primary producer or consumer used to set the baseline, $\Delta^{15}N$ is the expected level of $\delta^{15}N$ fractionation between predator and prey, and λ represents the trophic level of the baseline organism (2 for primary consumer). Choosing an appropriate trophic discrimination factor (TDF) is a crucial component of estimating trophic position (REF). Generally, TDFs should be as specific to the species, tissue type and environment (freshwater vs. marine vs. terrestrial) of the study organism(s) as possible. Due to the inherent difficulties of keeping deep-pelagic taxa alive, lab-based trophic discrimination studies have not been conducted for deep-pelagic organisms. Instead, I selected TDFs derived from laboratory experiments of marine fishes ($\Delta^{15}N = 3.15 \pm 1.28$; Sweeting et al 2007b), and crustaceans ($\Delta^{15}N = 2.60 \pm 0.30$) that examined discrimination factors in white muscle tissue. The TDF for fishes outlined by Sweeting et al. (2007b) was applied to cephalopods due to a lack of squid and octopus specific TDFs in the literature. Samples of the tunicate *Pyrosoma atlanticum* collected concurrently with micronekton were used to set the nitrogen isotopic baseline ($\delta^{15}N_{Base}$ in Equation 3). Pyrosomes are known to feed on suspended organic matter and have been used previously to delineate isotopic baselines in pelagic ecosystems (Cherel et al., 2008; Menard et

al., 2014). Pyrosomes have been shown to more accurately represent the primary consumer trophic position in low-latitude oligotrophic ecosystems like the pelagic GOM. In these ecosystems, phytoplankton communities are primarily comprised of small flagellates rather than large diatoms, which have been shown to be unassimilated during pyrosome feeding (Harbou et al., 2011; Pakhomov et al., 2019). Additionally, the $\delta^{15}N$ values of *P. atlanticum* (3.11 ± 0.44) are consistent with $\delta^{15}N$ values of epipelagic copepods (a dominate food source of migratory deep-pelagic fishes) reported from the northwestern (Holl et al. 2007) and northern (Wells et al., 2017) regions of the GOM. Considering the utility of estimating trophic position to ecosystem based models, I compared trophic position estimates made using stable isotope analysis (TP:SIA) to estimates made using stomach content data (TP:SCA) to examine whether or not TP:SIA estimates serve as an accurate alternative to estimates made using TP:SCA. Estimates of TP:SCA for fishes were taken from FishBase.org, while estimates for crustaceans and cephalopods, when available, were taken from SeaLifeBase.org. Estimates of TP:SCA derived from a single prey item in FishBase and SeaLifeBase were excluded from this analysis. For a detailed description of the methods used by FishBase and SeaLifeBase to calculate TP I refer the reader to Froese and Pauly (2018) and Mancinelli et al. (2012). Following TP estimates, I conducted linear regression to examine the relationship between TP:SIA and TP:SCA for both migratory and non-migratory species.

Feeding guild determination

Micronekton species were assigned to feeding guilds according to criteria identified and described by Hopkins et al. (1996) during their diet analysis of 164 species of deep-pelagic fishes collected from the GOM. To allow for the identification of ontogenetic shifts in diet, Hopkins et al. (1996) divided individuals from each species into 10 mm size classes which were used as the

base unit in subsequent cluster analyses (as opposed to species). Thus, some species were found to have individuals of differing sizes assigned to different feeding guilds. For species belonging to multiple feeding guilds, I averaged the size of the individuals included in our analysis and assigned all individuals to the corresponding feeding guild for that size class. For crustaceans, cephalopods and fish species not included in Hopkins et al. (1996), quantitative diet data were taken from primary literature sources and applied to the same feeding guild criteria used for fishes in Hopkins et al. (1996). While examination of deep-pelagic fish diets by Hopkins et al., (1996) was comprehensive, diets of leptocephalus larvae, an important component of pelagic fish diversity in the GOM (Moore et al., 2020), were not considered. Several studies have suggested that pelagic leptocephalus larvae feed on particulate organic matter (POM) including fecal pellets and discarded housings from pelagic larvaceans. I subsequently identified the leptocephalus congrid eel Rhynchoconger flavus as a detritivore, a feeding guild not included in the analysis by Hopkins et al. (1996). To see references used to assign each species to a feeding guild, see Appendix Table B-1.

Median depth of occurrence determination for micronekton

In order to investigate the effect of depth on $\delta^{13}C$ and $\delta^{15}N$ values of micronekton, median depth of occurrence for each species was derived from vertical depth distribution data in the primary literature or from data collected by the DEEPEND Consortium during MOCNESS sampling. To attain the highest resolution vertical distribution data possible, I estimated median depth of occurrence using data from studies employing opening and closing trawls only (MOCNESS, Tucker Trawl). I did not consider data from open net trawls where the relative capture location of an individual within a large swath of the water column (>400 m) could not be determined. If multiple discrete-depth, vertical distribution data sets were available, priority was

given to studies with the finest scale vertical distribution data. Additionally, depth distribution data derived from studies conducted in the GOM were given preference over data from the Atlantic Ocean or Pacific Ocean. For references used to assign species a median depth of occurrence, see Appendix Table B-1.

Statistical analysis

Trophic structure of the micronekton assemblage was first explored using hierarchical cluster analysis on per-species mean $\delta^{13}C$ and $\delta^{15}N$ values to determine the number of trophic groupings represented in the assemblage. Cluster analysis was performed using Ward's minimum variance clustering as it employs an analysis of variance approach to evaluate distances between clusters, producing the smallest possible increase in the error sum of squares. Statistically significant clusters were identified using similarity profile routines (SIMPROF) at a significance level of 0.05. Following cluster analysis, one-way analysis of variance (ANOVA) was used to examine patterns of isotopic differences among identified clusters. Assumptions of ANOVA were checked using Shapiro-Wilk test (normality) and Levene's test (homogeneity of variance). Following ANOVA, *a posteriori* differences among means were analyzed using Tukey's Honestly Significant Difference test (Tukey HSD).

Multiple linear regression was used to explain observed variation in $\delta^{13}C$ and $\delta^{15}N$ values of migratory and non-migratory micronekton. Specifically, I examined the relationship between $\delta^{13}C$ and $\delta^{15}N$ values with body length, median nighttime depth of occurrence, median daytime depth of occurrence, capture location (latitude and longitude), and sampling season (spring, summer). Additionally, because the stable isotope ratios of zooplanktivorous species were shown to be influenced by the Loop Current in Chapter II, water type (Loop Current (LCW), Gulf Common Water (GCW)) was included as a categorical factor during multiple linear

regression. A stepwise model selection procedure was used to identify and remove non-significant independent variables and interactions. Model fit was assessed using Akaike information criterion (AIC), while multicollinearity between independent variables was assessed using Variance Inflation Factors (VIF). For all models examined, VIF scores were < 3.0 indicating multicollinearity between independent variables was not an issue in our analysis. Normality for all multiple regression models were assessed visually using qqplots. Following model construction, variable importance was assessed by removing each retained independent variable from the final model and calculating the subsequent change in AIC (ΔAIC) and change in % deviance explained (ΔDE).

Results

In total, SIA was conducted on 471 individuals from 55 species of micronekton collected from the GOM. Species mean $\delta^{13}C$ values encompassed a relatively narrow range from -21.56 to -18.25‰, while mean $\delta^{15}N$ values was between 5.53‰ and 11.47‰. Using the criteria outlined by Hopkins et al. (1996), nine distinct feeding guilds spanning several putative food web levels from detritivores to piscivores were identified in the micronekton assemblage (Table 10).

To compare diet data with stable isotope data, all individual $\delta^{13}C$ and $\delta^{15}N$ values from the micronekton assemblage are shown in Figure 13 grouped by feeding guild. Relative positions of feeding guilds within isotope space aligned with known feeding relationships, with detritivores possessing lower mean $\delta^{13}C$ and $\delta^{15}N$ values, micronektonivores and piscivores characterized by higher $\delta^{13}C$ and $\delta^{15}N$ values, and mean isotope values of zooplanktivores intermediate (Figure 13). Notably, however, the range of individual $\delta^{15}N$ values for several feeding guilds of zooplanktivores (Zoo 1, Zoo 2, Zoo 5 from Table 10) was far greater than

Table 10. Description of feeding guilds used to classify species within the GOM micronekton assemblage.

Functional Group	Feeding Guild	Feeding Guild Description
Detritivore	Detritivore	Marine snow and other particulate organic matter including fecal pellets and discarded larvacean housings
Zooplanktivore	Zoo 1	Predominantly small crustaceans, with copepods the highest contributing category
Zooplanktivore	Zoo 2	Mixed crustacean diet with large contributions by both copepods and small euphausiids
Zooplanktivore	Zoo 3	Mixed crustacean diet primarily comprised of euphausiids and decapod crustaceans
Zooplanktivore	Zoo 4	Mixed crustacean diet with ostracods representing >40% of prey biomass
Zooplanktivore	Zoo 5	Mixed crustacean diet with amphipods representing >33% of prey biomass
Gelativore	Gelativore	Gelatinous prey items comprise more than two thirds of prey by biomass
Micronektonivore	Micronektonivore	Diet dominated by large decapod crustaceans, with fish and other miscellaneous prey supplementing
Micronektonivore	Piscivore	Diet dominated by fishes which represent >84% of prey items by number

expected given their narrow dietary breadth (Figure 13). For instance, the $\delta^{15}N$ values of species with diets dominated by copepods (Zoo 1), copepods/euphausiids (Zoo 2), and amphipods (Zoo 5) displayed $\delta^{15}N$ values spanning 8.02‰, 6.73‰, and 5.27‰, respectively, with individuals of each group frequently characterized by values exceeding those of piscivorous species (Figure 13). In contrast, the combined $\delta^{15}N$ range of micronektonivores (e.g. micronektonivores and piscivores) spanned a relatively narrow 4.16‰. The broad range of $\delta^{15}N$ values of zooplanktivores cannot be explained by dietary variation alone and suggests additional sources

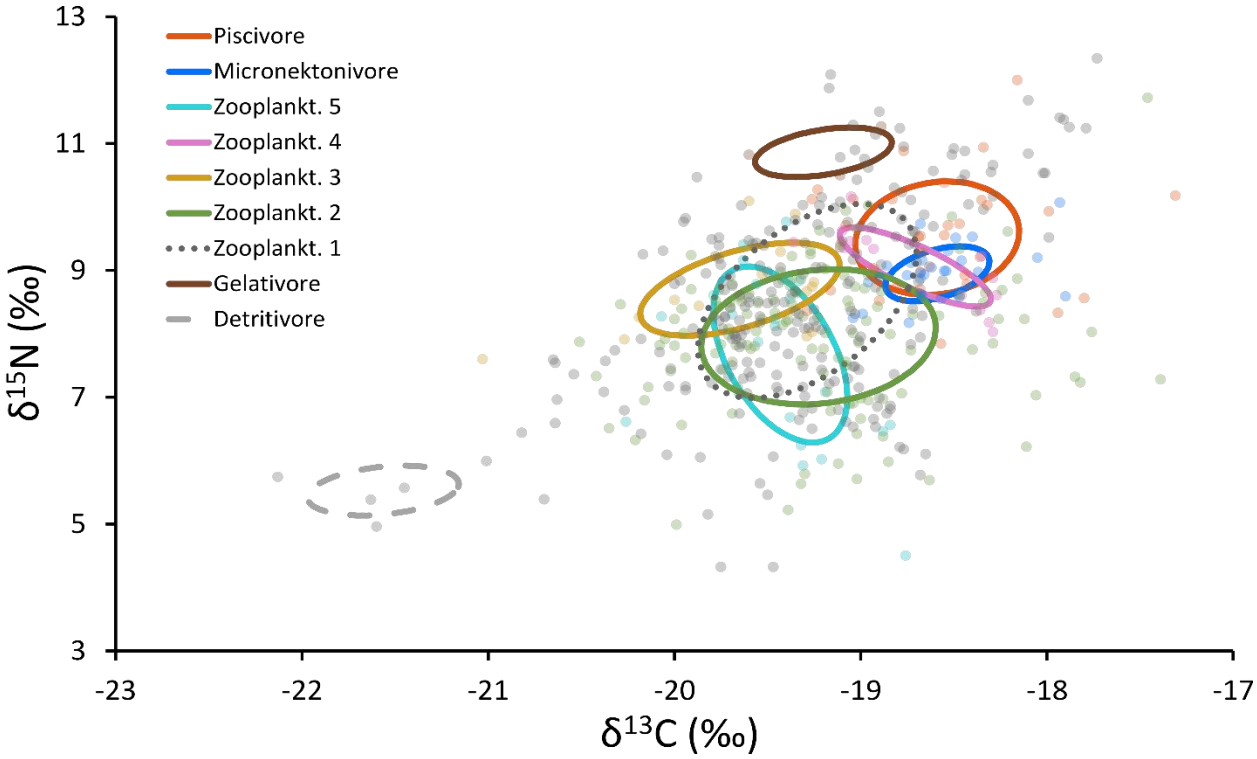

Figure 13. Individual $\delta^{13}C$ and $\delta^{15}N$ values of 55 species of micronekton grouped according to their assigned feeding guild (Table 10). Ellipses represent the standard ellipse area (SEA) drawn to encompass ~40% of the isotope data for each feeding guild.

of variation are influencing the isotopic values of some zooplanktivore feeding guilds (e.g. Zoo 1, Zoo 2, Zoo 5).

In contrast to the nine dietary guilds represented by the assemblage, hierarchical cluster analysis followed by SIMPROF routines on species mean $\delta^{13}C$ and $\delta^{15}N$ values yielded five significant clusters (Figure 14). Interestingly, species were not strictly clustered by feeding guild, with zooplanktivorous species frequently clustering with micronektonivores and piscivores (Figure 14; CLUSTER-4 and CLUST-5). Species assigned to CLUST-1 were characterized by low $\delta^{13}C$ (range: -21.56‰ to -19.24‰) and $\delta^{15}N$ values (range: 5.53‰ to 6.79‰), while species assigned to CLUST-5 displayed higher $\delta^{13}C$ (range: -19.20 to -18.25‰) and $\delta^{15}N$ values (9.64 to

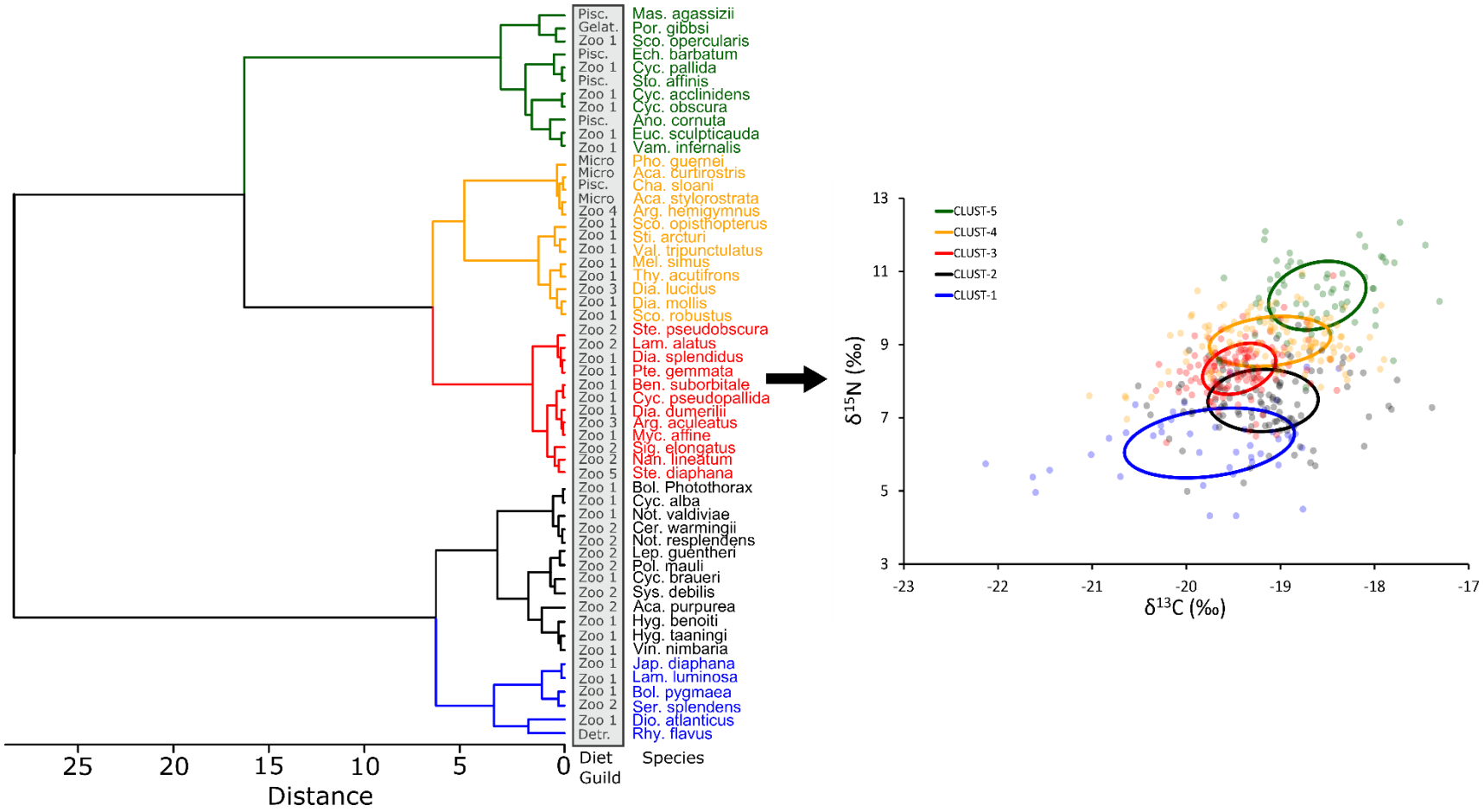

Figure 14. Dendrogram of cluster analysis derived from per-species mean $\delta^{13}C$ and $\delta^{15}N$ values of micronekton (left panel). Colors represent statistically significant clusters identified through similarity profile (SIMPROF) routines. The diet guild of each species is listed to illustrate discrepancies between stomach content and stable isotope data. Right Panel: Individual $\delta^{13}C$ and $\delta^{15}N$ values of 55 species of micronekton grouped according to cluster analysis and SIMPROF results. Ellipses represent the standard ellipse area (SEA) drawn to encompass ~40% of the isotope data for each cluster.

11.47‰) (Figure 14). CLUST-2 and CLUST-4 were characterized by $\delta^{13}C$ and $\delta^{15}N$ values intermediate to groups one and five, with $\delta^{15}N$ values enriching with each subsequent cluster (Figure 14). Isotopic separation among the five clusters occurred primarily along the ^{15}N axis as $\delta^{13}C$ values overlapped broadly among clusters (Figure 14). Statistically significant differences in the isotopic signatures among the five clusters was detected (MANOVA: $F_{4,50} = 13.81$; $p < 0.001$), with significant differences among clusters detected for $\delta^{15}N$ (ANOVA: $F_{4,50} = 154.72$; $p < 0.001$) and $\delta^{13}C$ values (ANOVA: $F_{4,50} = 7.11$; $p < 0.001$). Subsequent multiple comparisons suggested $\delta^{15}N$ values were significantly different among all clusters (Shaffer's MCP; $p < 0.001$, for each). Differences in $\delta^{13}C$ values of cluster groups were driven by CLUST-5 which possessed significantly higher $\delta^{13}C$ values relative to all other clusters (Shaffer's MCP; $p < 0.05$, for each) and CLUST-1 which possessed significantly lower $\delta^{13}C$ values relative to all other groups (Shaffer's MCP; $p < 0.05$, for each) except CLUST-3 (Shaffer's MCP; $p = 0.09$).

Multiple linear regression of $\delta^{13}C$ and $\delta^{15}N$ isotope values

Results of multiple linear regression of $\delta^{13}C$ values for migratory species yielded a best fit model which included length, longitude, and their interaction ($F_{3,236} = 34.97$; $p < 0.001$, $R^2 = 0.30$), with ^{13}C values increasing with length and decreasing when moving from west to east across the sampling grid (Figure 15 A,B). For $\delta^{13}C$ values of non-migratory species, the best fit model included length, median nighttime depth, and the interactions between length and median nighttime depth, and median nighttime depth and water type ($F_{4,162} = 18.57$; $p < 0.001$, $R^2 = 0.30$) (Figure 16). Within non-migrators, ^{13}C values were positively correlated with increasing length and median nighttime depth, with the slope of the relationship between $\delta^{13}C$ and nighttime depth differing between water types (Figure 16A, B). Additionally, ^{13}C values of non-migratory

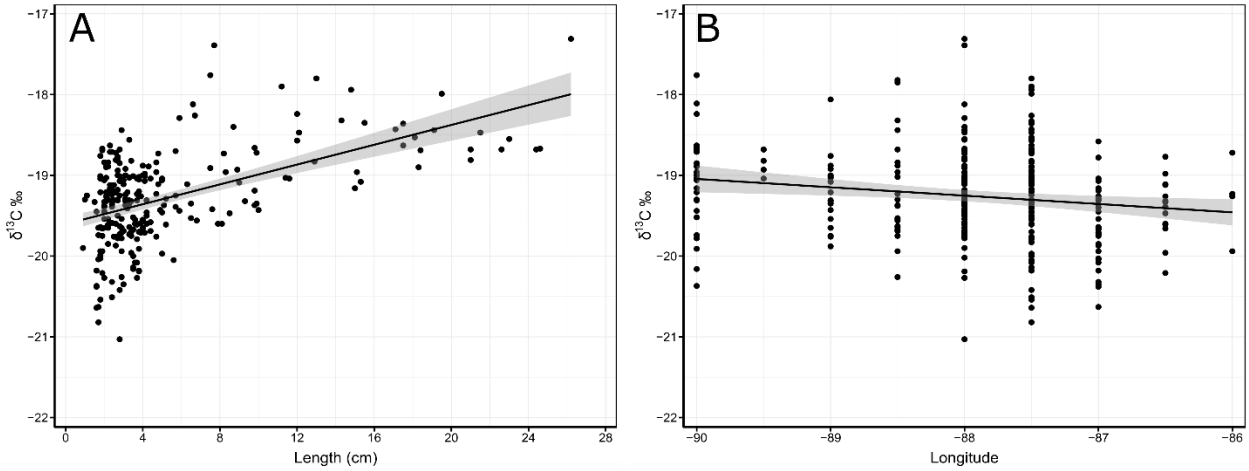

Figure 15. Multiple linear regression model selection results for $\delta^{13}C$ values of vertically migrating species relative to length (A) and longitude (B). Trend lines represent best fit lines for linear models, and gray bands represent 95% confidence intervals.

species were higher in LCW relative to GCW (Figure 16C). For both migratory and non-migratory species, length was the most important variable retained in final models explaining 28.3% and 12.2% of the observed variation in migrators and non-migrators, respectively.

The best fit model following multiple linear regression on $\delta^{15}N$ values of migratory species included length, median nighttime depth, median daytime depth and water type. Additionally, significant interactions between length and median nighttime depth, median nighttime depth and water type, and the interaction between median day and nighttime depths were retained in the final model ($F_{7,235} = 25.47$; $p < 0.001$, $R^2 = 0.42$). The $\delta^{15}N$ values of vertically migrating species increased with increasing length and increasing nighttime depth of occurrence, with the slope of the relationship between $\delta^{15}N$ values and nighttime depth varying between LCW and GCW (Figure 17A, B). Interestingly, the $\delta^{15}N$ values of migratory species

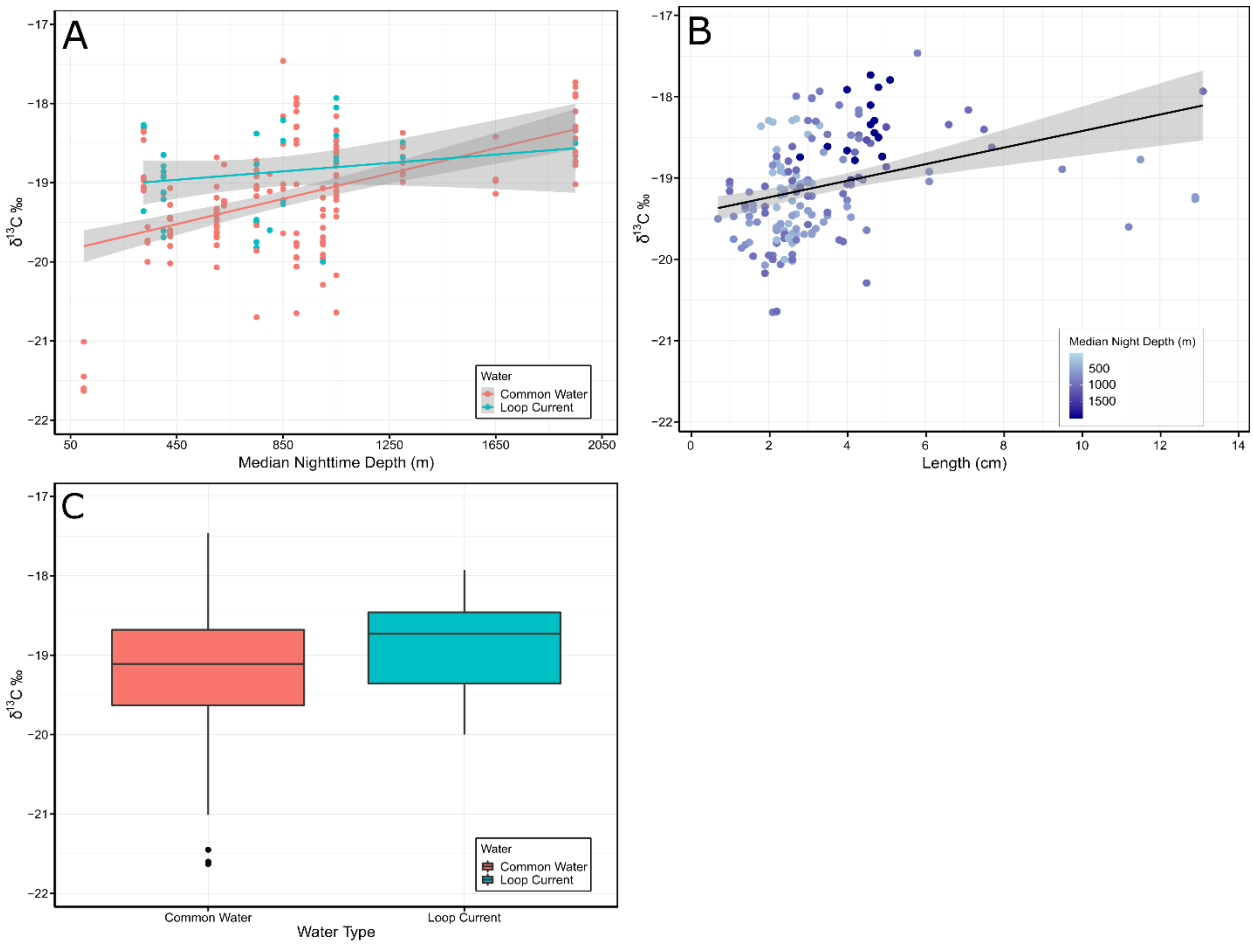

Figure 16. Multiple linear regression model selection results for $\delta^{13}C$ values of non-migratory species. Relationship between $\delta^{13}C$ and median nighttime depth and the interaction between depth and water type (A), length and the interaction between length and nighttime depth (B), and water type (C). Trend lines represent best fit lines for linear models, and gray bands represent 95% confidence intervals. Boxplots represent 25th%, 50th% and 75th% percentile, while whisker lengths represent 1.5*interquartile range. Outliers (filled circles) are observations falling beyond the range defined by the whiskers.

were found to be slightly elevated in GCW compared to LCW and showed a slight negative relationship with increasing median daytime depth (Figure 17D). The best fit model for non-migratory species included median nighttime depth, water type, and the interaction between length and water type ($F_{4,162} = 22.43$; $p < 0.001$, $R^2 = 0.34$), with $\delta^{15}N$ values increasing with

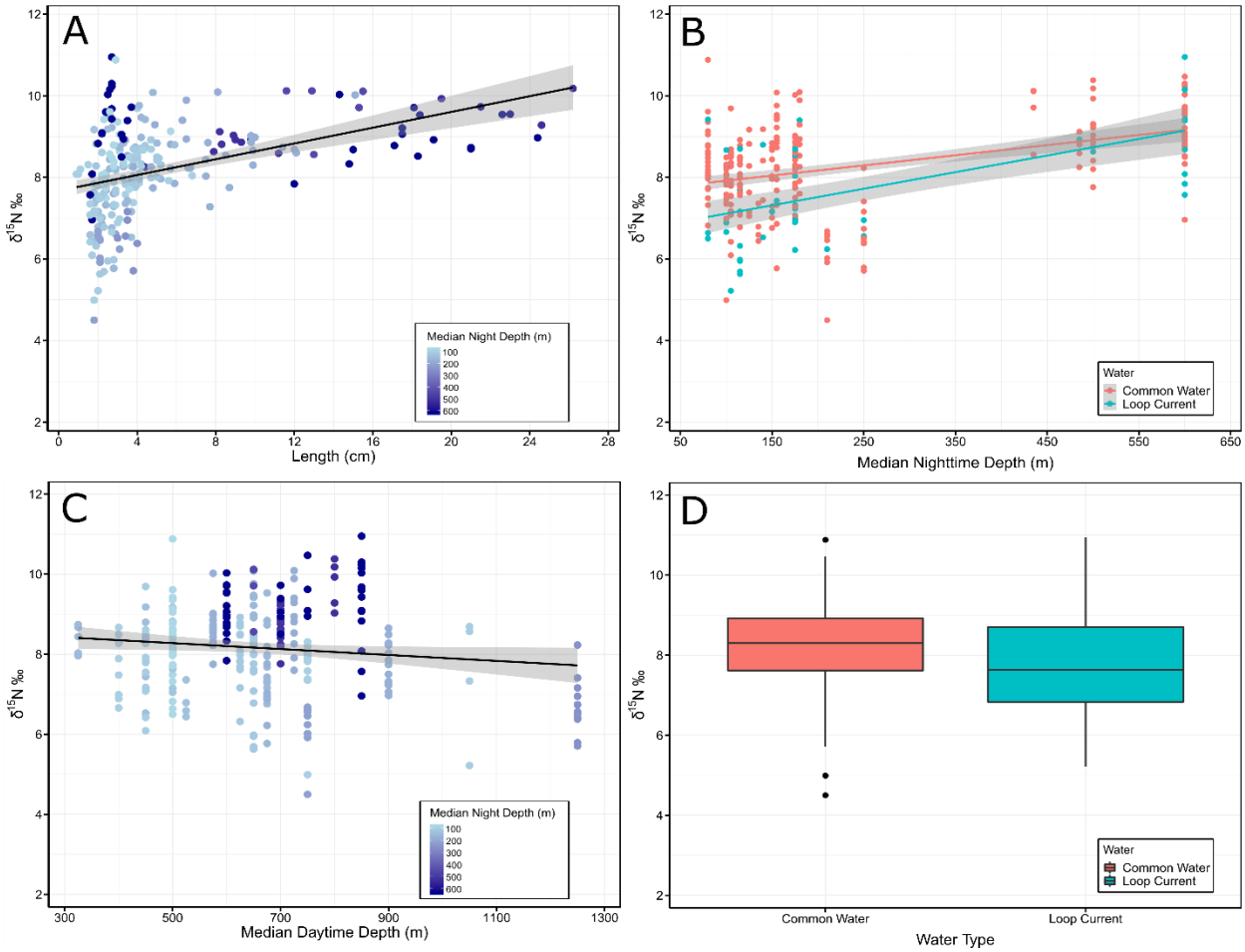

Figure 17. Multiple linear regression model selection results for $\delta^{15}N$ values of migratory species. Relationship between $\delta^{15}N$ and length and the interaction between length and nighttime depth (A), median nighttime depth and the interaction between nighttime depth and water type (B), median daytime depth and the interaction between daytime depth and nighttime depth (C), and water type (D). Trend lines represent best fit lines for linear models, and gray bands represent 95% confidence intervals. Boxplots represent 25th%, 50th% and 75th% percentile, while whisker lengths represent 1.5*interquartile range. Outliers (filled circles) are observations falling beyond the range defined by the whiskers

median nighttime depth. The effect of length on $\delta^{15}N$ values differed between the two water types, with the slope of the relationship increasing in LCW due in part to lower overall $\delta^{15}N$ values in LCW relative to GCW (Figure 18). Variable importance differed between migratory

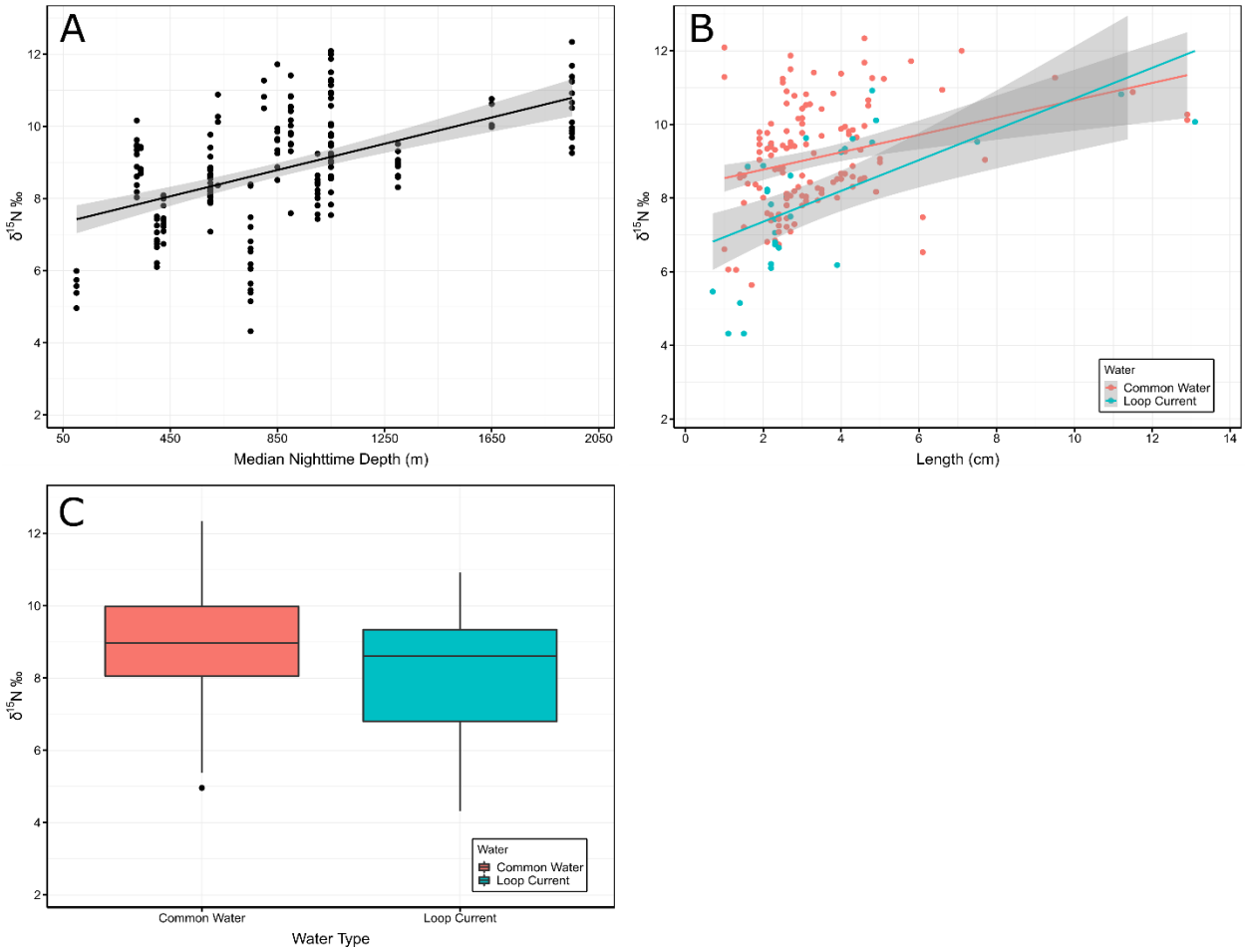

Figure 18. Multiple linear regression model selection results for $\delta^{15}N$ values of non-migratory species. Relationship between $\delta^{15}N$ and median nighttime depth (A), length and the interaction between length and water type (B), and water type (C). Trend lines represent best fit lines for linear models, and gray bands represent 95% confidence intervals. Boxplots represent 25th%, 50th% and 75th% percentile, while whisker lengths represent 1.5*interquartile range. Outliers (filled circles) are observations falling beyond the range defined by the whiskers

and non-migratory species, with length explaining 12.2% of variation in migratory species, with median nighttime depth explaining 9.2% of variance in non-migratory species (Table 11).

Table 11. Independent variables retained in final multiple regression models for migratory and non-migratory micronekton species in the Gulf of Mexico. Model fit was assessed with Akaike's information criterion (AIC) and % deviance explained (DE). Relative importance of each independent variable is given by the difference in AIC (ΔAIC) and DE (ΔDE) when this variable was removed from the final model. Explanatory variables that were included as categorical factors in models are denoted by (f).

	$\delta^{13}C$		$\delta^{15}N$	
Variable	Δ AIC	Δ DE	Δ AIC	Δ DE
Migrators	**AIC = 351.0**	**DE = 30.0**	**AIC = 628.1**	**DE = 41.5**
Length	80.1	28.3	54.6	15.6
Median night depth	--	--	3.9	1.7
Median day depth	--	--	8.3	2.8
Water Type (f)	--	--	11.1	3.5
Longitude	2.4	1.1		
Length:Median night depth	--	--	28.4	8.1
Median night depth:Water type	--	--	4.9	2.0
Median night depth:Median day depth	--	--	2.0	1.3
Length:Longitude	1.8	0.9	--	--
Non-migrators	**AIC = 264.2**	**DE = 30.0**	**AIC = 560.7**	**DE = 34.1**
Length	25.3	12.2	--	--
Median night depth	10.3	5.2	24.9	9.2
Water type (f)	--	--	12.5	5.6
Length:Water type	--	--	0.5	0.6
Length:Median night depth	17.2	8.3	--	--
Median night depth:Water type	6.1	3.3	--	--

Trophic position estimates

Mean TP:SIA estimates for the entire assemblage spanned two trophic levels between TP 2.8 (detritivore *R. flavus*) and TP 4.8 (zooplanktivore *E. sculpticauda*), with zooplanktivorous species (mean TP: 3.7) estimated to occupy a half trophic level below micronektonivores and piscivorous species (mean TP: 4.2). TP estimates for both zooplanktivores and micronektonivores/piscivores were 0.3 TPs higher in non-migratory species relative to migratory species (Figure 19A). For both migratory and non-migratory species, TP:SIA estimates were generally higher than TP:SCA, although the magnitude of difference between the two methods

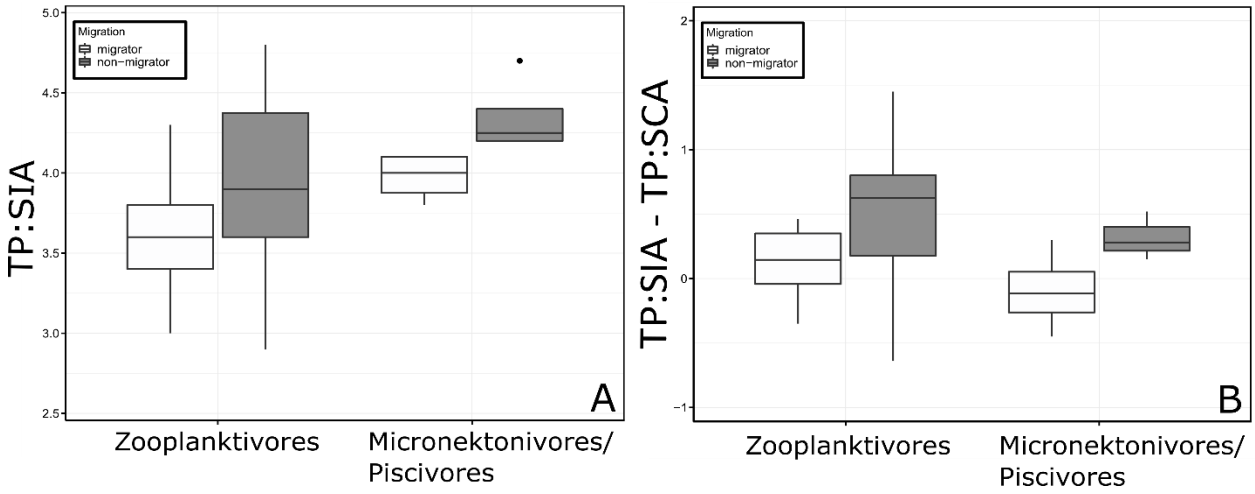

Figure 19. Boxplots depicting TP-SIA estimates of migratory (white) and non-migratory (gray) zooplanktivores and micronektonivores/piscivores (A). Boxplots depicting the difference in TP estimates made with TP:SIA and TP:SCA. Boxplots represent 25th%, 50th% and 75th% percentile, while whisker lengths represent 1.5*interquartile range. Outliers (filled circles) are observations falling beyond the range defined by the whiskers.

varied between lower and higher-order consumers and migration types (Figure 19B). Specifically, the difference between TP:SIA and TP:SCA estimates was 0.1 and 0.3 TL for migratory and non-migratory piscivores/micronektonivores, respectively, while differences in the two methods ranged between 0.1 TLs and 0.5 TLs for migratory and non-migratory zooplanktivores, respectively (Figure 19B). Alignment between TP estimation methods varied between migratory and non-migratory species, with linear regression indicating TP:SIA estimates agreed with TP:SCA estimates in migratory species ($F_{1,14} = 18.23$; $p < 0.001$; $R^2 = 0.54$) (Figure 20A) but not non-migratory species ($p = 0.61$) (Figure 20B). Because the precision between TP:SIA and TP:SCA varied by functional group and migration type, alignment between the two TP estimation methods varied among the major families of fishes examined, with precision increasing in families primarily comprised of migratory species. For instance, TP

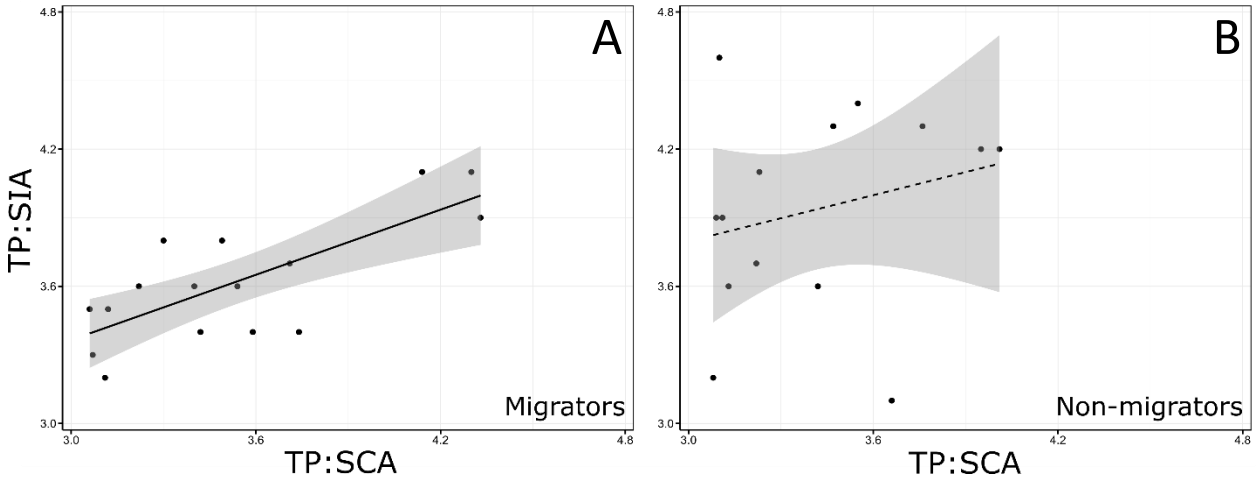

Figure 20. Linear regression analysis examining the relationship between trophic position estimates made using stomach content analysis (TP:SCA) and stable isotope analysis (TP:SIA) for migratory and non-migratory deep-pelagic micronekton. Trend lines represent best fit lines for linear models, and gray bands represent 95% confidence intervals. Solid regression line represents statistically significant relationship between the two methods.

estimations for migratory myctophids and stomiids varied by 0.2 and 0.1 TPs, respectively, while non-migratory members of the genus *Cyclothone* had TP:SIA estimates that were, on average, 0.6 TPs greater than TP:SCA estimates.

Discussion

Trophic structure of the deep-pelagic micronekton assemblage

Cluster analysis of SIA data taken from 55 species of micronekton with feeding modes ranging from detritivores to piscivores resulted in the identification of five distinct trophic groupings, which contrasted with the nine feeding guilds identified using stomach content data (Hopkins et al., 1994; Hopkins et al., 1996). The lower number of trophic groupings identified using SIA was driven primarily by the grouping of zooplanktivorous species known to feed on a

range of taxa including copepods, euphausiids, ostracods, and amphipods (Table 10; Figure14). Interestingly, the range $\delta^{15}N$ values for many zooplanktivorous species known to feed primarily on copepods (e.g. *Cyclothone spp., E. sculpticauda, V. infernalis*) exceeded two trophic levels, and these taxa were grouped in the same cluster (CLUST-5) as larger-bodied piscivores (e.g. *E. barbatum* and *A. cornuta*) (Figure 14). The dissonance between SIA and SCA data is likely driven by the differing time scales over which feeding information is incorporated by the two methods. Because SCA data provides only a "snapshot" of an animal's diet, SCA analysis can be heavily influenced by random feeding events resulting in high variation among individuals, particularly if a species feeds on a wide range of prey items. Additionally, in SCA studies where the taxonomic resolution of identified prey is high (genus or species level), as was the case in the diet analyses referenced in this study (Hopkins et al., 1994; Hopkins et al., 1996), variability among consumers will increase, leading to the identification of a greater number of diet guilds than would be identified if taxonomic resolution of prey was lower (class level). In contrast, because isotope ratios represent the "average" of an organism's feeding events over a period of weeks to months (Post 2002), variation among populations and species tends to be lower resulting in the identification of fewer trophic groupings. Variation in isotope signatures among species is also reduced in ecosystems like the deep-pelagic that are supported by few isotopically distinct carbon and nitrogen sources (Choy et al., 2015; Parzanini et al., 2017). Because pelagic production derived from phytoplankton represents the dominate carbon source to deep-pelagic food webs (Drazen and Sutton, 2017), consumers may be observed to feed diversely during stomach content analysis, but that variability may not translate to isotopic variation at higher trophic levels, as all prey items are isotopically similar. The somewhat contrasting depictions of trophic structure identified through SCA and SIA clearly demonstrates the importance of

stomach content data when interpreting the results of stable isotope analysis and highlights the importance of combining the two data types. It is important to note that the diet data used in this analysis comes from studies conducted in the northern GOM in the 1980s and that changes in feeding habits among species could have occurred during that time. However, more recent diet analyses in both the Atlantic Ocean and GOM of many of the species examined by Hopkins et al. (1996) suggests that the feeding patterns of many species has been conserved through time (McClain-Counts et al., 2017; Olivar et al., 2019).

Depth of occurrence as a driver of variation in $\delta^{13}C$ and $\delta^{15}N$ values

Results of multiple linear regression indicated that length, depth of occurrence and water type were important predictors of $\delta^{15}N$ values in both migratory and non-migratory species, with the relative importance of each variable varying between the two groups (Table 11). For both migratory and non-migratory species, $\delta^{15}N$ values displayed a positive relationship with nighttime depth of occurrence, however, the strength of the relationship was greater in non-migratory species and explained the greatest proportion of variance of the variables retained in the final model. The positive relationship between $\delta^{15}N$ and depth in non-migratory species did not appear to be confounded by higher-order consumers (piscivores/micronektonivores) occupying the deepest depths within the assemblage, as zooplanktivorous species were frequently characterized by elevated $\delta^{15}N$ values relative to piscivores occupying similar depths. The observed enrichment in ^{15}N with increasing depth regardless of trophic status strongly suggests that variation in the $\delta^{15}N$ values of non-migratory species is driven by increased reliance on food webs with enriched nitrogen baselines in the meso- and bathypelagic, similar to what was observed in the zooplanktivorous species examined in Chapter II. In pelagic ecosystems, phytoplankton and other sinking particulate organic matter (POM) represent the

primary source of carbon to consumers throughout the water column (Hannides et al., 2013; Choy et al., 2016). SIA examinations of POM throughout the deep-pelagic have shown that as POM sinks, bacterial degradation results in the physical breakdown of POM into smaller, more slowly sinking particles and the removal of isotopically light nitrogen (^{14}N), leaving the residual material isotopically enriched relative to POM at shallower depths (Mintenbeck et al., 2007; Hannides et al., 2013). Analyses using a combination of SIA and amino acid compound specific stable isotope analysis (AA-CSIA) have demonstrated that the pattern of ^{15}N enrichment with depth observed in POM is reflected in the tissues of non-migratory zooplankton and micronekton, with utilization of isotopically enriched POM increasing with depth (Hannides et al., 2013, Gloeckler et al., 2018). Although the trend of enrichment with depth is clear in non-migratory species, the range of $\delta^{15}N$ values observed among non-migratory species with differing diets occupying similar depths is considerable and suggests use of ^{15}N enriched baselines could depend on trophic status (zooplanktivores, piscivores) as well as depth. Suspended, isotopically enriched POM that has been re-worked by bacteria has been shown to of poorer nutritional quality relative to surface derived production (Mintenbeck et al., 2007; Hannides et al., 2013). That small bodied zooplanktivorous species such as *Cyclothone spp.* appear to be more likely to feed within food webs supported by enriched ^{15}N baselines suggests that the energetic demands of larger, actively swimming piscivores like *A. cornuta* and *C. sloani* might preclude them from relying heavily on food webs supported by degraded POM at depth. Direct and indirect evidence for this theory is supported by the results of Chapter II and Chapter III which suggest that use of food webs with isotopically enriched baselines is most evident in non-migratory zooplanktivorous species inhabiting the bathypelagic, while larger-bodied, higher trophic level predators are largely supported by surface derived production (Chapter III).

Combined, these results suggest that non-migratory micronektonivores and piscivores occupying depths within the meso- and bathypelagic likely access surface derived production indirectly by consuming migratory prey that forage in the epipelagic (Sutton et al., 1996b; Gloeckler et al., 2018; Richards et al., 2018).

Median nighttime depth was significantly correlated with $\delta^{15}N$ values in migratory species, but the relationship was not nearly as pronounced as the relationship in non-migratory taxa. Because migratory taxa feed almost exclusively at night within the epipelagic zone, all species are likely feeding within similar food webs supported by a uniform isotopic baseline. Unlike the trends observed in non-migratory species, the slight positive trend in $\delta^{15}N$ values and depth appears to be driven primarily by larger, higher-trophic level consumers occupying the deepest depths of the migratory assemblage. Many of these piscivorous species (*C. sloani, E. barbatum, S. affinis*) are asynchronous migrators, meaning only a portion of the population migrates into the epipelagic at night to feed while the remaining individuals remain in the meso- or bathypelagic (Sutton and Hopkins, 1996a; Sutton and Hopkins, 1996b). In these species, the cue for migration has been linked to stomach fullness and feeding occurs primarily in migrating individuals foraging in the epipelagic (Sutton and Hopkins, 1996b). Thus, despite having a deeper median nighttime depth of occurrence due to some individuals remaining at depth during the night, these species carry $\delta^{15}N$ values suggestive of reliance on surface derived primary production. The conclusion that median depth of occurrence more strongly influences the $\delta^{15}N$ values of non-migratory species is consistent with previous examinations of micronekton trophic structure in the Pacific Ocean (Gloeckler et al., 2018; Romero-Romero et al., 2019) and Mediterranean (Valls et al., 2014) and suggests depth is likely an important driver of trophic structure in low-latitude oligotrophic ecosystems worldwide.

Length-based variation in $\delta^{13}C$ and $\delta^{15}N$ values

Body length was significantly and positively correlated with $\delta^{13}C$ and $\delta^{15}N$ values in migratory species and with $\delta^{13}C$ values in non-migrators, explaining most of the variation in multiple regression models where it was retained (Table 11). The conclusion that size more strongly influences $\delta^{15}N$ values in migratory rather than non-migratory species, is identical to the results of Romero et al., (2019) who examined $\delta^{15}N$ values of micronekton in the Pacific Ocean. That variation in the isotopic signatures of migratory species was largely explained by body length, as opposed to depth, again suggests that migratory species within the GOM assemblage feed on prey supported by carbon sources with similar isotopic baselines (Layman et al., 2005). Due to shared reliance on a similar isotopic baseline, it follows that separation along the nitrogen axis in migratory species would be primarily driven by body length. Increases in body length have been commonly linked to ontogenetic shifts in diet and trophic position, as larger individuals with expanded gape sizes are capable of consuming larger prey of higher trophic status (Post, 2003).

Although there is clear enrichment in ^{15}N between the smallest and largest migratory species, the pattern is asymptotic due to a wide range of $\delta^{15}N$ values in small, zooplanktivorous species (Figure 17). Large variation in $\delta^{15}N$ values of smaller-bodied species is interesting and cannot be explained by differences in nighttime depth of occurrence within the epipelagic zone (Figure 17B). Within migratory species, larger-bodied *S. elongatus* and various stomiids account for all samples larger than 9.0 cm and do not contribute to the enrichment of ^{15}N with increasing size of migratory species, particularly in small individuals (Figure 21. Thus, the wide range of $\delta^{15}N$ values in smaller migrating individuals was detected almost entirely within zooplanktivorous species. Specifically, lanternfish (Family Myctophidae), the numerically

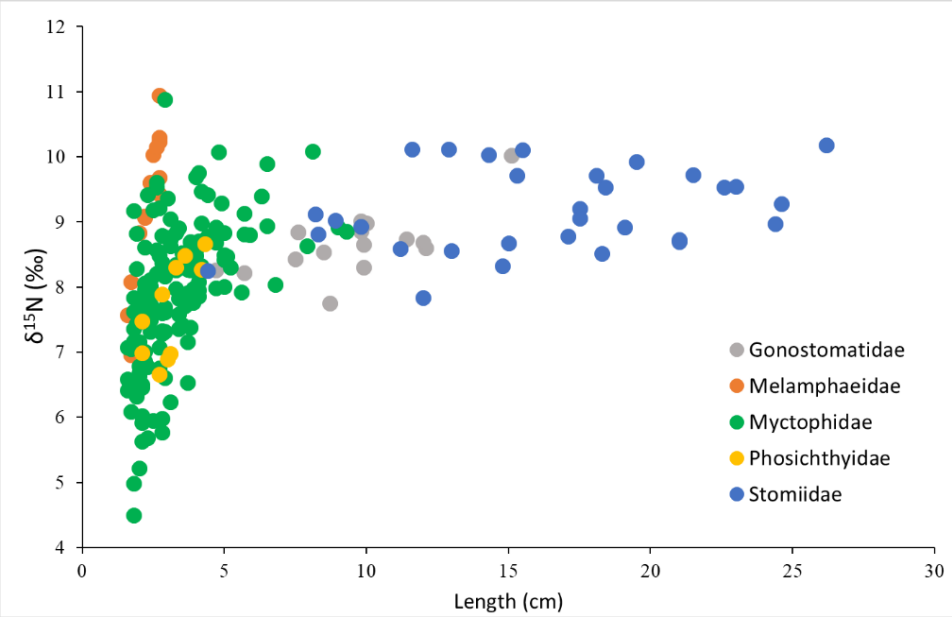

Figure 21. Relationship between $\delta^{15}N$ values and length for major families of migratory fishes

dominant family of vertically migrating fishes in GOM deep-pelagic assemblages, account for almost all the observed $\delta^{15}N$ variation in smaller-bodied migrators (Figure 21). Hopkins and Gartner (1992) conducted a detailed diet and vertical distribution analysis of 17 species of lanternfish collected in the GOM to test for resource partitioning within the assemblage. Cluster analysis suggested that myctophids within the GOM partition resources both intra- and interspecifically via differences in their vertical distribution and through variations in the type and size of their prey (Hopkins and Gartner, 1992), with larger individuals within species occupying deeper depths and consuming larger prey. Although the myctophids examined in this study do have differing median depths of distribution at night, those differences do not appear to have translated into depth-driven $\delta^{15}N$ variation, as the relationship between median nighttime depth and $\delta^{15}N$ within the myctophid assemblage was non-significant ($F_{1,152} = 2.12$; $p = 0.15$).

Thus, the broad range of $\delta^{15}N$ values observed within myctophids is likely due to differences in length which have been shown to be correlated with the size and trophic status of prey consumed (Hopkins and Gartner, 1992). Indeed, length within the myctophid assemblage was significantly correlated with $\delta^{15}N$ values ($F_{1,143} = 54.64$, $p < 0.001$, $R^2 = 0.27$), with the shape of the relationship (i.e., asymptotic) mirroring that of the larger assemblage. The asymptotic shape of enrichment in ^{15}N within the myctophid assemblage (Figure 21) is likely due to interspecific differences and ontogenetic shifts in gape size, with gape size increasing more rapidly in smaller individuals allowing for a more rapid shift in $\delta^{15}N$ relative to larger individuals and sizes where increases in length/gape decrease significantly (Post, 2003; Wells et al., 2008).

Influence of the Loop Current on micronekton $\delta^{13}C$ and $\delta^{15}N$ values

Final regression models for non-migratory $\delta^{13}C$ and $\delta^{15}N$, and migratory $\delta^{15}N$ included water mass as a significant explanatory variable. In both migratory and non-migratory species, $\delta^{15}N$ values were lower in samples collected from LCW relative to samples collected from GCW, while $\delta^{13}C$ values were higher in LCW. The pattern of higher $\delta^{13}C$ and lower $\delta^{15}N$ values in samples collected from LCW has been demonstrated previously in the isotopic values of epipelagic zooplankton and in epi- and mesopelagic micronekton (Wells et al., 2017). Although the observed differences between LCW and GCW of 0.5‰ and 0.8‰ for migratory and non-migratory species, respectively, were not large, it is interesting that an isotopic signal between the two water masses was detectable despite the trophic and life history variation in the assemblage examined. Differences in the isotopic composition of consumers collected from the two water masses are driven by differences in sources of nitrogen fueling the base of the food web (Biggs, 1992). The warm waters of the Loop Current are characterized by deep nitracline depths which result in primary production in the epipelagic primarily relying on isotopically light

nitrogen derived from nitrogen fixing cyanobacteria (*Trichodesmium* spp.) (Montoya et al., 2002; Dorado et al., 2012; Wells et al., 2017). In contrast, primary production in neritic waters (i.e., common water) is largely supported by isotopically enriched deep-water nitrate resulting in higher $\delta^{15}N$ values of consumers (Biggs, 1992).

Interestingly, the interaction between water type and median nighttime depth was retained in the final models for migratory $\delta^{15}N$ and non-migratory $\delta^{13}C$ (Figures 16, 17). In both instances, the differences in slope between the regression lines for LCW and GCW were greatest at shallower depths (Figure 16A, 17B). The diminishing effect of water type on isotope values with increasing depth is consistent with previous analysis of meso- and bathypelagic micronekton which found that isotopic differences between the two water masses decreased with depth of occurrence (Chapter II). The Loop Current dominates circulation in near-surface waters of the GOM but use of unique salinity-temperature-depth profiles inherent to LCW and GCW demonstrated that substantial mixing between the two water masses begins in the upper-mesopelagic (Cardona and Bracco, 2016; Johnston et al., 2019). Thus, it is logical that both migratory and non-migratory species foraging within the upper or lower-mesopelagic are less likely to incorporate isotopic signatures specific to a water mass.

Trophic position estimates of deep-pelagic micronekton

Trophic position estimates for deep-pelagic micronekton spanned two trophic levels between a low of 2.8 and high of 4.8 and were similMcar to estimations for micronekton assemblages in the GOM and Pacific (Choy et al., 2013; McClain-Counts et al., 2017). Although TP estimates were, on average higher for micronektonivores and piscivores (mean TL: 4.2) relative to zooplanktivores (mean TL: 3.7), there was considerable overlap in TP estimations between the two groups (Figure 19). In general, relative to published TP:SCA values, TP:SIA

estimations were overestimated to a greater extent in non-migrators, with overestimation found to be greater in zooplanktivores (Figure 19). The overestimation in TP:SIA in non-migratory taxa likely stems from increased reliance on food webs supported by enriched isotopic baselines at depth and suggests that the pyrosome, *P. atlanticum*, does not adequately characterize the nitrogen baseline for non-migratory species. Despite overestimations in TP:SIA in non-migrators, TP:SIA estimations agreed well with TP:SCA in migratory species suggesting *P. atlanticum* characterizes the nitrogen baseline for migratory taxa well (Figure 20). The agreement between the two methods in migratory taxa is useful as it suggests that TP:SIA, which requires fewer samples and is a more accessible method (less reliance on taxonomic expertise), adequately describes trophic positions for a variety of ecologically important groups including myctophids and stomiids. Although it is tempting to use an alternative baseline such as POM collected from the meso- or bathypelagic to estimate TPs of non-migratory species, the high level of observed variation in $\delta^{15}N$ values in non-migratory species suggests that relative use of isotopically enriched baselines varies by species so a "one size fits all" approach is unlikely to adequately describe trophic positions.

CHAPTER V

CONCLUSIONS

As research into the structure and function of deep-pelagic ecosystems expands, an emerging theme is that deep-pelagic ecosystems and communities are far more complex and interconnected than previously thought. The degree of complexity observed in the deep pelagic is astounding considering deep-pelagic ecosystems lack physical habitat structure, are characterized by relatively uniform abiotic conditions throughout the lower meso- and bathypelagic zones and are largely supported by a single carbon source (phytoplankton). Once considered to be 'biological deserts' recent faunal inventories have revealed that the deep pelagic harbors extremely diverse and unique assemblages of species. Emerging research in the Gulf of Mexico (GOM) suggests its deep-pelagic realm is incredibly diverse, displays a high degree of connectivity both vertically within the pelagic ocean and horizontally with coastal and shelf ecosystems, and possesses an incredibly complex and interconnected food web. By examining the trophic structure of GOM deep-pelagic assemblages using dietary tracers (SIA), this project provides the most thorough description of deep-pelagic food web structure in the GOM to date.

Detailed analysis of stable isotope values in zooplanktivorous fishes in the first chapter of this dissertation highlighted the importance of phytoplankton-based epipelagic primary production (PP) to deep-pelagic micronekton. Interestingly, the importance of epipelagic PP to zooplanktivorous micronekton was dependent on the depth range and vertical migration behavior of each species. All vertically migrating species relied heavily on primary production from the epipelagic, while non-migratory species, such as *C. obscura* and *A. hemigymnuts,* fed within food webs supported by recycled carbon and marine snow at depth, with reliance on deep

suspended marine snow increasing with depth. This finding corroborates recent evidence from the Pacific Ocean which suggests that small, suspended particles represent a previously unknown carbon source supporting the production of deep-pelagic fauna. Additionally, the discovery that stable isotope ratios of deep-pelagic micronekton can differ significantly between mesoscale oceanographic features provides important context to the degree of vertical connectivity in the pelagic GOM and provides important context for the interpretation of stable isotope data in future studies of the pelagic GOM.

Following the results in Chapter II which suggested that the relative use of particulate organic matter in the epipelagic was dependent on depth of distribution and vertical migration type, I conducted a similar trophic analysis on an understudied group of piscivorous micronekton collected within the northern GOM. This chapter provided some of the first estimations of trophic position and resource use dynamics for several of these circumglobally distributed species. Surprisingly, despite vertical distributions extending into the bathypelagic (> 1,000 m), all the species examined received the majority (>73%) of their carbon from primary production in the epipelagic zone. These species, which often do not vertically migrate, access primary production in the epipelagic zone indirectly by consuming vertically migrating micronekton which forage in the epipelagic at night before migrating to daytime depths in the meso- and bathypelagic zones. The dependence of non-migratory predatory fishes on epipelagic production through an intermediate vector (migratory species) underscores the spatial complexity and extent of vertical connectivity in pelagic GOM food webs.

Finally, by examining the stable isotope values of 55 species of micronekton in the northern GOM, I identified five unique trophic guilds and provided trophic position estimates for each species. The five trophic groupings identified through SIA were in stark contrast to

estimates made using stomach content data in the primary literature which identified 19 distinct trophic groupings. The disparity between stable isotope and diet data highlights the contrasting views of food web structure created by the two methods. Additionally, using multiple linear regression, I demonstrated that depth in the water column, length, and location in the GOM relative to mesoscale features such as the Loop Current are important determinants of trophic structure in micronekton assemblages in the GOM.

One of the key goals of my dissertation research was to expand our basic understanding of the trophic and food web structure of deep-pelagic communities using dietary tracer analysis. Gaining a better understanding of deep-pelagic trophic structure is important, considering the current paucity of data on deep-pelagic ecosystems despite increased fisheries production and natural resource extraction. The data presented here, which include comprehensive estimates of trophic position, identification of environmental and biological factors contributing to variation in trophic structure, and contribution estimates of particulate organic matter from different regions of the water column to the production of micronekton, will provide information critical to the development of effective management plans.

REFERENCES

Altabet, M. A. (1988). Variations in nitrogen isotopic composition between sinking and suspended particles: Implications for nitrogen cycling and particle transformation in the open ocean. *Deep Sea Research Part A. Oceanographic Research Papers*, *35*(4), 535-554.

Altabet, M. A., Deuser, W. G., Honjo, S., & Stienen, C. (1991). Seasonal and depth-related changes in the source of sinking particles in the North Atlantic. *Nature*, *354*(6349), 136.

Angel, M. V., & Baker, A. (1982). Vertical distribution of the standing crop of plankton and micronekton at three stations in the northeast Atlantic. *Biological Oceanography*, *2*(1), 1-30.

Biggs, D. C. (1992). Nutrients, plankton, and productivity in a warm-core ring in the western Gulf of Mexico. *Journal of Geophysical Research: Oceans*, *97*(C2), 2143-2154.

Boecklen, W. J., Yarnes, C. T., Cook, B. A., & James, A. C. (2011). On the use of stable isotopes in trophic ecology. *Annual Review of Ecology, Evolution, and Systematics*, *42*, 411-440.

Bradley, C. J., Wallsgrove, N. J., Choy, C. A., Drazen, J. C., Hetherington, E. D., Hoen, D. K., & Popp, B. N. (2015). Trophic position estimates of marine teleosts using amino acid compound specific isotopic analysis. *Limnology and Oceanography: Methods*, *13*(9), 476-493.

Burghart, S. E., Hopkins, T. L., & Torres, J. J. (2010). Partitioning of food resources in bathypelagic micronekton in the eastern Gulf of Mexico. *Marine Ecology Progress Series*, *399*, 131-140.

Cardona, Y., & Bracco, A. (2016). Predictability of mesoscale circulation throughout the water column in the Gulf of Mexico. *Deep Sea Research Part II: Topical Studies in Oceanography*, *129*, 332-349.

Caut, S., Angulo, E., & Courchamp, F. (2008). Caution on isotopic model use for analyses of consumer diet. *Canadian Journal of Zoology*, *86*(5), 438–445.

Cherel, Y., Ducatez, S., Fontaine, C., Richard, P., & Guinet, C. (2008). Stable isotopes reveal the trophic position and mesopelagic fish diet of female southern elephant seals breeding on the Kerguelen Islands. *Marine Ecology Progress Series*, *370*, 239–247.

Cherel, Y., Fontaine, C., Richard, P., & Labatc, J. P. (2010). Isotopic niches and trophic levels of myctophid fishes and their predators in the Southern Ocean. *Limnology and Oceanography*, *55*(1), 324-332.

Chikaraishi, Y., Ogawa, N. O., Kashiyama, Y., Takano, Y., Suga, H., Tomitani, A., *et al*. (2009). Determination of aquatic food-web structure based on compound-specific nitrogen isotopic composition of amino acids. *Limnology and Oceanography: Methods*, *7*(11), 740-750.

Choy, C. A., Davison, P. C., Drazen, J. C., Flynn, A., Gier, E. J., Hoffman, J. C., McClain-Counts, J. P., *et al.* (2012). Global trophic position comparison of two dominant mesopelagic fish families (Myctophidae, Stomiidae) using amino acid nitrogen isotopic analyses. *PLoS ONE*, *7*(11), e50133.

Choy, C. A., Portner, E., Iwane, M., & Drazen, J. C. (2013). Diets of five important predatory mesopelagic fishes of the central North Pacific. *Marine Ecology Progress Series*, *492*, 169–184.

Choy, C. A., Popp, B. N., Hannides, C. C. S., & Drazen, J. C. (2015). Trophic structure and food resources of epipelagic and mesopelagic fishes in the North Pacific Subtropical Gyre ecosystem inferred from nitrogen isotopic compositions. *Limnology and Oceanography*, *60* (4), 1156-1171.

Choy, C. A., Wabnitz, C. C., Weijerman, M., Woodworth-Jefcoats, P. A., & Polovina, J. J. (2016). Finding the way to the top: how the composition of oceanic mid-trophic micronekton groups determines apex predator biomass in the central North Pacific. *Marine Ecology Progress Series*, *549*, 9-25.

Clarke, T. A., & Wagner, P. J. (1976). Vertical distribution and other aspects of the ecology of certain mesopelagic fishes taken near Hawaii. *Fish. Bull*, *74*(3), 635-645.

Cook, A., Bernard, A.M., Boswell, K.M., Bracken-Grissom, H.D., D'Elia, M.A., DeRada, S., *et al.* (in press). A Multidisciplinary Aproach to Investigate Deep-pelagic Ecosystem Dynamics in the Gulf of Mexico Following Deepwater Horizon. *Frontiers in Marine Science*

Cornic, M., & Rooker, J. R. (2018). Influence of oceanographic conditions on the distribution and abundance of blackfin tuna (*Thunnus atlanticus*) larvae in the Gulf of Mexico. *Fisheries Research, 201*, 1-10.

Danovaro, R., Gambi, C., Dell'Anno, A., Corinaldesi, C., Fraschetti, S., Vanreusel, A., Vincx, M., *et al.* (2008). Exponential Decline of Deep-Sea Ecosystem Functioning Linked to Benthic Biodiversity Loss. *Current Biology, 18*(1), 1–8.

Davis, R. W., Ortega-Ortiz, J. G., Ribic, C. A., Evans, W. E., Biggs, D. C., Ressler, P. H., *et al*. (2002). Cetacean habitat in the northern oceanic Gulf of Mexico. *Deep Sea Research Part I: Oceanographic Research Papers*, *49*(1), 121-142.

DeNiro, M. J., & Epstein, S. (1978). Influence of diet on the distribution of carbon isotopes in animals. *Geochimica et Cosmochimica Acta*, *42*(5), 495-506.

Dorado, S., Rooker, J. R., Wissel, B., & Quigg, A. (2012). Isotope baseline shifts in pelagic food webs of the Gulf of Mexico. *Marine Ecology Progress Series*, *464*, 37-49.

Drazen, J., Smith, C., Gjerde, K., Au, W., Black, J., Carter, G., *et al*. (2019). Report of the workshop Evaluating the nature of midwater mining plumes and their potential effects on midwater ecosystems. *Research Ideas and Outcomes*, 5, e33527.

Drazen, J. C., & Sutton, T. T. (2017). Dining in the deep: the feeding ecology of deep-sea fishes. *Annual Review of Marine Science, 9*, 337-366.

Emeis, K. C., Mara, P., Schlarbaum, T., Möbius, J., Dähnke, K., Struck, U., *et al.* (2010). External N inputs and internal N cycling traced by isotope ratios of nitrate, dissolved reduced nitrogen, and particulate nitrogen in the eastern Mediterranean Sea. *Journal of Geophysical Research: Biogeosciences*, *115*(G4).

Fernández-Carrera, A., Rogers, K. L., Weber, S. C., Chanton, J. P., & Montoya, J. P. (2016). Deep Water Horizon oil and methane carbon entered the food web in the Gulf of Mexico. *Limnology and Oceanography*, *61*(S1), S387–S400.

Froese, R., & Pauly, D. (2010). FishBase.

Gartner Jr, J. V. (1987). The lanternfishes (Pisces: Myctophidae) of the eastern Gulf of Mexico. *Fishery Bulletin US*, *85*, 81-98.

Gartner, J. V. (1991). Life histories of three species of lanternfishes (Pisces: Myctophidae) from the eastern Gulf of Mexico. *Marine Biology*, *111*(1), 11-20.

Gloeckler, K., Choy, C. A., Hannides, C. C., Close, H. G., Goetze, E., Popp, B. N., & Drazen, J. C. (2018). Stable isotope analysis of micronekton around Hawaii reveals suspended particles are an important nutritional source in the lower mesopelagic and upper bathypelagic zones. *Limnology and Oceanography*, *63*(3), 1168-1180.

Halpern, B. S., Walbridge, S., Selkoe, K. A., Kappel, C. V., Micheli, F., D'Agrosa, C., *et al*. (2008). A global map of human impact on marine ecosystems. *science*, *319*(5865), 948-952.

Hannides, C. C., Popp, B. N., Choy, C. A., & Drazen, J. C. (2013). Midwater zooplankton and suspended particle dynamics in the North Pacific Subtropical Gyre: A stable isotope perspective. *Limnology and Oceanography*, *58(*6), 1931-1946.

von Harbou, L., Dubischar, C. D., Pakhomov, E. A., Hunt, B. P., Hagen, W., & Bathmann, U. V. (2011). Salps in the Lazarev Sea, Southern Ocean: I. Feeding dynamics. *Marine Biology*, *158*(9), 2009-2026.

Hoffman, J. C., & Sutton, T. T. (2010). Lipid correction for carbon stable isotope analysis of deep-sea fishes. *Deep-Sea Research Part I: Oceanographic Research Papers*, *57*(8), 956–964.

Holl, C. M., Villareal, T. A., Payne, C. D., Clayton, T. D., Hart, C., & Montoya, J. P. (2007). Trichodesmium in the western Gulf of Mexico: 15N2-fixation and natural abundance stable isotopic evidence. *Limnology and Oceanography*, *52*(5), 2249-2259.

Hopkins, T. L., & Baird, R. C. (1985). Feeding ecology of four hatchetfishes (Sternoptychidae) in the eastern Gulf of Mexico. *Bulletin of Marine Science*, *36*(2), 260-277.

Hopkins, T. L., & Gartner, J. V. 1992. Resource-partitioning and predation impact of a low-latitude myctophid community. *Marine Biology*, *114*(2), 185-197.

Hopkins, T. L., Flock, M. E., Gartner Jr, J. V., & Torres, J. J. (1994). Structure and trophic ecology of a low latitude midwater decapod and mysid assemblage. *Marine Ecology Progress Series*, 143-156.

Hopkins, T. L., Sutton, T. T., & Lancraft, T. M. (1996). The trophic structure and predation impact of a low latitude midwater fish assemblage. *Progress in Oceanography*, *38*(3), 205-239.

Hyslop, E. J. (1980). Stomach contents analysis—a review of methods and their application. *Journal of fish biology*, *17*(4), 411-429.

Irigoien, X., Klevjer, T. A., Røstad, A., Martinez, U., Boyra, G., Acuña, J. L., *et al*. (2014). Large mesopelagic fishes biomass and trophic efficiency in the open ocean. *Nature communications*, *5*(1), 1-10.

Jackson, A. L., Inger, R., Parnell, A. C., & Bearhop, S. (2011). Comparing isotopic niche widths among and within communities: SIBER–Stable Isotope Bayesian Ellipses in R. *Journal of Animal Ecology*, *80*(3), 595-602.

Johnston, M. W., Milligan, R. J., Easson, C. G., DeRada, S., English, D. C., Penta, B., & Sutton, T. T. (2019). An empirically validated method for characterizing pelagic habitats in the Gulf of Mexico using ocean model data. *Limnology and Oceanography: Methods*, *17*(6), 362-375.

Lancraft, T. M., Hopkins, T. L., & Torres, J. J. (1988). Aspects of the ecology of the mesopelagic fish Gonostoma elongatum(Gonostomatidae, Stomiiformes) in the eastern Gulf of Mexico. *Marine ecology progress series. Oldendorf*, *49*(1), 27-40.

Layman, C. A., Winemiller, K. O., Arrington, D. A., & Jepsen, D. B. (2005). Body size and trophic position in a diverse tropical food web. *Ecology*, *86*(9), 2530-2535.

Layman, C. A., Arrington, D. A., Montaña, C. G., & Post, D. M. (2007). Can stable isotope ratios provide for community-wide measures of trophic structure?. *Ecology*, *88*(1), 42-48.

Longhurst, A. R., Bedo, A. W., Harrison, W. G., Head, E. J. H., & Sameoto, D. D. (1990). Vertical flux of respiratory carbon by oceanic diel migrant biota. *Deep Sea Research Part A. Oceanographic Research Papers*, *37*(4), 685-694.

Lotze, H. K., Lenihan, H. S., Bourque, B. J., Bradbury, R. H., Cooke, R. G., Kay, M. C., *et al.* (2006). Depletion, degradation, and recovery potential of estuaries and coastal seas. *Science*, *312*(5781), 1806-1809.

Mancinelli, G., Vizzini, S., Mazzola, A., Maci, S., & Basset, A. (2013). Cross-validation of δ15N and FishBase estimates of fish trophic position in a Mediterranean lagoon: the importance of the isotopic baseline. *Estuarine, Coastal and Shelf Science*, *135*, 77-85.

McCann, K. S. 2000. The diversity–stability debate. Nature, *405*(6783), 228-233.

McClain-Counts, J. P., Demopoulos, A. W., & Ross, S. W. (2017). Trophic structure of mesopelagic fishes in the Gulf of Mexico revealed by gut content and stable isotope analyses. *Marine Ecology*, *38*(4), e12449.

McClelland, J. W., & Montoya, J. P. (2002). Trophic relationships and the nitrogen isotopic composition of amino acids in plankton. *Ecology*, *83*(8), 2173-2180.

McEachran J. D., & Fechhelm J. D. (1998). *Fishes of the Gulf of Mexico, Volume 1: Myxiniformes to Gasterosteiformes*. Austin, TX: University of Texas Press

Ménard, F., Benivary, H. D., Bodin, N., Coffineau, N., Le Loc'h, F., Mison, T., *et al*. (2014). Stable isotope patterns in micronekton from the Mozambique Channel. *Deep Sea Research Part II: Topical Studies in Oceanography*, *100*, 153-163.

Mengerink, K. J., Van Dover, C. L., Ardron, J., Baker, M., Escobar-Briones, E., Gjerde, K., *et al*. (2014). A call for deep-ocean stewardship. *Science*, *344*(6185), 696-698.

Milligan, R. J., Bernard, A. M., Boswell, K. M., Bracken-Grissom, H. D., D'Elia, M. A., DeRada, S., *et al*. (2018). The Application of Novel Research Technologies by the Deep Pelagic Nekton Dynamics of the Gulf of Mexico (DEEPEND) Consortium. *Marine Technology Society Journal*, *52*(6), 81-86.

Moore, J. A., Fenolio, D. B., Cook, A. B., & Sutton, T. T. (2020). Hiding in Plain Sight: Elopomorph Larvae Are Important Contributors to Fish Biodiversity in a Low-Latitude Oceanic Ecosystem. *Frontiers in Marine Science*.

Myers, R. A., & Worm, B. (2003). Rapid worldwide depletion of predatory fish communities. *Nature*, *423*(6937), 280-283.

Minagawa, M., & Wada, E. (1984). Stepwise enrichment of 15N along food chains: further evidence and the relation between δ^{15}N and animal age. *Geochimica et Cosmochimica Acta*, *48*(5), 1135-1140.

Mintenbeck, K., Jacob, U., Knust, R., Arntz, W. E., & Brey, T. (2007). Depth-dependence in stable isotope ratio δ^{15}N of benthic POM consumers: the role of particle dynamics and organism trophic guild. *Deep Sea Research Part I: Oceanographic Research Papers*, *54*(6), 1015-1023.

Montoya, J. P., Carpenter, E. J., & Capone, D. G. (2002). Nitrogen fixation and nitrogen isotope abundances in zooplankton of the oligotrophic North Atlantic. *Limnology and Oceanography*, *47*(6), 1617-1628.

Moore, J. A., Vecchione, M., Collette, B. B., Gibbons, R., Hartel, K. E., Galbraith, J. K., *et al*. (2003). Biodiversity of Bear Seamount, New England seamount chain: results of exploratory trawling. *Journal of Northwest Atlantic Fishery Science*, *31*.

Morato, T., Watson, R., Pitcher, T. J., & Pauly, D. (2006). Fishing down the deep. *Fish and fisheries*, *7*(1), 24-34.

Moteki, M., Arai, M., Tsuchiya, K., & Okamoto, H. (2001). Composition of piscine prey in the diet of large pelagic fish in the eastern tropical Pacific Ocean. *Fisheries Science*, *67*(6), 1063-1074.

Murawski S.A., Hollander D.J., Gilbert S., Gracia A. (2020) Deepwater Oil and Gas Production in the Gulf of Mexico and Related Global Trends. In: Murawski S. et al. (eds) Scenarios and Responses to Future Deep Oil Spills. Springer, Cham

Olivar, M. P., Bode, A., López-Pérez, C., Hulley, P. A., & Hernández-León, S. (2019). Trophic position of lanternfishes (Pisces: Myctophidae) of the tropical and equatorial Atlantic estimated using stable isotopes. *ICES Journal of Marine Science*, *76*(3), 649-661.

Pakhomov, E. A., Perissinotto, R., and McQuaid, C. D. 1996. Prey composition and daily rations of myctophid fishes in the Southern Ocean. *Marine Ecology Progress Series*, 134: 1–14.

Pakhomov, E. A., Henschke, N., Hunt, B. P., Stowasser, G., & Cherel, Y. (2019). Utility of salps as a baseline proxy for food web studies. *Journal of Plankton Research*, *41*(1), 3-11.

Parzanini, C., Parrish, C. C., Hamel, J. F., & Mercier, A. (2017). Trophic ecology of a deep-sea fish assemblage in the Northwest Atlantic. *Marine Biology*, *164*(10), 206.

Passarella, K. C., & Hopkins, T. L. (1991). Species composition and food habits of the micronektonic cephalopod assemblage in the eastern Gulf of Mexico. *Bulletin of Marine Science*, *49*(1-2), 638-659.

Pauly, D., Trites, A. W., Capuli, E., and Christensen, V. 1998. Diet composition and trophic levels of marine mammals. *ICES Journal of Marine Science*, *55*(3), 467-481.

Peterson, B. J., & Fry, B. (1987). Stable isotopes in ecosystem studies. *Annual Review of Ecology and Systematics*, *18*(1), 293-320.

Pethybridge, H. R., Choy, C. A., Polovina, J. J., & Fulton, E. A. (2018). Improving marine ecosystem models with biochemical tracers. *Annual Review of Marine Science*, *10*, 199-228.

Polis, G. A., & Strong, D. R. (1996). Food web complexity and community dynamics. *The American Naturalist*, *147*(5), 813-846.

Popp, B. N., Graham, B. S., Olson, R. J., Hannides, C. C., Lott, M. J., López-Ibarra, G. A., *et al*. (2007). Insight into the trophic ecology of yellowfin tuna, *Thunnus albacares*, from compound-specific nitrogen isotope analysis of proteinaceous amino acids. *Terrestrial Ecology*, *1*, 173-190.

Porteiro, F. M., & Sutton, T. T. (2007). Midwater fish assemblages and seamounts. *In* Seamounts: Ecology, Conservation and Management, pp. 101-116. Ed. by T.J. Pitcher, T. Morato, P.J.B. Hart, M.R. Clark, N. Haggan, and R.S. Santos. Oxford: Blackwell, Fish and Aquatic Resources Series.

Post, D. M. (2002). Using stable isotopes to estimate trophic position: models, methods, and assumptions. *Ecology*, *83*(3), 703-718.

Post, D. M. (2003). Individual variation in the timing of ontogenetic niche shifts in largemouth bass. *Ecology*, *84*(5), 1298-1310.

Post, D. M., Layman, C. A., Arrington, D. A., Takimoto, G., Quattrochi, J., & Montana, C. G. (2007). Getting to the fat of the matter: models, methods and assumptions for dealing with lipids in stable isotope analyses. *Oecologia*, *152*(1), 179-189.

Raclot, T., Groscolas, R., & Cherel, Y. (1998). Fatty acid evidence for the importance of myctophid fishes in the diet of king penguins, Aptenodytes patagonicus. *Marine Biology*, *132*(3), 523-533.

Ramirez-Llodra, E., Tyler, P. A., Baker, M. C., Bergstad, O. A., Clark, M. R., Escobar, E., *et al*. (2011). Man and the last great wilderness: human impact on the deep sea. *PLoS one*, *6*(8), e22588.

Richards, T. M., Gipson, E. E., Cook, A., Sutton, T. T., & Wells, R. D. (2018). Trophic ecology of meso-and bathypelagic predatory fishes in the Gulf of Mexico. *ICES Journal of Marine Science*, *76*(3), 662-672.

Robison, B. H. (2004). Deep pelagic biology. *Journal of experimental marine biology and ecology*, *300*(1-2), 253-272.

Robison, B. H. (2009). Conservation of deep pelagic biodiversity. *Conservation Biology*, *23*(4), 847-858.

Romero-Romero, S., Choy, C. A., Hannides, C. C., Popp, B. N., & Drazen, J. C. (2019). Differences in the trophic ecology of micronekton driven by diel vertical migration. *Limnology and oceanography*, *64*(4), 1473-1483.

Rooker, J. R., Kitchens, L. L., Dance, M. A., Wells, R. D., Falterman, B., & Cornic, M. (2013). Spatial, temporal, and habitat-related variation in abundance of pelagic fishes in the Gulf of Mexico: potential implications of the Deepwater Horizon oil spill. *PLoS ONE*, *8*(10), e76080.

Schoener, T. W. (1968). The Anolis lizards of Bimini: resource partitioning in a complex fauna. *Ecology*, *49*(4), 704-726.

Shaffer, J. P. (1986). Modified sequentially rejective multiple test procedures. *Journal of the American Statistical Association*, *81*(395), 826-831.

Stock, B. C., and Semmens, B. X. 2015. MixSIAR.

Sutton, T. T., & Hopkins, T. L. (1996a). Species composition, abundance, and vertical distribution of the stomiid (Pisces: Stomiiformes) fish assemblage of the Gulf of Mexico. *Bulletin of Marine Science*, *59*(3), 530-542.

Sutton, T. T., & Hopkins, T. L. (1996). Trophic ecology of the stomiid (Pisces: Stomiidae) fish assemblage of the eastern Gulf of Mexico: strategies, selectivity and impact of a top mesopelagic predator group. *Marine Biology*, *127*(2), 179-192.

Sutton, T. T., Porteiro, F. M., Heino, M., Byrkjedal, I., Langhelle, G., Anderson, C. I. H., *et al*. (2008). Vertical structure, biomass and topographic association of deep-pelagic fishes in relation to a mid-ocean ridge system. *Deep Sea Research Part II: Topical Studies in Oceanography*, *55*(1-2), 161-184.

Sutton, T. T., Wiebe, P. H., Madin, L., & Bucklin, A. (2010). Diversity and community structure of pelagic fishes to 5000 m depth in the Sargasso Sea. *Deep Sea Research Part II: topical studies in oceanography*, *57*(24-26), 2220-2233.

Sutton, T. T. (2013). Vertical ecology of the pelagic ocean: classical patterns and new perspectives. *Journal of fish biology*, *83*(6), 1508-1527.

Sutton, T.T., Cook, A.B., Moore, J.A., Frank, T., Judkins, H., Vecchione, M., Nizinski, M., & Youngbluth, M., (2017a). Inventory of Gulf oceanic fauna data including species, weight, and measurements. Meg Skansi cruises from Jan. 25–Sept. 30, 2011 in the Northern Gulf of Mexico. Distributed by: Gulf of Mexico Research Initiative Information and Data Cooperative (GRIIDC), Harte Research Institute, Texas A &M University – Corpus Christi. ⟨http://doi.org/10.7266/N7VX0DK2⟩.

Sutton, T. T., Clark, M. R., Dunn, D. C., Halpin, P. N., Rogers, A. D., Guinotte, J., *et al*. (2017b). A global biogeographic classification of the mesopelagic zone. *Deep Sea Research Part I: Oceanographic Research Papers*, *126*, 85-102.

Sutton T.T., Frank T., Judkins H., Romero I.C. (2020) As Gulf Oil Extraction Goes Deeper, Who Is at Risk? Community Structure, Distribution, and Connectivity of the Deep-Pelagic Fauna. In: Murawski S. et al. (eds) Scenarios and Responses to Future Deep Oil Spills. Springer, Cham

Sweeting, C. J., Barry, J. T., Polunin, N. V. C., & Jennings, S. (2007). Effects of body size and environment on diet-tissue δ13C fractionation in fishes. *Journal of Experimental Marine Biology and Ecology*, *352*(1), 165-176.

Sweeting, C. J., Barry, J., Barnes, C., Polunin, N. V. C., & Jennings, S. (2007b). Effects of body size and environment on diet-tissue δ15N fractionation in fishes. *Journal of Experimental Marine Biology and Ecology*, *340*(1), 1-10.

Syvitski, J. P., Vörösmarty, C. J., Kettner, A. J., & Green, P. (2005). Impact of humans on the flux of terrestrial sediment to the global coastal ocean. *science*, *308*(5720), 376-380.

Thurber, A. R., Sweetman, A. K., Narayanaswamy, B. E., Jones, D. O., Ingels, J., & Hansman, R. L. (2014). Ecosystem function and services provided by the deep sea. *Biogeosciences*, *11*(14), 3941-3963.

Trueman, C. N., Johnston, G., O'Hea, B., & MacKenzie, K. M. (2014). Trophic interactions of fish communities at midwater depths enhance long-term carbon storage and benthic production on continental slopes. *Proceedings of the Royal Society B: Biological Sciences*, *281*(1787), 20140669.

Valls, M., Olivar, M. P., de Puelles, M. F., Molí, B., Bernal, A., & Sweeting, C. J. (2014). Trophic structure of mesopelagic fishes in the western Mediterranean based on stable isotopes of carbon and nitrogen. *Journal of Marine Systems*, *138*, 160-170.

Vereshchaka, A. L., Lunina, A. A., & Sutton, T. (2019). Assessing Deep-Pelagic Shrimp Biomass to 3000 m in The Atlantic Ocean and Ramifications of Upscaled Global Biomass. *Scientific Reports*, *9*(1), 5946.

Vukovich, F. M., & Crissman, B. W. (1986). Aspects of warm rings in the Gulf of Mexico. *Journal of Geophysical Research: Oceans*, *91*(C2), 2645-2660.

Wada, E., Mizutani, H., & Minagawa, M. (1991). The use of stable isotopes for food web analysis. *Critical Reviews in Food Science & Nutrition*, *30*(4), 361-371.

Webb, T. J., Berghe, E. V., & O'Dor, R. (2010). Biodiversity's big wet secret: the global distribution of marine biological records reveals chronic under-exploration of the deep pelagic ocean. *PloS one*, *5*(8), e10223.

Wells, R. D., Cowan Jr, J. H., & Fry, B. (2008). Feeding ecology of red snapper Lutjanus campechanus in the northern Gulf of Mexico. *Marine Ecology Progress Series*, *361*, 213-225.

Wells, R. D., Rooker, J. R., Quigg, A., & Wissel, B. (2017). Influence of mesoscale oceanographic features on pelagic food webs in the Gulf of Mexico. *Marine biology*, *164*(4), 92.

Wilson, R. W., Millero, F. J., Taylor, J. R., Walsh, P. J., Christensen, V., Jennings, S., & Grosell, M. (2009). Contribution of fish to the marine inorganic carbon cycle. *Science*, *323*(5912), 359-362.

Winemiller, K. O., & Polis, G. A. (1996). Food webs: what can they tell us about the world?. In *Food Webs*. Boston, MA: Springer.

Wissel, B., & Fry, B. (2005). Tracing Mississippi River influences in estuarine food webs of coastal Louisiana. *Oecologia*, *144*(4), 659-672.

Yarnes, C. T., & Herszage, J. (2017). The relative influence of derivatization and normalization procedures on the compound-specific stable isotope analysis of nitrogen in amino acids. *Rapid Communications in Mass Spectrometry*, *31*(8), 693-704.

Zanden, M. J. V., & Rasmussen, J. B. (2001). Variation in $\delta^{15}N$ and $\delta^{13}C$ trophic fractionation: implications for aquatic food web studies. *Limnology and oceanography*, *46*(8), 2061-2066.

APPENDIX A

Table A-1. Results of least-squares linear regression of POM $\delta^{13}C$ and $\delta^{15}N$ with latitude and longitude.

	Latitude	Longitude
$\delta^{13}C$		
Epipelagic	$r = 0.01$, $p = 0.18$	**$r = 0.04$, $p < 0.05$**
Mesopelagic	$r = 0.02$, $p = 0.19$	$r = –0.03$, $p = 0.82$
Bathypelagic	$r = 0.08$, $p = 0.13$	$r = –0.04$, $p = 0.63$
$\delta^{15}N$		
Epipelagic	$r = 0.02$, $p = 0.07$	$r = –0.01$, $p = 0.80$
Mesopelagic	$r = –0.03$, $p = 0.97$	$r = –0.02$, $p = 0.58$
Bathypelagic	$r = 0.06$, $p = 0.15$	$r = –0.05$, $p = 0.70$

Table A-2. Results of all pairwise comparisons between species $\delta^{15}N$ and $\delta^{13}C$ values conducted using Tukey's HSD test.

	A. cornuta	*C. atlantica*	*C. sloani*	*G. chuni*	*G. indica*	*O. lowii*	*P. guernei*
$\delta^{13}C$							
C. atlantica	0.25						
C. sloani	0.77	0.96					
G. chuni	**< 0.01**	0.85	0.13				
G. indica	**< 0.01**	0.86	0.15	1			
O. lowii	1	**< 0.05**	0.22	**< 0.01**	**< 0.01**		
P. guernei	0.43	0.99	0.99	0.26	0.30	**< 0.05**	
S. affinis	0.11	**< 0.01**	**< 0.01**	**< 0.01**	**< 0.01**	0.31	**<0.01**
$\delta^{15}N$							
C. atlantica	**< 0.01**						
C. sloani	**< 0.01**	0.47					
G. chuni	1	**< 0.01**	**< 0.01**				
G. indica	0.56	**< 0.05**	**< 0.01**	0.55			
O. lowii	**< 0.01**	1	0.81	**< 0.01**	**< 0.01**		
P. guernei	**< 0.01**	**< 0.01**	0.65	**< 0.01**	**< 0.01**	**< 0.05**	
S. affinis	**< 0.01**	1	0.28	**< 0.01**	**< 0.05**	0.98	**< 0.01**

Table A-3. Trophic position estimates for all fishes using mean POM $\delta^{15}N$ from the epipelagic to set isotopic baseline and TP estimates using $\delta^{15}N$ of euphausiids (McClain-Counts *et al.*, 2017).

	TP (± s.d.) POM baseline	TP (± s.d.) Euphausiid baseline
A. cornuta	3.4 ± 0.31	3.7 ± 0.31
C. sloani	2.9 ± 0.14	3.2 ± 0.14
C. atlantica	3.0 ± 0.26	3.4 ± 0.26
G. chuni	3.4 ± 0.34	3.7 ± 0.34
G. indica	3.3 ± 0.20	3.6 ± 0.20
O. lowii	3.0 ± 0.19	3.3 ± 0.19
P. guernei	2.8 ± 0.20	3.1 ± 0.20
S. affinis	3.0 ± 0.28	3.4 ± 0.28

APPENDIX B

Table B-1. Diet and depth references for each micronekton species included Chapter IV analysis.

Species	Diet Reference(s)	Depth Reference(s)
Argyropelecus aculeatus	Hopkins & Baird, 1985; Hopkins et al., 1996	Hopkins & Baird, 1985
Benthosema suborbitale	Hopkins et al., 1996	Gartner et al., 1987
Bolinichthys photothorax	Hopkins et al., 1996	Gartner et al., 1987
Ceratoscopelus warmingii	Hopkins et al., 1996	Gartner et al., 1987
Chauliodus sloani	Hopkins et al., 1996; Sutton et al., 1996B	Sutton et al., 1996A; Cook & Sutton, 2017
Diaphus dumerilii	Hopkins et al., 1996	Gartner et al., 1987
Diaphus lucidus	Hopkins et al., 1996	Gartner et al., 1987
Diaphus mollis	Hopkins et al., 1996	Gartner et al., 1987
Diaphus splendidus	Hopkins et al., 1996	Gartner et al., 1987
Diogenichthys atlanticus	McEachran & Fechhelm, 1998	Gartner et al., 1987
Echiostoma barbatum	Hopkins et al., 1996; Sutton et al., 1996B	Sutton et al., 1996A; Cook & Sutton, 2017
Hygophum benoiti	Hopkins et al., 1996	Gartner et al., 1987
Hygophum taaningi	Hopkins et al., 1996	Gartner et al., 1987
Lampadena luminosa	Hopkins et al., 1996	Gartner et al., 1987
Lampanyctus alatus	Hopkins et al., 1996	Gartner et al., 1987
Lepidophanes guentheri	Hopkins et al., 1996	Gartner et al., 1987
Melamphaes simus	Hopkins et al., 1996	Cook & Sutton, 2017
Myctophum affine	Hopkins et al., 1996	Gartner et al., 1987
Nannobrachium lineatum	McEachran & Fechhelm, 1998	Cook & Sutton, 2017
Notolychnus valdiviae	Hopkins et al., 1996	Gartner et al., 1987
Notoscopelus resplendens	Hopkins et al., 1996	Gartner et al., 1987; Cook & Sutton, 2017
Photostomias guernei	Hopkins et al., 1996; Sutton et al., 1996B	Sutton et al., 1996A; Cook & Sutton, 2017
Pollichthys mauli	Hopkins et al., 1996	Cook & Sutton, 2017
Sigmops elongatus	Lancraft et al., 1988; Hopkins et al., 1996	Lancraft et al., 1988
Stomias affinis	Hopkins et al., 1996; Sutton et al., 1996B	Sutton et al., 1996A;
Vinciguerria nimbaria	Hopkins et al., 1996	Cook & Sutton, 2017
Pterygioteuthis gemmata	Passarella & Hopkins, 1991	Judkins & Vecchione, 2020
Stigmatoteuthis arcturi	McEachran & Fechhelm, 1998	Judkins & Vecchione, 2020
Acanthephyra purpurea	Hopkins et al., 1994	Hopkins et al., 1994
Sergia splendens	Hopkins et al., 1994	Hopkins et al., 1994; Burghart et al., 2007
Systellaspis debilis	Hopkins et al., 1994	Hopkins et al., 1994
Thysanopoda acutifrons	SeaLifeBase.org	Frank et al., 2020
Anoplogaster cornuta	Hopkins et al., 1996	Clarke & Wagner, 1976
Argyropelecus hemigymnus	Hopkins & Baird, 1985; Hopkins et al., 1996	Hopkins & Baird, 1985
Cyclothone acclinidens	Hopkins et al., 1996	Cook & Sutton, 2017
Cyclothone alba	Hopkins et al., 1996	Miya & Nemoto, 1986; Cook & Sutton, 2017
Cyclothone braueri	Hopkins et al., 1996	Cook & Sutton, 2017
Cyclothone obscura	Burghart et al., 2010	McEachran & Fechhelm; Cook & Sutton, 2017
Cyclothone pallida	Hopkins et al., 1996	Badcock & Merrett, 1976; Cook & Sutton, 2017
Cyclothone pseudopallida	Hopkins et al., 1996	Badcock & Merrett, 1976; Cook & Sutton, 2017
Poromitra gibbsi	Hopkins et al., 1996	Cook & Sutton, 2017
*Rhynchoconger flavus**	Quattrini et al.,	Cook & Sutton, 2017
Scopeloberyx opercularis	McEachran & Fechhelm, 1998	Cook & Sutton, 2017
Scopeloberyx opisthopterus	Hopkins et al., 1996	Cook & Sutton, 2017
Scopeloberyx robustus	McEachran & Fechhelm, 1998	Cook & Sutton, 2017
Sternoptyx diaphana	Hopkins & Baird, 1985; Hopkins et al., 1996	Hopkins & Baird, 1985
Sternoptyx pseudobscura	Hopkins & Baird, 1985; Hopkins et al., 1996	Hopkins & Baird, 1985; Cook & Sutton, 2017
Valenciennellus tripunctulatus	Hopkins et al., 1996	Hopkins & Baird, 1981

Bolitaena pygmaea	Passarella & Hopkins, 1991	Judkins & Vecchione, 2020
Japatella diaphana	Passarella & Hopkins, 1991	Judkins & Vecchione, 2020
Mastigoteuthis agassizii	Passarella & Hopkins, 1991	Judkins & Vecchione, 2020
Vampyroteuthis infernalis	Golikov et al., 2019	Judkins & Vecchione, 2020
Acanthephyra curtirostris	Hopkins et al., 1994	Hopkins et al., 1994; Burdett et al., 2017
Acanthephyra stylorostrata	Hopkins et al., 1994	Hopkins et al., 1994; Burdett et al., 2017
Eucopia sculpticauda	Hopkins et al., 1994; Burghart et al., 2010	Hopkins et al. 1994; Burghart et al., 2007

Table B-1 Continued